Accepted Manuscript

Synthesis, molecular docking and *Brugia malayi* thymidylate kinase (BmTMK) enzyme inhibition study of novel derivatives of [6]-shogaol

Vinay Kr. Singh, Pawan K. Doharey, Vikash Kumar, J.K. Saxena, M.I. Siddiqi, Sushma Rathaur, Narender Tadigoppula

PII: S0223-5234(15)00055-0

DOI: 10.1016/j.ejmech.2015.01.035

Reference: EJMECH 7651

To appear in: *European Journal of Medicinal Chemistry*

Received Date: 5 September 2014

Revised Date: 15 January 2015

Accepted Date: 19 January 2015

Please cite this article as: V.K. Singh, P.K. Doharey, V. Kumar, J.K. Saxena, M.I. Siddiqi, S. Rathaur, N. Tadigoppula, Synthesis, molecular docking and *Brugia malayi* thymidylate kinase (BmTMK) enzyme inhibition study of novel derivatives of [6]-shogaol, *European Journal of Medicinal Chemistry* (2015), doi: 10.1016/j.ejmech.2015.01.035.

Graphical Abstract

Synthesis, molecular docking and *Brugia malayi* thymidylate kinase (BmTMK) enzyme inhibition study of novel derivatives of [6]-shogaol

Leave this area blank for abstract info.

Vinay Kr. Singh[a], Pawan K. Doharey[b], Vikash Kumar[c], J. K. Saxena[b], M. I. Siddiqi[c], Sushma Rathaur[d], Narender Tadigoppula[a]*

[a]*Medicinal and Process Chemistry Division, CSIR-Central Drug Research Institute, (CSIR-CDRI), BS-10/1, Sector 10, Jankipuram extension, Sitapur Road, P.O. Box 173, Lucknow 226031, India*

[b]*Biochemistry Division, CSIR-Central Drug Research Institute, (CSIR-CDRI), BS-10/1, Sector 10, Jankipuram extension, Sitapur Road, P.O. Box 173, Lucknow 226031, India*

[c]*Molecular & Structural Biology Division, CSIR-Central Drug Research Institute, (CSIR-CDRI), BS-10/1, Sector 10, Jankipuram extension, Sitapur Road, P.O. Box 173, Lucknow 226031, India*

[d]*Department of Biochemistry, Banaras Hindu University, Varanasi 221005, India*

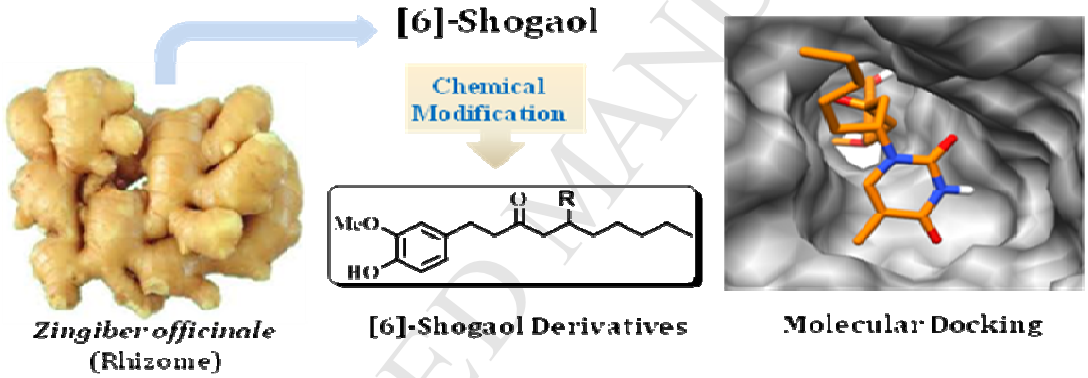

Synthesis, molecular docking and *Brugia malayi* thymidylate kinase (BmTMK) enzyme inhibition study of novel derivatives of [6]-shogaol

Vinay Kr. Singh[a], Pawan K. Doharey[b], Vikash Kumar[c], J. K. Saxena[b], M. I. Siddiqi[c], Sushma Rathaur[d], Narender Tadigoppula[a]*

[a]*Medicinal and Process Chemistry Division, CSIR-Central Drug Research Institute, (CSIR-CDRI), BS-10/1, Sector 10, Jankipuram extension, Sitapur Road, P.O. Box 173, Lucknow 226031, India*

[b]*Biochemistry Division, CSIR-Central Drug Research Institute, (CSIR-CDRI), BS-10/1, Sector 10, Jankipuram extension, Sitapur Road, P.O. Box 173, Lucknow 226031, India*

[c]*Molecular & Structural Biology Division, CSIR-Central Drug Research Institute, (CSIR-CDRI), BS-10/1, Sector 10, Jankipuram extension, Sitapur Road, P.O. Box 173, Lucknow 226031, India*

[d]*Department of Biochemistry, Banaras Hindu University, Varanasi 221005, India*

Abstract: [6]-Shogaol (**1**) was isolated from *Zingiber officinale*. Twelve novel compounds have been synthesized and evaluated for their *Brugia malayi* thymidylate kinase (BmTMK) inhibition activity, which plays important role for the DNA synthesis in parasite. [6]-Shogaol (**1**) and shogaol with thymine head group (**2**), 5-bromouracil head group (**3**), adenine head group (**4**) and 2-amino-3-methylpyridine head group (**5**) showed potential inhibitory effect on BmTMK activity. Further molecular docking studies were carried out to explore the putative binding mode of compounds **1**-**5**.

Key Words: [6]-Shogaol; *Zingiber officinale;* Filariasis*; Brugia malayi;* Thymidylate kinase; Molecular Modelling; Enzyme inhibitor

*** Address correspondence to this author**

E-mail: t_narendra@cdri.res.in (T. Narender); Phone: +91 522 2612411, Fax: +91 522 2623405# CDRI Manuscript No.xxx/2013/TN

1. Introduction

Filariasis is a challenging problem for tropical and subtropical countries, about 140 million people world-wide are affected and about 1.20 billion people are at risk of infection [1]. Human lymphatic filariasis is mainly caused by the parasites *Wuchereria bancrofti* and *Brugia malayi*. Lymphatic filariasis (LF) is a complex human infection with a wide spectrum of clinical manifestations. Although the most active antifilarial drugs diethylcarbamazine (DEC), ivermectin and albendazole are effective against microfilariae (mf) stage, they are unable to kill adult parasite which produces millions of microfilariae and are responsible for the chronic pathological lesions [2]. Indications of resistance have also been reported for albendazole and ivermectin [3,4]. So there is an urgent need to develop new antifilarial drugs having effectiveness against both the adult and microfilariae stages of the parasite. Ginger suggested that enzyme inhibitors can be used as drugs by targeting selected enzyme involved in essential metabolic pathways which may be lethal to parasite [5]. Thymidylate kinase (EC 2.7.4.9, ATP:TMP phosphotransferase, TMPK), has emerged as an attractive therapeutic target as it catalyzes the conversion of thymidine monophosphate (dTMP) into thymidine diphosphate (dTDP) (Figure 1) in the presence of ATP as the preferred phosphoryl donor. This is an obligatory step in the synthesis of thymidine triphosphate (dTTP) either from thymidine via thymidine kinase (salvage pathway) or from dUMP via thymidylate synthase in all living cells [6]. Therefore the inhibition of TMK function can block DNA synthesis in the replicating organisms [7]. TMK phosphorylates thymidine monophosphate (dTMP) to thymidine diphosphate (dTDP), using ATP as a phosphoryl donor [6]. In addition, TMK is the last specific enzyme in the pathway for the synthesis of thymidine triphosphate (dTTP), which is an essential component in DNA synthesis [8].

Recently we cloned, expressed and characterized *Brugia malayi* thymidylate kinase (BmTMK), which showed substrate specificity and utilizes pyrimidine nucleosides only. In our studies nucleoside analogues selectively inhibited the BmTMK as compared to human TMK and the specificity of nucleoside analogues was validated by docking studies [9]. In continuation of this program to develop BmTMK inhibitors, we screened few natural products available in our laboratory and discovered the activity in [6]-Shogaol isolated from *Zingiber officinale*. Shogaols and gingerols have been identified as main active and pungent constituents from the plant, Ginger, *Z. officinale* (Zingiberaceae). Shogaols are dehydrated products of gingerols. Ginger is used world-wide not only as a spice in culinary preparations, but also in various folk medicines against different ailments. It has found to have antioxidant, anticancer, antimicrobial, and anti-inflammatory properties [10]. Molecular targets involved in their

therapeutic properties include matrix metalloproteinases MMP-2 and MMP-9 [11], nuclear-factor-kB (NF-kB) [12], cyclooxygenase (COX) and lipooxygenase (LOX) [13], and peroxisome proliferator-activated receptor (PPARγ) [14]. In addition, gingerols and shogaols have been reported to activate the transient receptor potential channels, TRPV1 [15] and TRPA1 [16], which belong respectively to the TRPV (vanilloid) and TRPA (ankyrin) subfamilies of the large transient receptor potential (TRP) cation channel family [17].

Most of the reported TMK inhibitors are thymidine derived (Figure 2) [18-24]. Although, inhibitor design has been enhanced by utilizing protein structures, computer aided design, and quantitative structure-activity relationship (QSAR) methods, the thymine head group of the inhibitors always remains the same (Figure 2). We desired to introduce the thymine head group into the natural products i.e. [6]-shogaol to improve their TMK inhibitory activity. We herein report the synthesis, enzyme inhibitory activity and molecular docking study of novel derivatives of [6]-shogaol as *B. malayi* TMK inhibitors.

2. Chemistry

2.1. Isolation of [6]-Shogaol from *Z. officinale*

The fresh ginger rhizomes were collected from local market of Lucknow (India). The rhizomes (5kg) were cut and powdered and placed in a glass percolator with 95% ethanol and allowed to stand at room temperature for 24 h. The percolate was collected and this process was repeated for four times. The combined percolates were concentrated under reduced pressure using rotary evaporator at 40^{o}C to get brown residual mass. This residue was fractionated using chloroform to get chloroform soluble fraction which was further subjected to column chromatography on silica gel using ethylacetate and n-hexane as solvent system to obtain [6]-shogaol and [6]-gingerol (Figure 3).

2.2. Synthesis of target compounds

Targeted [6]-shogaol derivatives were synthesized using Scheme 1 and Scheme 2. We applied the aza-Michael reaction for synthesizing the target compounds. Two series of compounds have been synthesized. In the first series (compounds **2-4**, **2a-2f**) [6]-shogaol was transformed to aza-Michael products with thymine and adenine which were further transformed to esters (scheme 1 and scheme 2) using appropriate acid chlorides in the presence of triethylamine as base. The second series of compounds (**5-7** and **6a**) have been synthesized from 2-aminopicolines using the same procedures.

3. Results and Discussion

3.1. BmTMK Inhibitory activity

All of the synthesized compounds (twelve) with [6]-shogaol were screened for their inhibitory activity against recombinant *B. malayi* thymidylate kinase (BmTMK). Since the standard inhibitor of the BmTMK is not known therefore the Km value of BmTMK for its substrate dTMP can be considered as a control. The calculated Km value for thymidine monophosphate (dTMP) is 17.00µM. Thus, the compounds having Ki value lower than 17 µM will show more affinity for the enzyme hence should be considered as more active. Results are shown in Table 1. Compounds **1**-**4** and **5** showed better activity profile with *Ki* value 10.78±0.55µM, 6.57±0.42µM, 8.32±0.39µM, 9.01±0.50µM, 11.06±0.50 µM respectively. It is noteworthy to mention here that shogaol with thymine head group (**2**) showed the most potent activity (6.57 µM). Compound **3** with 5-bromouracil head group, compound **4** with adenine group and compound **5** with a 2-amino-3-methylpyridine group in place of thymine head group also showed better inhibitory effect on BmTMK activity. Compounds **2a, 2b**, **2d**, **2e**, **2f**, **6**, **6a**, and **7** showed poor activity with *Ki* 66.12±3.40 µM, 45.68±2.50 µM, 20.05±1.05 µM, 20.30±1.02 µM, 44.41±2.43 µM, 21.57±1.35 µM, 30.45±1.75 µM, 40.60±1.86 µM, respectively as compared to the control (dTMP; *Km*=17.00 µM). From the above data the structure activity relationship indicated that protection of phenolic hydroxyl group (as in compounds **2a, 2b, 2d, 2e, 2f, 6**, **6a** and **7**) results in poor activity. On the other hand, compounds having free phenolic hydroxyl group with thymine or adenine or 2-amino-3-methylpyridine group (as in **1**-**4** and **5**), showed better activity which suggests that free phenolic group and head group is crucial for activity.

3.2. Molecular docking studies

We investigated the possible binding pose of mentioned inhibitors (**1**-**4** and **5**) in TMP binding site of BmTMK. Due to lack of crystal structure of BmTMK, a homology model was constructed using the crystal structure of HumanTMK (HsTMK) and *Plasmodium falciparum* TMK (PfTMK) [9]. Crystal structure of HsTMK with its substrate shows that, thymine ring of TMP makes π-π stacking interaction with Phe72 (Fig.4a). Apart from this, one of carbonyl groups of thymine ring is involved in H-bonding with side chain of Arg76. Docking studies using Autodock4.2 revealed that binding conformation of parent compound [6]-shogaol,**1** and its derivatives (Fig.4b, 4c, 4d, 4e and 4f) are consistent with the experimentally derived TMP bound conformation [9,25]. We observed that, feruloyl group of inhibitors occupied the narrow cavity and engaged in π-π stacking interaction with Phe73 residue. Besides the hydrophobic interaction, H-bond between phenolic hydroxyl group and His70 was found to be important for activity. However Arg77 (Arg76 in HsTMK) was not involved in H-bonding with any of inhibitors, in this case H–bond with His70 may have compensating effect. We observed that protection of phenolic hydroxyl group resulted in loss of activity, which in turn validates the importance of H-bond with His70. Through computational study we did not establish the effect of substitution at β-position to keto group of parent compound as calculated binding affinities of all compounds were almost similar. In the previous studies [9] few residues inside/near TMP binding of BmTMK were highlighted, which differs from HsTMK. Interestingly thymine ring and adenine ring of compound **2** and **4** respectively found to make H-bond with Tyr106, a residue which is substituted by Phe105 in HsTMK. Docking simulation was also carried out with HsTMK, to reveal any possible differences in binding pose of mentioned inhibitors in the TMP binding site. In case of HsTMK (see supporting information), feruloyl group of all inhibitors were found to be involved in π-π stacking interaction with Phe72, as also seen in BmTMK. In addition, phenolic group of all inhibitors were involved in H-bonding with Arg76. Also the interaction pattern of β-substituents of [6]-shogaol derivatives were different from those observed in the case of BmTMK. In the current study we do not see major differences in the binding modes of compounds when compared to TMP binding pocket of HsTMK, however consideration of receptor flexibility might help in pointing the exact binding mode. The above docking studies reveal the putative binding pose of [6]-shogaol, **1** and its derivatives, which may help in design and optimization of novel BmTMK inhibitors.

4. Conclusion

In conclusion, we isolated [6]-shogaol from *Z. officinale* and discovered its *B. malayi* thymidylate kinase (BmTMK) inhibitory activity for the first time. Twelve novel compounds (**2, 2a-f, 3-6, 6a** and **7**) have been synthesized and evaluated for their inhibitory effect against *B. malayi* thymidylate kinase (BmTMK) activity. Compounds **1-4** and **5** showed potential inhibitory activity profile with *Ki* value 10.78± 0.55 µM, 6.57±0.42 µM, 8.32±0.39 µM, 9.01±0.50 µM, 11.06±0.54 µM respectively. A homology model was constructed using the crystal structure of HumanTMK (HsTMK) and *P. falciparum* TMK (PfTMK) and docking studies were carried out, which revealed that binding conformation of parent compound [6]-shogaol, **1** and its derivatives **2**-**5** (Fig. 4b, 4c, 4d, 4e and 4f) are consistent with the experimentally derived TMP bound conformation. [6]-Shogaol without a thymine head group (**1**), and shogaol with thymine (**2**), 5-bromouracil (**3**), adenine (**4**) and 2-amino-3-methylpyridine (**5**) head groups also showed better activity than its substrate (dTMP) and compound **2** is of further interest to explore.

5. Experimental

5.1. Chemistry

5.1.1. General Information

All reagents were procured from commercial suppliers and were used without further purification. Chromatography was carried on silica gel (60-120 and 100-200 mesh). All reactions were monitored by TLC; silica gel plates with fluorescence F254 were used. ^{1}H NMR and ^{13}C NMR spectra were determined on 400 MHz and 100 MHz, respectively, using $CDCl_3$ and CD_3OD as solvents and TMS as internal standard. All chemical shifts were given in (ppm). IR spectra were recorded on in the range of 500~400cm^{-1} and multiplicity (s = singlet, brs = broad singlet, d = doublet, brd = broad doublet, dd = double doublet, t = triplet, q = quartet, m = multiplet).

5.1.2. General procedure for the synthesis of compounds 2-7

Nitrogenous compounds (1eq. each) viz. thymine (for **2**), 5-bromouracil (for **3**), adenine (for **4**), were first dissolved in warm DMSO. To this solution TEA and a solution of [6]-Shogaol (1eq.) in DMSO was added. Reaction mixture was stirred at room temperature for 24 h. The crude product was extracted using ethyl acetate (3×50 mL). The combined organic layers were dried

over Na_2SO_4, filtered, and concentrated under reduced pressure to get crude product as a syrupy residue which was further purified by flash chromatography to afford the corresponding pure product.

5.1.2.1. 1-(1-(4-Hydroxy-3-methoxyphenyl)-3-oxodecan-5-yl)-5-methylpyrimidine-2,4-(1H,3H)-dione (2)

Yield: 67%; FT-IR (Neat, cm^{-1}): 3416, 3022, 1673, 1216, 760; ^{1}H NMR (400 MHz, $CDCl_3$) δ (ppm): 9.36 (s, 1H), 6.99 (S, 1H), 6.79 (d, *J* = 7.97 Hz, 1H), 6.65 (d, 1H), 6.60 (d, *J* = 7.77 Hz, 1H), 5.92 (br s, 1H), 4.43 (m, 1H), 3.84 (s, 3H), 3.14 (dd, 1H), 2.78 (t, 2H), 2.71 (t, 2H), 2.67 (dd, 1H), 2.62 (s, 3H), 2.16 (s, 2H), 1.90 (s, 3H), 1.60 (m, 1H), 1.25 (m, 8H), 0.86 (t, 3H); ^{13}C NMR (100 MHz, $CDCl_3$) δ (ppm): 207.66, 164.17, 150.81, 146.62, 144.10, 140.19, 132.32, 120.72, 114.58, 111.19, 110.12, 55.90, 46.04, 44.66, 40.83, 32.48, 31.21, 29.31, 25.88, 22.38, 13.91, 12.40; ESI-MS (*m/z*): 403.1 $[M+H]^+$; HRMS (*m/z*): calcd for $C_{22}H_{30}N_2O_5$ $[M+H]^+$ 403.2155, found: 403.2238.

5.1.2.2. 5-Bromo-1-(1-(4-hydroxy-3-methoxyphenyl)-3-oxodecan-5-yl)-pyrimidine-2,4-(1H,3H)-dione (3)

Yield: 43%; FT-IR (Neat, cm^{-1}): 3401, 2927, 1692, 1216, 758; ^{1}H NMR (400 MHz, $CDCl_3$) δ (ppm): 9.06 (s, 1H), 7.55 (s, 1H), 6.82 (d, *J* = 7.92 Hz, 1H), 6.68-6.62 (m, 3H), 5.50 (br s, 1H, OH), 4.44 (m, 1H), 3.87 (s, 3H), 3.15 (dd, 1H), 2.83 (t, 2H), 2.74-2.68 (m, 4H), 1.91 (m, 2H), 1.60 (m, 2H), 1.27 (m, 10H), 0.86 (t, 3H); ^{13}C NMR (100 MHz, $CDCl_3$) δ (ppm): 207.56, 159.40, 149.98, 146.55, 144.06, 143.97, 132.21, 120.74, 114.53, 111.16, 95.92, 55.95, 45.70, 44.57, 32.34, 31.17, 29.68, 29.38, 25.90, 22.36, 13.91; ESI-MS (*m/z*): 467.2 $[M+H]^+$ 469.2 $[M+2]^+$; HRMS (*m/z*): calcd for $C_{21}H_{27}BrN_2O_5$ $[M+H]^+$ 467.1103, found: 467.1188 $[M+H]^+$ 469.1167 $[M+2]^+$.

5.1.2.3. 5-(6-Amino-9H-purin-9-yl)-1-(4-hydroxy-3-methoxyphenyl)decan-3-one (4)

Yield: 38%; FT-IR (Neat, cm^{-1}): 3412, 3021, 1632, 1215, 761, 670; ^{1}H NMR (400 MHz, $CDCl_3$) δ (ppm): 8.28 (s, 1H), 7.77 (s, 1H), 6.74 (d, *J* = 8.14 Hz, 1H), 6.54 (s, 1H),6.51 (d, *J* = 8.41 Hz, 1H), 5.86 (s, H, OH), 4.80 (m, 1H), 3.81 (s, 3H), 3.49 (dd, 1H), 2.90 (dd, 1H), 2.70 (t, 2H), 2.64 (t, 2H), 2.19 (m, 1H), 1.80 (m, 1H), 1.21 (br m, 8H), 0.82 (t, 3H); ^{13}C NMR (100 MHz, $CDCl_3$) δ (ppm): 207.29, 155.52, 152.33, 149.46, 146.68, 144.10, 141.09, 132.13, 120.55, 114.67, 111.13, 55.83, 53.16, 46.46, 44.80, 40.90, 33.40, 31.03, 29.17, 25.84, 22.31, 13.84; ESI-MS (*m/z*): 412.3 $[M+H]^+$; HRMS (*m/z*): calcd for $C_{22}H_{29}N_5O_3$ $[M+H]^+$ 412.2270, found: 412.2348.

5.1.2.4. 1-(4-Hydroxy-3-methoxyphenyl)-5-(3-methylpyridin-2-ylamino)decan-3-one (5)

Yield: 57%; FT-IR (Neat, cm^{-1}): 3431, 3019, 1628, 1215, 757; ^{1}H NMR (400 MHz, $CDCl_3$) δ (ppm): 7.32 (dd, *J* = 8.40 Hz, 1H), 6.80 (d, *J* = 8.26 Hz, 1H), 6.66 (d, *J* = 1.92 Hz, 1H), 6.63 (dd, *J* = 7.92 Hz, 2.01 Hz, 1H), 6.42 (d, *J* = 7.18 Hz, 1H), 6.21 (d, *J* = 8.34 Hz, 1H), 4.79 (br s, 1H,), 4.09 (m, 1H), 3.85 (s, 3H), 2.80 (t, 2H), 2.73 (t, 2H), 2.65 (d, 1H), 2.58 (d, 1H), 2.35 (s, 3H), 1.51 (m, 2H), 1.27 (br m, 6H), 0.87 (t, 3H); ^{13}C NMR (100 MHz, $CDCl_3$) δ (ppm): 209.38, 157.55, 146.42, 143.92, 138.22, 132.86, 120.78, 114.34, 112.04, 111.05, 103.36, 55.85, 48.30, 48.09, 45.50, 35.44, 31.66, 29.32, 25.79, 23.94, 22.52, 13.99; ESI-MS (*m/z*): 385.1 $[M+H]^+$; HRMS (*m/z*): calcd for $C_{23}H_{32}N_2O_3$ $[M+H]^+$ 385.2413, found: 385.2492.

5.1.2.5. 1-(4-Hydroxy-3-methoxyphenyl)-5-(4-methylpyridin-2-ylamino)decan-3-one (6)

Yield: 54%; FT-IR (Neat, cm^{-1}): 3409, 3019, 2931, 1615, 1514, 1216, 759; ^{1}H NMR (400 MHz, $CDCl_3$) δ (ppm): 7.90 (s, 1H), 6.80 (d, *J* = 7.78 Hz, 1H), 6.66 (s, 1H), 6.63 (d, *J* = 8.60 Hz, 1H), 6.40 (d, *J* = 5.40 Hz, 1H), 6.22 (s, 1H), 4.69 (d, 1H, NH), 4.17 (m, 1H), 3.85 (s, 3H), 2.79 (t, 2H), 2.72 (m, 2H), 2.64 (t, 2H), 2.23 (s, 3H), 1.52 (m, 2H), 1.27 (br m, 6H), 0.87 (t, 3H); ^{13}C NMR (100 MHz, $CDCl_3$) δ (ppm): 209.64, 158.17, 148.78, 147.15, 146.53, 144.01, 132.81, 120.77, 114.44, 111.12, 107.59, 55.84, 48.19, 47.79, 45.47, 35.30, 31.68, 29.30, 25.85, 22.53, 21.21, 13.99; ESI-MS (*m/z*): 385.1 $[M+H]^+$; HRMS (*m/z*): calcd for $C_{23}H_{32}N_2O_3$ $[M+H]^+$ 385.2413, found: 385.2492.

5.1.2.6. 1-(4-Hydroxy-3-methoxyphenyl)-5-(5-methylpyridin-2-ylamino)decan-3-one (7)

Yield: 50%; FT-IR (Neat, cm^{-1}): 3426, 3021, 1622, 1215, 760, 670; ^{1}H NMR (300 MHz, $CDCl_3$) δ (ppm): 7.85 (s, 1H), 7.25 (d, *J* = 8.64 Hz, 1H), 6.80 (d, *J* = 7.97 Hz, 1H), 6.66 (s, 1H), 6.63 (d, *J* = 8.64 Hz, 1H), 6.35 (d, *J* = 8.64 Hz, 1H), 4.66 (d, 1H), 4.13 (m, 1H), 3.88 (m, 1H), 3.85 (s, 3H), 3.59 (t, 1H), 3.41 (t, 1H), 2.78-2.69 (m, 4H), 2.63 (t, 2H), 2.41 (m, 2H), 2.17 (s, 3H), 1.50 (t, 2H), 1.27 (m, 11H), 0.86 (t, 3H); ^{13}C NMR (100 MHz, $CDCl_3$) δ (ppm): 209.64, 160.79, 156.15, 146.72, 146.63, 144.07, 138.92,

132.75, 121.47, 120.75, 114.55, 111.20, 107.17, 55.83, 55.35, 54.19, 48.46, 47.84, 46.07, 45.44, 39.79, 35.34, 31.67, 29.29, 25.83, 22.52, 17.31, 13.99; ESI-MS (*m/z*): 385.2 $[M+H]^+$; HRMS (*m/z*): calcd for $C_{23}H_{32}N_2O_3$ $[M+H]^+$ 385.2413, found: 385.2482.

5.1.3. General procedure for the synthesis of compounds 2a-2f and 6a

Compound **3** (1eq) was dissolved in dry DCM and cooled the solution at 0^oC. To this solution added triethylamine followed by the addition of a solution of appropriate acid chloride (1.1eq) in dry DCM. Reaction mixture was stirred for 2h at RT. After the reaction was completed, the crude product was extracted in DCM (3×50 mL). The combined organic layers were dried over Na_2SO_4, filtered, and concentrated under reduced pressure to get crude product which was further purified by column chromatography to afford pure products with good yield. Compound **6** was used as substrate for compound **6a**.

5.1.3.1. 2-Methoxy-4-(5-(5-methyl-2,4-dioxo-3,4-dihydropyrimidin-1(2H)-yl)-3-oxodecyl)phenyl methanesulfonate (2a)

Yield: 82%; FT-IR (Neat, cm^{-1}): 3443, 3019, 1637, 1215, 757; ^1H NMR (400 MHz, $CDCl_3$) δ (ppm): 8.79 (s, 1H, NH), 7.19 (d, *J* = 8.02 Hz, 1H), 7.01 (s, 1H), 6.82 (s, 1H), 6.74 (dd, *J* = 8.19 Hz, 1.86 Hz, 1H), 4.48 (m, 1H), 3.88 (s, 3H), 3.20 (s, 3H), 3.05 (dd, 1H), 2.87 (t, 2H), 2.80-2.69 (m, 3H), 1.90 (s, 3H), 1.27 (br m, 6H), 0.88 (t, 3H); ^{13}C NMR (100 MHz, $CDCl_3$) δ (ppm): 206.92, 164.03, 151.25, 150.76, 141.29, 139.92, 136.71, 124.38, 120.68, 113.26, 110.26, 55.98, 46.11, 44.05, 38.30, 32.60, 31.21, 29.30, 25.85, 22.38, 13.91; ESI- MS $C_{23}H_{32}N_2O_7S$, *m/z* 481.2 $[M+1]^+$, 503.2 $[M+Na]^+$

5.1.3.2. 2-Methoxy-4-(5-(5-methyl-2,4-dioxo-3,4-dihydropyrimidin-1(2H)-yl)-3-oxodecyl)phenyl 4-methylbenzenesulfonate (2b)

Yield: 78%; FT-IR (Neat, cm^{-1}): 3444, 1654, 1215, 756; ^1H NMR (400 MHz, $CDCl_3$) δ (ppm): 8.83 (s, 1H), 7.77 (d, *J* = 7.77 Hz, 2H), 7.32 (d, *J* = 7.77 Hz, 2H), 7.01 (dd, 2H), 6.67-6.65 (m, 2H), 4.47 (m, 1H), 3.56 (s, 3H), 3.16 (dd, 1H), 2.83 (t, 2H), 2.72 (m, 3H), 2.46 (s, 3H), 1.93 (s, 3H), 1.27 (br m, 6H), 0.88 (t, 3H); ^{13}C NMR (100 MHz, $CDCl_3$) δ (ppm): 206.92, 163.97, 151.67, 150.79, 144.95, 140.95, 139.97, 136.76, 133.41, 129.36, 128.55, 123.85, 120.16, 112.94, 110.29, 56.48, 55.55, 46.05, 44.14, 32.55, 31.22, 29.31, 25.87, 22.39, 21.66, 13.91; ESI-MS (*m/z*): 557.2 $[M+H]^+$; HRMS (*m/z*): calcd for $C_{29}H_{36}N_2O_7S$ $[M+H]^+$ 557.2243, found: 557.2308.

5.1.3.3. 2-Methoxy-4-(5-(5-methyl-2,4-dioxo-3,4-dihydropyrimidin-1(2H)-yl)-3-oxodecyl)phenyl 6-chloronicotinate (2c)

Yield: 74%; FT-IR (Neat, cm^{-1}): 3446, 1656, 758; ^1H NMR (400 MHz, $CDCl_3$) δ (ppm): 9.03 (s, 1H, NH), 8.58 (dd, *J* = 4.80 Hz, 1.9 Hz, 1H), 8.42 (dd, *J* = 7.75 Hz, 1.97 Hz, 1H), 7.40 (dd, *J* = 7.75 Hz, 1.90 Hz, 1H), 7.06 (d, *J* = 7.99 Hz, 1H), 7.01 (s, 1H), 6.83 (d, *J* = 1.92 Hz, 1H), 6.77 (dd, *J* = 7.99 Hz, 1.90 Hz, 1H), 4.48 (m, 1H), 3.82 (s, 3H), 3.16 (dd, 1H), 2.89 (t, 2H), 2.80-2.69 (m, 3H), 1.92 (s, 3H), 1.91 (m, 1H), 1.64 (m, 1H), 1.26 (br m, 6H), 0.87 (t, 3H); ^{13}C NMR (100 MHz, $CDCl_3$) δ (ppm): 207.09, 164.03, 162.52, 152.31, 150.83, 150.77, 150.64, 140.96, 140.21, 139.98, 137.73, 126.16, 122.52, 122.19, 120.44, 112.90, 110.25, 55.93, 46.13, 44.26, 32.56, 31.21, 29.43, 25.86, 22.39, 14.03, 13.91; ESI-MS (*m/z*): 542.2 $[M+H]^+$, 564.2 $[M+Na]^+$; HRMS (*m/z*): calcd for $C_{28}H_{32}ClN_3O_6$ $[M+H]^+$ 542.1980, found: 542.2047.

5.1.3.4. 2-Methoxy-4-(5-(5-methyl-2,4-dioxo-3,4-dihydropyrimidin-1(2H)-yl)-3-oxodecyl)-phenyl 4-methoxybenzoate (2d)

Yield: 76%; FT-IR (Neat, cm^{-1}): 3431, 3019, 1654, 1215, 757; ^1H NMR (400 MHz, $CDCl_3$) δ (ppm): 8.16 (d, *J* = 8.89 Hz, 2H), 7.87 (d, *J* = 8.68 Hz, 2H), 7.12 (s, 1H), 7.03 (d, *J* = 8.05 Hz, 1H), 6.98 (d, *J* = 8.89 Hz, 2H), 6.94 (d, *J* = 8.68 Hz, 2H), 6.79 (d, *J* = 1.95 Hz, 1H), 6.75 (dd, *J* = 8.05 Hz, 1.86 Hz, 1H), 4.50 (br s, 1H), 3.90 (s, 3H), 3.85 (s, 3H), 3.77 (s, 3H), 2.87 (t, 2H), 2.77-2.73 (m, 3H), 1.98 (s, 3H), 1.29 (br s, 6H), 0.90 (t, 3H); ^{13}C NMR (100 MHz, $CDCl_3$) δ (ppm): 207.26, 167.87, 165.11, 164.60, 163.83, 162.75, 151.31, 149.92, 139.43, 138.45, 132.95, 132.38, 124.37, 122.95, 121.75, 120.32, 114.51, 113.79, 112.77, 110.43, 55.92, 55.64, 55.50, 46.12, 44.47, 32.49, 31.58, 31.20, 29.54, 25.95, 22.65, 22.43, 14.11; ESI-MS $C_{30}H_{36}N_2O_7$, *m/z* 671.2 $[M+H]^+$, 693.3 $[M+Na]^+$ 716.1 $[M+2Na]^+$

5.1.3.5. 4-(5-(3-(Furan-2-carbonyl)-5-methyl-2,4-dioxo-3,4-dihydropyrimidin-1(2H)-yl)-3-oxodecyl)-2-methoxyphenyl furan-2-carboxylate (2e)

Yield: 72%; FT-IR (Neat, cm^{-1}): 3444, 1647, 1215, 756; ^1H NMR (400 MHz, $CDCl_3$) δ (ppm): 7.68 (dd, 1H), 7.58 (br s, 1H), 7.09 (s, 1H), 7.04 (d, *J* = 8.12 Hz, 1H), 6.81 (d, *J* = 1.90 Hz, 1H), 6.76 (dd, *J* = 8.12 Hz, 2.09 Hz, 1H), 6.60 (m, 2H), 4.49 (m, 1H), 3.80 (s, 3H), 3.17 (dd, 1H), 2.88 (t, 2H), 2.82-2.71 (m, 3H), 1.97 (s, 3H), 1.29 (br m, 6H), 0.89 (t, 3H); ^{13}C NMR (100 MHz, $CDCl_3$) δ (ppm): 207.20, 162.47, 157.57, 156.60, 151.16, 149.69, 148.54, 147.44, 147.03, 143.89, 139.88, 137.48, 122.82,

122.48, 120.33, 119.45, 113.48, 112.79, 112.15, 110.40, 55.92, 46.02, 44.43, 32.44, 31.18, 29.47, 25.87, 22.41, 13.91; ESI-MS (*m/z*): 591.2 $[M+H]^+$, 613.2 $[M+Na]^+$, 636.1 $[M+2Na]^+$; HRMS (*m/z*): calcd for $C_{27}H_{32}N_2O_7$ $[M+H]^+$ 591.2264, found: 591.2335.

5.1.3.6. (E)-2-Methoxy-4-(5-(5-methyl-2,4-dioxo-3,4-dihydropyrimidin-1(2H)-yl)-3-oxodecyl)phenyl 3-(4-fluorophenyl)-acrylate (2f)

Yield: 70%; FT-IR (Neat, cm^{-1}): 3441, 3019, 1638, 1215, 757; ^1H NMR (400 MHz, $CDCl_3$) δ (ppm): 8.89 (s, 1H), 7.85 (d, *J* = 8.46 Hz, 1H), 7.60 (d, *J* = 8.77 Hz, 1H), 7.58 (d, *J* = 7.57 Hz, 1H), 7.12 (t, 2H), 7.01 (s, 1H), 7.00 (d, *J* = 9.37 Hz, 1H), 6.81 (s, 1H), 6.75 (dd, *J* = 8.12 Hz, 1H), 6.60 (d, *J* = 15.82 Hz, 1H), 4.50 (m, 1H), 3.83 (s, 3H), 3.16 (dd, 1H), 2.89 (t, 2H), 2.81-2.69 (m, 3H), 1.94 (s, 3H), 1.60 (m, 2H), 1.28 (br s, 6H), 0.89 (t, 3H); ^{13}C NMR (100 MHz, $CDCl_3$) δ (ppm): 207.20, 165.36, 165.07, 164.13, 162.86, 151.06, 150.72, 145.27, 145.06, 140.04, 139.58, 138.08, 130.54, 130.27, 130.18, 122.77, 120.38, 117.37, 116.78, 116.24, 116.02, 112.81, 110.24, 56.54, 55.91, 46.15, 44.31, 32.58, 31.22, 29.69, 29.44, 25.87, 22.40, 13.92, 12.43; ESI-MS $C_{31}H_{35}FN_2O_6$, *m/z* 551.3 $[M+H]^+$, 573.3$[M+Na]^+$.

5.1.3.7. 2-Methoxy-4-(5-(4-methylpyridin-2-ylamino)-3-oxodecyl)phenyl-6-chloro nicotinate (6a)

Yield: 78%; FT-IR (Neat, cm^{-1}): 3433, 3019, 1627, 1215, 757; ^1H NMR (400 MHz, $CDCl_3$) δ (ppm): 8.59 (dd, *J* = 4.81 Hz, 1.98 Hz, 1H), 8.41 (dd, *J* = 7.77 Hz, 1.98 Hz, 1H), 8.17 (d, 1H), 7.41 (d, *J* = 8.03 Hz, 1H), 7.40 (d, *J* = 8.03 Hz, 1H), 7.09 (d, *J* = 7.71 Hz, 1H), 7.02 (m, 2H), 6.90-6.84 (m, 3H), 5.06 (m, 1H), 3.84 (s, 3H), 3.18 (dd, 1H), 2.96-2.79 (m, 5H), 2.23 (s, 3H), 1.80 (m, 1H), 1.28 (m, 7H), 0.87 (t, 3H); ^{13}C NMR (100 MHz, $CDCl_3$) δ (ppm): 207.76, 162.48, 152.28, 150.79, 150.63, 149.63, 149.38, 148.40, 147.10, 140.88, 140.80, 137.90, 137.64, 126.26, 123.88, 123.67, 122.45, 122.15, 121.67, 120.51, 112.92, 55.95, 46.52, 44.44 32.92, 31.49, 29.68, 29.57, 26.22, 22.48, 20.82, 13.99; HRMS (*m/z*): calcd for $C_{29}H_{34}ClN_3O_4$ $[M+H]^+$ 524.2238, found: 524.2308.

5.2. Pharmacology

5.2.1. BmTMK Inhibition Assay

Compounds were screened against recombinant BmTMK using a coupled assay with pyruvate kinase and lactate dehydrogenase [26]. The reaction mixture (1.0) ml contained 50 mM Tris/HCl (pH 7.4), 50 mM KCl, 1.0 mM phosphoenolpyruvate, 1.0 mM $MgCl_2$, 0.05 mM NADH, 2 U pyruvate kinase, 2 U lactate dehydrogenase 0.05 mM dTMP and 0.5 mM ATP whereas the concentrations of analogues varied between 0.005 and 0.25 mM. The reaction was initiated by the addition of the BmTMK. Activity was measured spectrophotometrically by following the change in absorption at 340 nm due to the oxidation of NADH. The assay was carried out using dTMP as substrate (Km = 17 μM). Control spectrophotometric assays were performed to verify that the compounds were inhibitors of BmTMK and not of the coupling enzymes, by using ADP as substrate and the two coupling enzymes pyruvate kinase and lactate dehydrogenase, but no BmTMK or TMP [25]. For each inhibitor, at least three independent experiments with duplicate reactions were performed.

Percentage inhibition was determined at different concentrations of inhibitors against BmTMK and percentage inhibition data were fit to the standard IC_{50} equation to calculate IC_{50}. K_i's were calculated from the Cheng−Prusoff relationship for competitive inhibitors (Ki = IC_{50}/(1 + ([S]/ Km)) where [S] and Km are the dTMP concentration and Michaelis constant for dTMP, respectively. Mode of inhibition of all compounds were also tested by measuring the initial velocity of the reaction at a fixed saturating concentration of ATP and different concentrations of dTMP, both in the absence and presence of inhibitors [27]

5.2.2. Molecular Docking studies of BmTMK inhibitors

All docking studies were carried out using Autodock4.2 [28]. Optimized 3D conformations of compounds were generated using Marvin sketch [29]. We used homology model of BmTMK [9] and crystal structure of HsTMK (PDB-ID: 1E2D) [30] as receptors. During docking, compounds were treated flexible and grid was constructed, enclosing the TMP binding pocket [30]. Lamarckian genetic algorithm [31] was used to generate 30 conformations of each compound. For visualization and image generation UCSFChimera1.6 [32] was used.

Acknowledgments

The authors are grateful to the Director, CSIR-CDRI, Lucknow, India, for constant encouragement in drug development program, SAIF for NMR, IR, and Mass spectral data. V. K. Singh is thankful to UGC, New Delhi, P. K. Doharey to CSIR, New Delhi and Vikash Kumar to DBT, New Delhi for financial support.

Supplementary data

Supplementary data associated with this article can be found, in the online version, at www.sciencedirect.com.

References

[1] (a) Behm, C. A.; Bendig, M. M.; McCarter, J. P.; Sluder, A. E. RNAi-based discovery and validation of new drug targets in filarial nematodes. *Trends Parasitol.* **2005,** 21, 97. (b) Sashidhara, K. V.; Rao, K. B.; Kushwaha, V.; Modukuri, R. K.; Verma, R.; Murti, P. K. Synthesis and antifilarial activity of chalcone-thiazole derivatives against a human lymphatic filarial parasite, *Brugia malayi*. *Eur. J. Med. Chem.* **2014**, 81, 473. (c) Carreño Otero, A. L.; Vargas Méndez, L. Y.; Jonny, E. D. L.; Kouznetsov, V. V. Design, synthesis, acetylcholinesterase inhibition and larvicidal activity of girgensohnine analogs on *Aedes aegypti*, vector of dengue fever. *Eur. J. Med. Chem.* **2014**, 78, 392.

[2] Gaur, R. L.; Sahoo, M. K.; Dixit, S.; Fatma, N.; Rastog, S.; Kulshreshtha, D. K.; Chatterjee, R. K.; Murthy, P.K. Antifilarial activity of *Caesalpinia bonducella* against experimental filarial infections. *Indian J. Med. Res.* **2008**, 128, 65.

[3] Osei-Atweneboana, M.Y.; Eng, J.K.; Boakye, D.A.; Gyapong, J.O.; Prichard, P.K. Prevalence and intensity of Onchocerca volvulus infection and efficacy of ivermectin in endemic communities in Ghana: a two-phase epidemiological study. *Lancet* **2007**, 369, 2021.

[4] Schwab, A.E.; Churcher, T.S.; Schwab, A.J.; Basanez, M.G.; Prichard, R.K. An analysis of the population genetics of potential multi-drug resistance in *Wuchereria bancrofti* due to combination chemotherapy. *Parasitology* **2007**, 134, 1025.

[5] Ginger, C. D.; Enzyme Inhibitors in the Chemotherapy of Filariasis, Report of a Scientific Working Group on the Biochemistry of Filarial and Allied Parasites WHO/OCP/OCT/83.1. World Health Organization, Geneva, **1983**.

[6] Anderson, E. Nucleoside and nucleotide kinases. In the Enzymes, (Boyer, P. D., ed) 3rd Ed.; Academic Press: New York, **1973**; Vol. 8, pp 49-96.

[7] Kandeel, M.; Kato, A.; Kitamura, Y.; Kitade, Y. Thymidylate kinase: the lost chemotherapeutic target. *Nucleic Acids Symp. Ser.(Oxford)* **2009**, 53, 283.

[8] Van Calenbergh, S. Structure-aided design of inhibitors of Mycobacterium tuberculosis thymidylate kinase. *Verh. K. Acad. Geneeskd. Belg.* **2006**, 68, 223.

[9] Doharey, P. K.; Suthar, M.K.; Verma, A.; Kumar, V.; Yadav, S.; Balaramnavar, V. M.; Rathaur, S.; Saxena, A. K.; Siddiqi, M. I.; Saxena, J. K. Molecular cloning and characterization of Brugia malayi thymidylate kinase. *Acta Trop.* **2014**, 133C, 83.

[10] (a) Butt, M. S.; Sultan, M. T. Ginger and its health claims: molecular aspects. Crit. Rev. Food Sc. Nutr. 2011, 51, 383; (b) Ali, B. H.; Blunden, G.; Tanira, M. O.; Nemmar, A. Some phytochemical, pharmacological and toxicological properties of ginger (*Zingiber officinale* Roscoe): a review of recent research. *Food Chem. Toxicol.* **2008**, 46, 409.

[11] Lee, H. S.; Seo, E. Y.; Kang, N. E.; Kim, W. K. [6]-Gingerol inhibits metastasis of MDA-MB-231 human breast cancer cells. *J. Nutr. Biochem.* **2008**, 19, 313.

[12] Rhode, J.; Fogoros, S.; Zick, S.; Wahl, H.; Griffith, K. A.; Huang, J.; Liu, J. R. Ginger inhibits cell growth and modulates angiogenic factors in ovarian cancer cells. *BMC Complement. Altern Med.* **2007**, 7, 44.

[13] Kiuchi, F.; Iwakami, S.; Shibuya, M.; Hanaoka, F.; Sankawa, U. Inhibition of prostaglandin and leukotriene biosynthesis by gingerols and diarylheptanoids. *Chem. Pharm. Bull.* **1992**, 40, 387.

[14] Yasuka Isa, Y.; Miyakawa, Y.; Yanagisawa, M.; Goto, T.; Kang, M.-S.; Kawada, T.; Morimitsu, Y.; Kubota, K.; Tsuda, T. 6-Shogaol and 6-gingerol, the pungent of ginger, inhibit TNF-alpha mediated down regulation of adiponectin expression via different mechanisms in 3T3-L1 adipocytes. *Biochem. Biophys. Res. Commun.* **2008**, 373, 429.

[15] (a) Iwasaki, Y.; Morita, A.; Iwasawa, T.; Kobata, K.; Sekiwa, Y.; Morimitsu, Y.; Kubota, K.; Watanabe, T. A nonpungent component of steamed ginger--[10]-shogaol--increases adrenaline secretion via the activation of TRPV1. *Nutr. Neurosci.* **2006**, 9, 169; (b) Dedov, V. N.; Tran, V. H.; Duke, C. C.; Connor, M.; Christie, M. J.; Mandadi, S.; Roufogalis, B. D. Gingerols: a novel class of vanilloid receptor (VR1) agonists. Br. *J. Pharmacol.* **2002**, 137, 793.

[16] Bandell, M.; Story, G. M.; Hwang, S. W.; Viswanath, V.; Eid, S. R.; Petrus, M. J.; Earley, T. J.; Patapoutian, A. Noxious cold ion channel TRPA1 is activated by pungent compounds and bradykinin. *Neuron* **2004**, 41, 849.

[17] (a) Li, M.; Yu, Y.; Yang, J. Structural biology of TRP channels. *Adv. Exp. Med. Biol.* **2011**, 704, 1; (b) Vennekens, R.; Owsianik, G.; Nilius, B. Vanilloid transient receptor potential cation channels: an overview. *Curr. Pharm. Des.* **2008**, 14, 18; (c) Appendino, G.; Minassi, A.; Pagani, A.; Ech-Chahad, A. The role of natural products in the ligand

deorphanization of TRP channels. *Curr. Pharm. Des.* **2008**, 14, 2; (d) Venkatachalam, K.; Montell, C. TRP channels. *Annu. Rev. Biochem.* **2007**, 76, 387; (e) Gharat, L.; Szallasi, A. Medicinal chemistry of the vanilloid (Capsaicin) TRPV1 receptor: current knowledge and future perspectives. *Drug Develop. Res.* **2007**, 68, 477; (f) Minke, B. TRP channels and Ca2+ signalling. *Cell Calcium* **2006**, 40, 261.

[18] Andrade, C. H.; Pasqualoto, K. F.; Ferreira, E. I.; Hopfinger, A. J. 3D-Pharmacophore mapping of thymidine-based inhibitors of TMPK as potential antituberculosis agents. *J. Comput.-Aided Mol. Des.* **2010**, 24, 157.

[19] Cui, H.; Ruiz-Perez, L. M.; Gonzalez-Pacanowska, D.; Gilbert, I. H. Potential application of thymidylate kinase in nucleoside analogue activation in *Plasmodium falciparum*. *Bioorg. Med. Chem.* **2010**, 18, 7302.

[20] Familiar, O.; Munier-Lehmann, H.; Ainsa, J. A.; Camarasa, M. J.; Perez-Perez, M. J. Design, synthesis and inhibitory activity against *Mycobacterium tuberculosis* thymidine monophosphate kinase of acyclic nucleoside analogues with a distal imidazoquinolinone. *Eur. J. Med. Chem.* **2010**, 45, 5910.

[21] Frecer, V.; Seneci, P.; Miertus, S. Computer-assisted combinatorial design of bicyclic thymidine analogs as inhibitors of *Mycobacterium tuberculosis* thymidine monophosphate kinase. *J. Comput.-Aided Mol. Des.* **2011**, 25, 31.

[22] Andrade, C. H.; Pasqualoto, K. F.; Ferreira, E. I.; Hopfinger, A. J. Rational design and 3D-pharmacophore mapping of 5'-thiourea-substituted alpha-thymidine analogues as mycobacterial TMPK inhibitors. *J. Chem. Inf. Model.* **2009**, 49, 1070.

[23] Douguet, D.; Munier-Lehmann, H.; Labesse, G.; Pochet, S. LEA3D: a computer-aided ligand design for structure-based drug design. *J. Med. Chem.* **2005**, 48, 2457.

[24] Van Daele, I.; Munier-Lehmann, H.; Froeyen, M.; Balzarini, J.; Van Calenbergh, S. Rational design of 5'-thiourea-substituted alpha-thymidine analogues as thymidine monophosphate kinase inhibitors capable of inhibiting mycobacterial growth. *J. Med. Chem.* **2007**, 50, 5281.

[25] Whittingham, J. L.; Carrero-Lerida, J.; Brannigan, J. A.; Ruiz-Perez, L. M.; Silva, A. P.; Fogg, M, J.; Wilkinson, A. J.; Gilbert, I. H.; Wilson, K. S.; González-Pacanowska, D. Structural basis for the efficient phosphorylation of AZT-MP (3'-azido-3'-deoxythymidine monophosphate) and dGMP by Plasmodium falciparum type I thymidylate kinase. *Biochem J.* **2010**, 428, 499.

[26] Blondin, C.; Serina, L.; Weismuller, L.; Gilles, A.M.; Barzu, O. "Improved Spectrophotometric Assay of Nucleoside Monophosphate Kinase Activity Using the Pyruvate Kinase/Lactate Dehydrogenase Coupling System. *Anal. Biochem.* **1994**, 220, 219

[27] Segel, I. H., 1993, Enzyme Kinetics, Wiley-Interscience Publications, John Wiley, New York.

[28] Morris, G. M.; Huey, R.; Lindstrom, W.; Sanner, M. F.; Belew, R. K.; Goodsell, D. S.; Olson, A. J. AutoDock4 and AutoDockTools4: Automated docking with selective receptor flexibility. *J Comput Chem.* **2009**, 30, 2785.

[29] http://www.chemaxon.com/products/marvin/marvinsketch/

[30] Ostermann, N.; Schlichting, I.; Brundiers, R.; Konrad, M.; Reinstein, J.; Veit, T.; Goody, R. S.; Lavie, A. Insights into the phosphoryltransfer mechanism of human thymidylate kinase gained from crystal structures of enzyme complexes along the reaction coordinate. *Structure.* **2000**, 8, 629.

[31] Morris, G. M.; Goodsell, D. S.; Halliday, R. S.; Huey, R.; Hart, W. E.; Belew, R. K.; Olson, A. J. Automated docking using a Lamarckian genetic algorithm and an empirical binding free energy function. *J Comput Chem*. **1998**, 19, 1639.

[32] Pettersen, E. F.; Goddard, T. D.; Huang, C. C.; Couch, G. S.; Greenblatt, D. M.; Meng, E. C.; Ferrin, T. E. UCSF Chimera-a visualization system for exploratory research and analysis. *J Comput Chem.* **2004**; 25, 1605.

Captions to illustrations:

Scheme 1: Synthesis of aza-Michael derivatives of [6]-Shogaol

Scheme 2: Synthesis of 2-aminopicoline based [6]-shogaol derivatives

Table 1: Inhibitory activity of compounds against recombinant BmTMK

Figure 1: Conversion of dTMP into dTDP

Figure 2: Known TMK inhibitors

Figure 3: Flow chart for the isolation of [6]-Shogaol and [6]-Gingerol

Figure 4: Co-crystallized conformation of TMP (orange) bound to Human Thymidylate kinase (a), Predicted binding pose of [6]-shogaol:**1** (b), **2** (c), **3** (d), **4** (e), and **5** (f) in TMP binding site of *Brugia malayi* thymidylate kinase. Hydrogen bonds are shown in black dotted line. Protein is shown in mixed representation (ribbon and stick). Only important residues involved in interaction are shown.

Scheme 1: Synthesis of aza-Michael derivatives of [6]-Shogaol

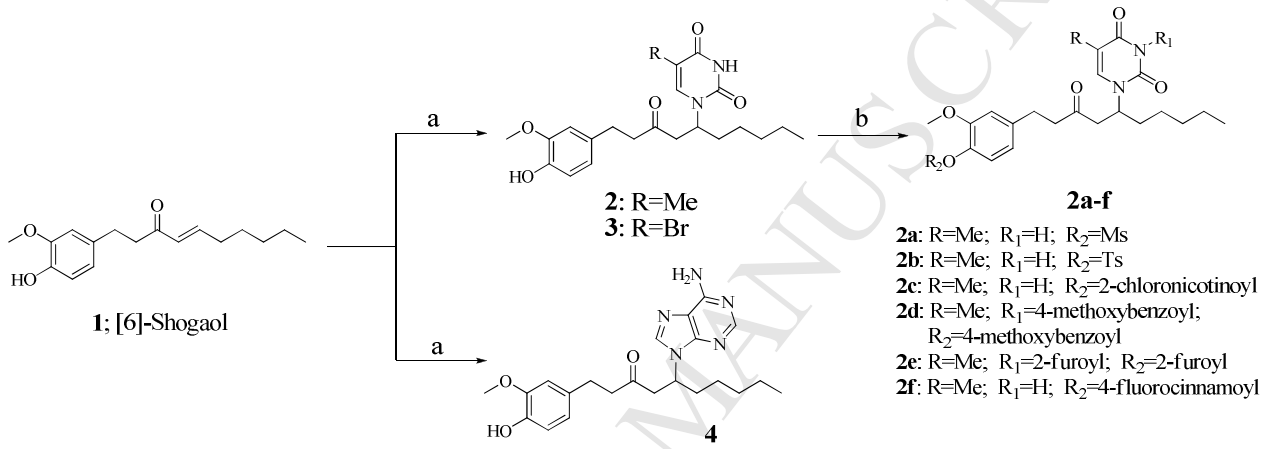

Reagents and conditions: (a) thymine (for **2**), 5-bromouracil (for **3**), adenine (for **4**), TEA, DMSO, rt, 12hr; (b) Appropriate acid chloride, dry DCM, TEA, 0^{o}C-rt, 2hr

Scheme 2: Synthesis of 2-aminopicoline based [6]-shogaol derivatives

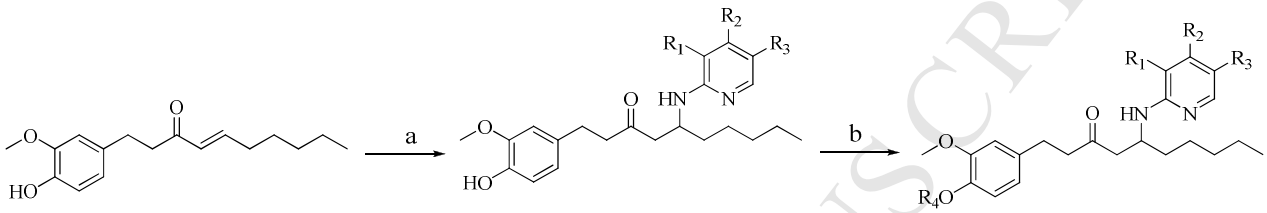

[6]-Shogaol: **1**

5: R_1=Me; R_2=H; R_3=H
6: R_1=H; R_2=Me; R_3=H
7: R_1=H; R_2=H; R_3=Me

6a: R_1=H; R_2=Me; R_3=H; R_4=2-chloronicotinoyl

Reagents and conditions: (a) appropriate 2-aminopicoline, TEA, DMSO, rt, 12hr; (b) Acid chloride, dry DCM, TEA, 0 ^{o}C-rt, 2hr

Table 1: Inhibitory activity of compounds against recombinant BmTMK

Entry	Compound	*Ki* value (μM)	Entry	Compound	*Ki* value (μM)
	dTMP	17.00[a]			
1	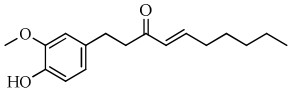 **1:** [6]-Shogaol	10.78± 0.55	8	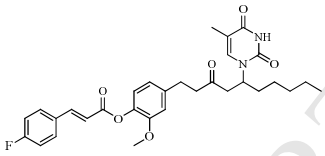 **2f**	44.41±2.43
2	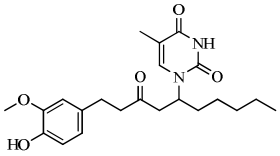 **2**	6.57±0.42	9	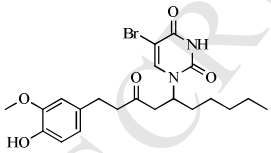 **3**	8.32± 0.39
3	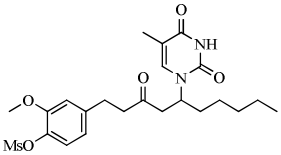 **2a**	66.12±3.40	10	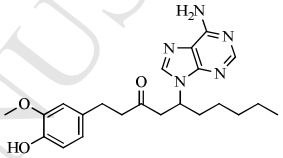 **4**	9.01±0.50
4	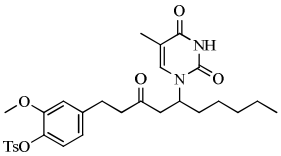 **2b**	45.68±2.50	11	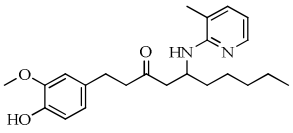 **5**	11.06± 0.54
5	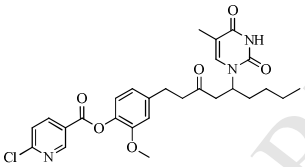 **2c**	No inhibition	12	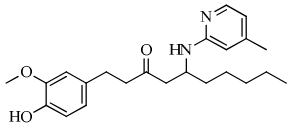 **6**	21.57±1.35
6	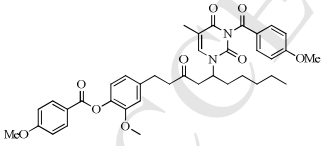 **2d**	20.05±1.03	13	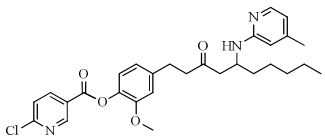 **6a**	30.45±1.72
7	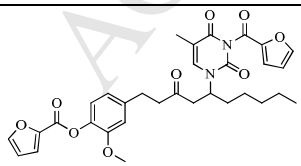 **2e**	20.30±1.02	14	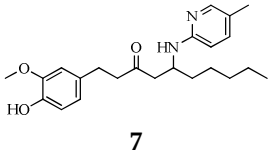 **7**	40.60±1.86

[a]Km value for dTMP

Ki values ± SEM given are representative of three independent experiments.

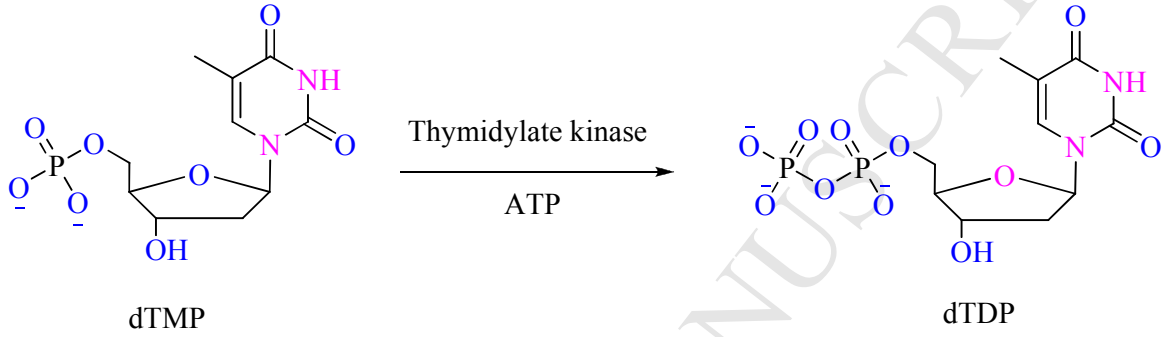

Figure 1: Conversion of dTMP into dTDP

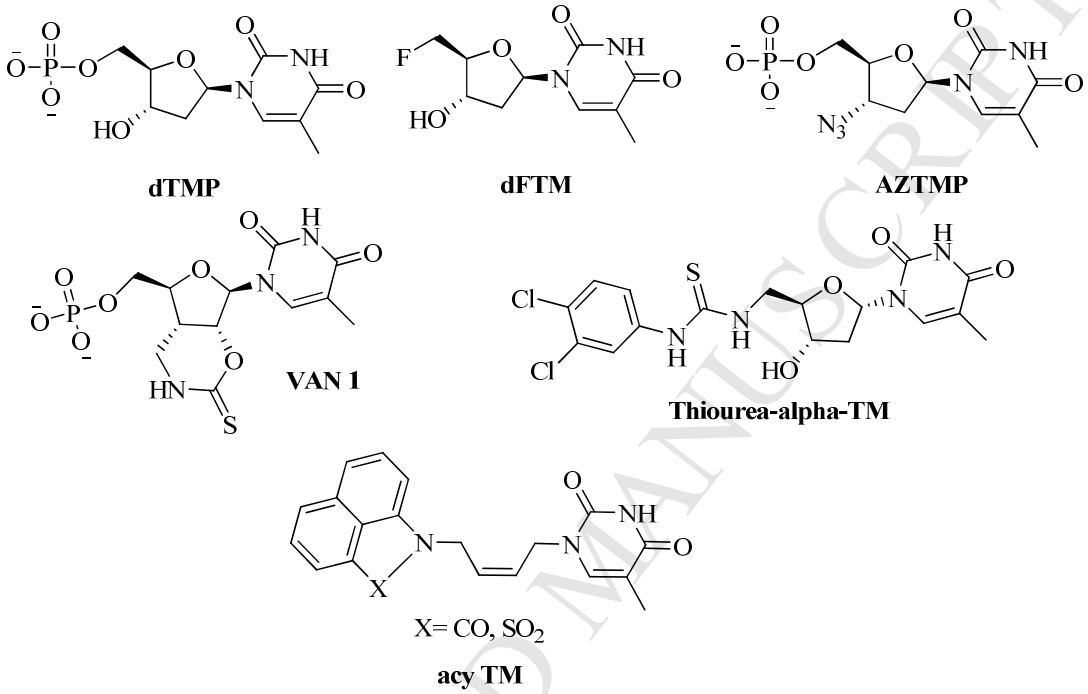

Figure 2: Known TMK inhibitors

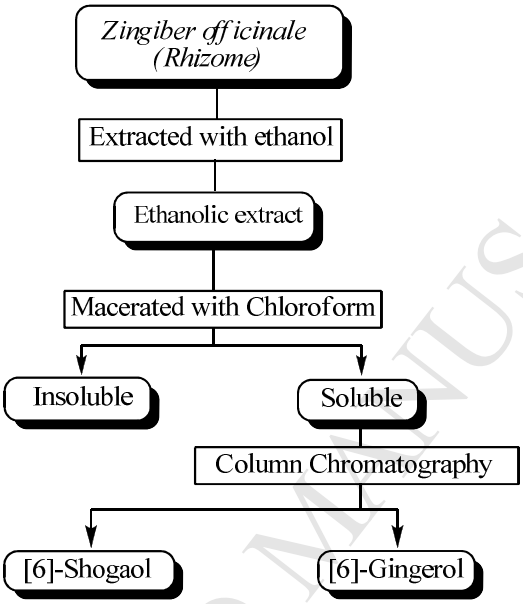

Figure 3: Flow chart for the isolation of [6]-Shogaol and [6]-Gingerol

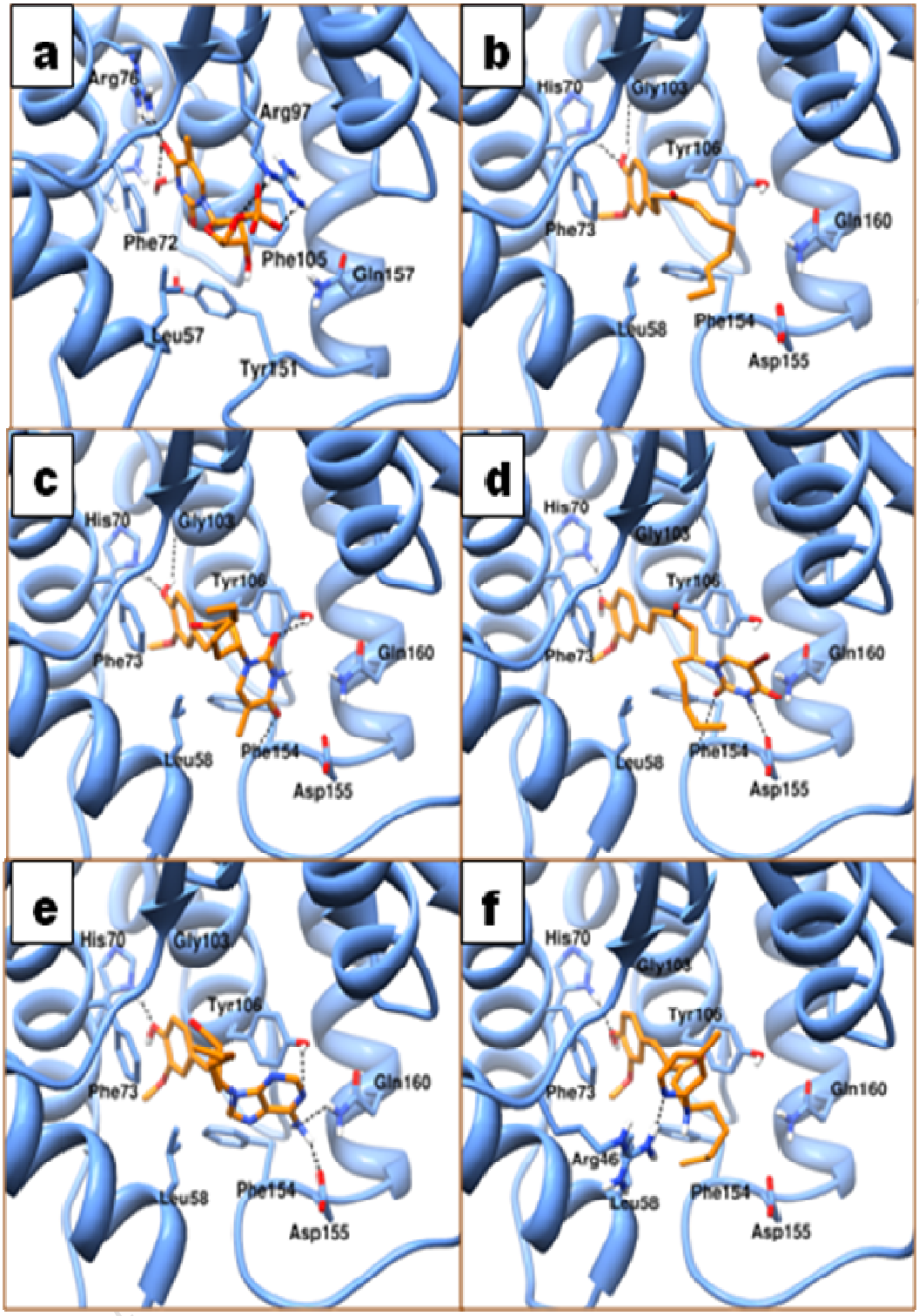

Figure 4: Co-crystallized conformation of TMP (orange) bound to Human Thymidylate kinase (a), Predicted binding pose of [6]-shogaol:**1** (b), **2** (c), **3** (d), **4** (e), and **5** (f) in TMP binding site of *Brugia malayi* thymidylate kinase. Hydrogen bonds are shown in black dotted line. Protein is shown in mixed representation (ribbon and stick). Only important residues involved in interaction are shown.

Research Highlights

- Twelve novel derivatives of [6]-shogaol have been synthesized
- 5 compounds showed potential *Brugia malayi* thymidylatekinase inhibition activity
- Binding conformation of parent compound and its derivatives were consistent with the TMP bound conformation.

Supporting Information

Synthesis, molecular docking and *Brugia malayi* thymidylate kinase (BmTMK) enzyme inhibition study of novel derivatives of [6]-shogaol

Vinay Kr. Singh[a], Pawan K. Doharey[b], Vikash Kumar[c], J. K. Saxena[b], M. I. Siddiqi[c], Sushma Rathaur[d], Narender Tadigoppula[a]*

[a]*Medicinal and Process Chemistry Division, CSIR-Central Drug Research Institute, (CSIR-CDRI), BS-10/1, Sector 10, Jankipuram extension, Sitapur Road, P.O. Box 173, Lucknow 226031, India*
[b]*Biochemistry Division, CSIR-Central Drug Research Institute, (CSIR-CDRI), BS-10/1, Sector 10, Jankipuram extension, Sitapur Road, P.O. Box 173, Lucknow 226031, India*
[c]*Molecular & Structural Biology Division, CSIR-Central Drug Research Institute, (CSIR-CDRI), BS-10/1, Sector 10, Jankipuram extension, Sitapur Road, P.O. Box 173, Lucknow 226031, India*
[d]*Department of Biochemistry, Banaras Hindu University, Varanasi 221005, India*

Email Address: t_narendra@cdri.res.in

Table of Contents

General Methods:

All reagents were procured from commercial suppliers and were used without further purification. Chromatography was carried on silica gel (60-120 and 100-200 mesh). All reactions were monitored by TLC; silica gel plates with fluorescence F254 were used. The ^{1}H NMR and ^{13}C NMR spectra were determined on 400MHz and 100MHz, respectively, using $CDCl_3$ and CD_3OD as solvents and TMS as internal standard. All chemical shifts were given in ppm. Multiplicity (s = singlet, brs = broad singlet, d = doublet, brd = broad doublet, dd = double doublet, t = triplet, q = quartet, m = multiplet).

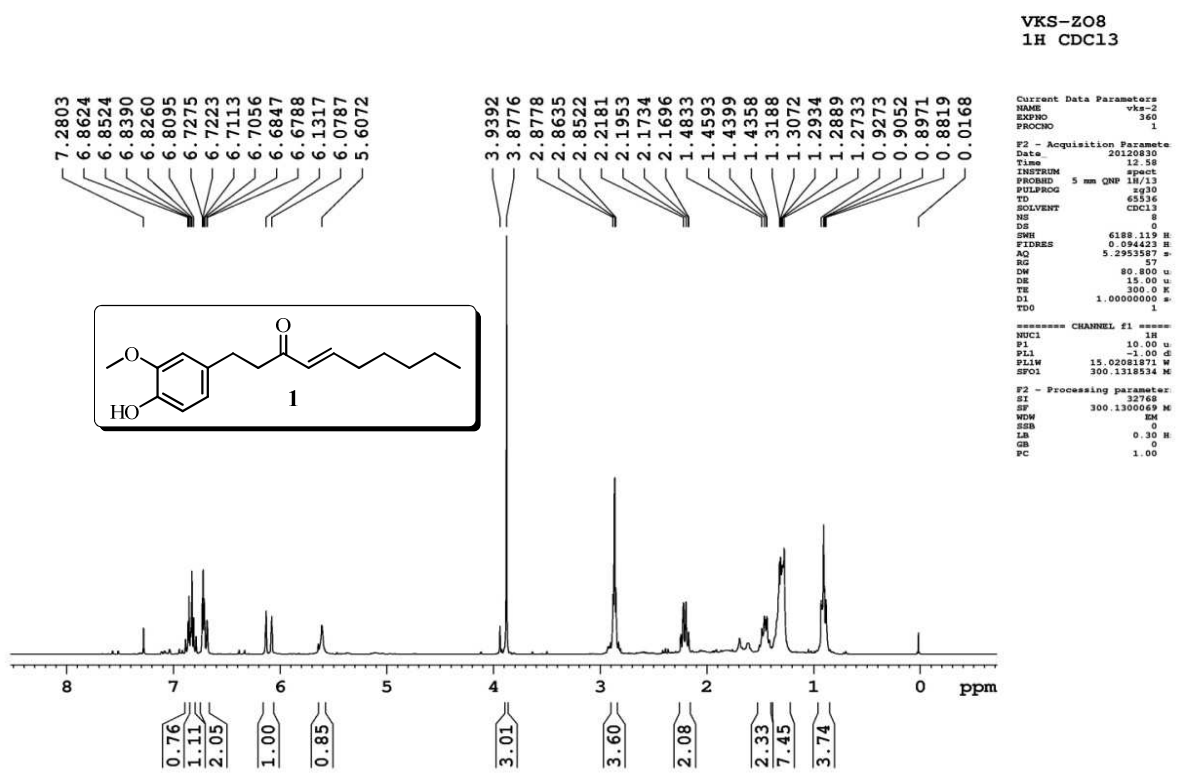

Figure 1. ^{1}**H NMR spectrum of 1 (300 MHz, CDCl$_3$)**

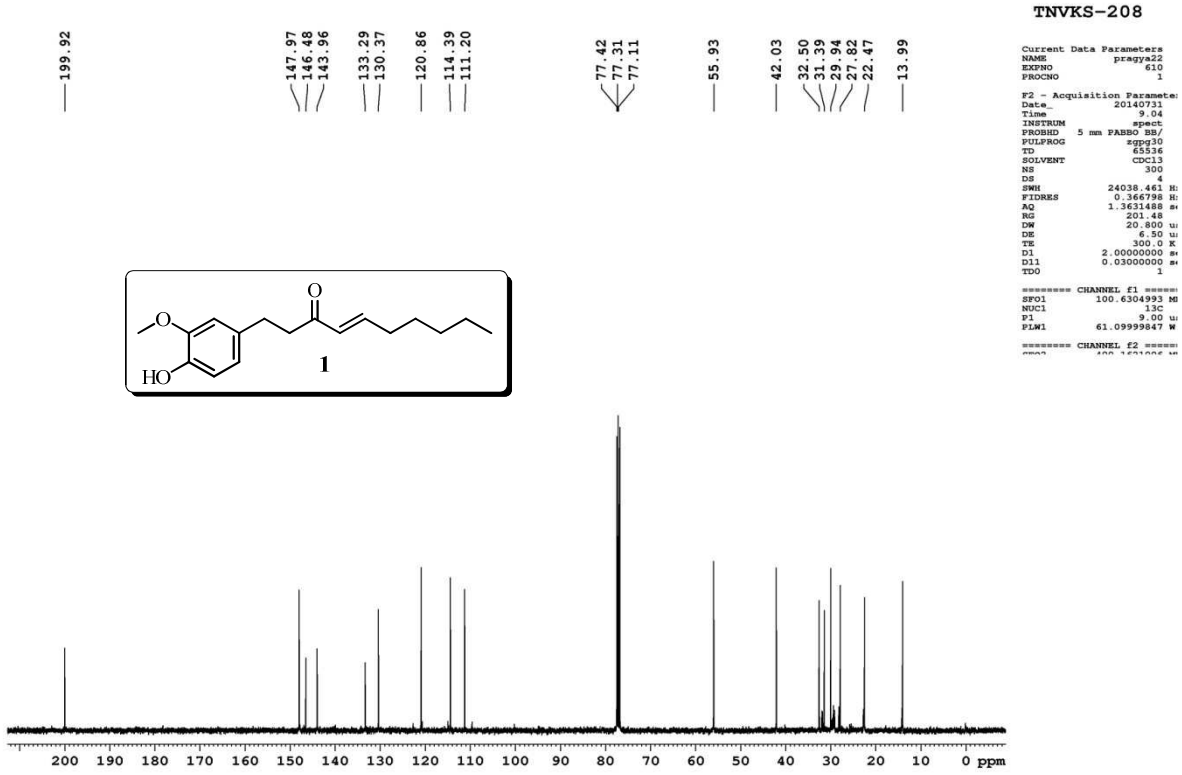

Figure 2. ^{13}**C NMR spectrum of 1 (100 MHz, CDCl$_3$)**

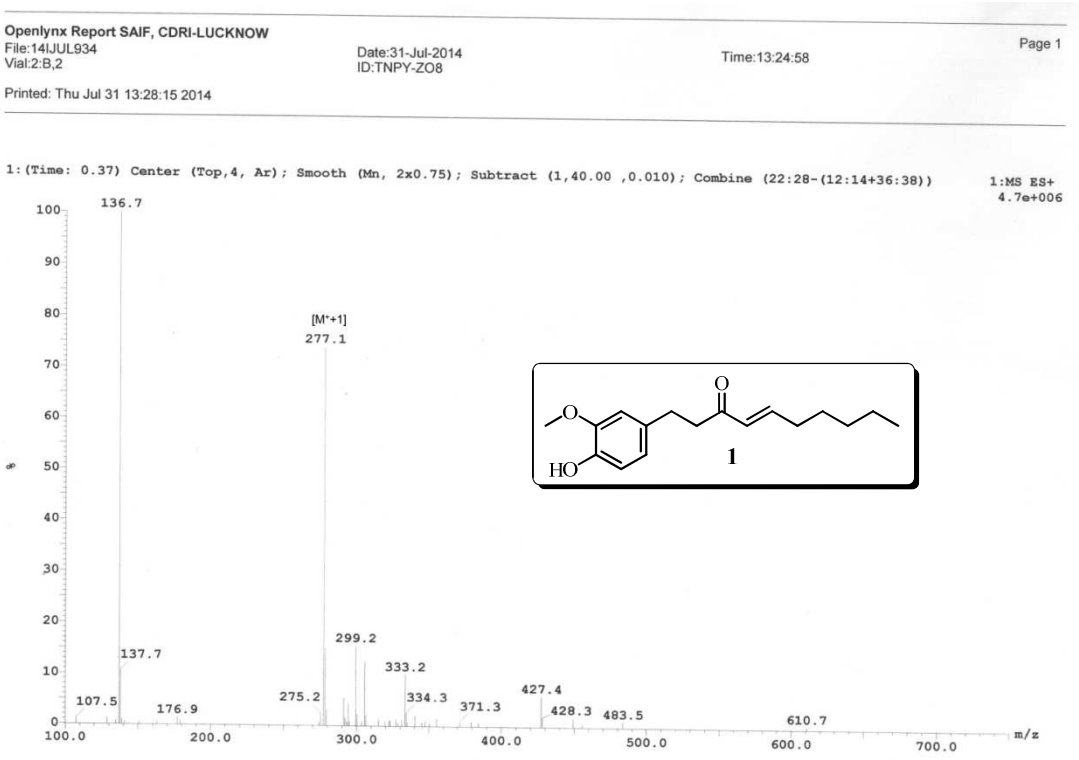

Figure 3. MS (ESI) of 1

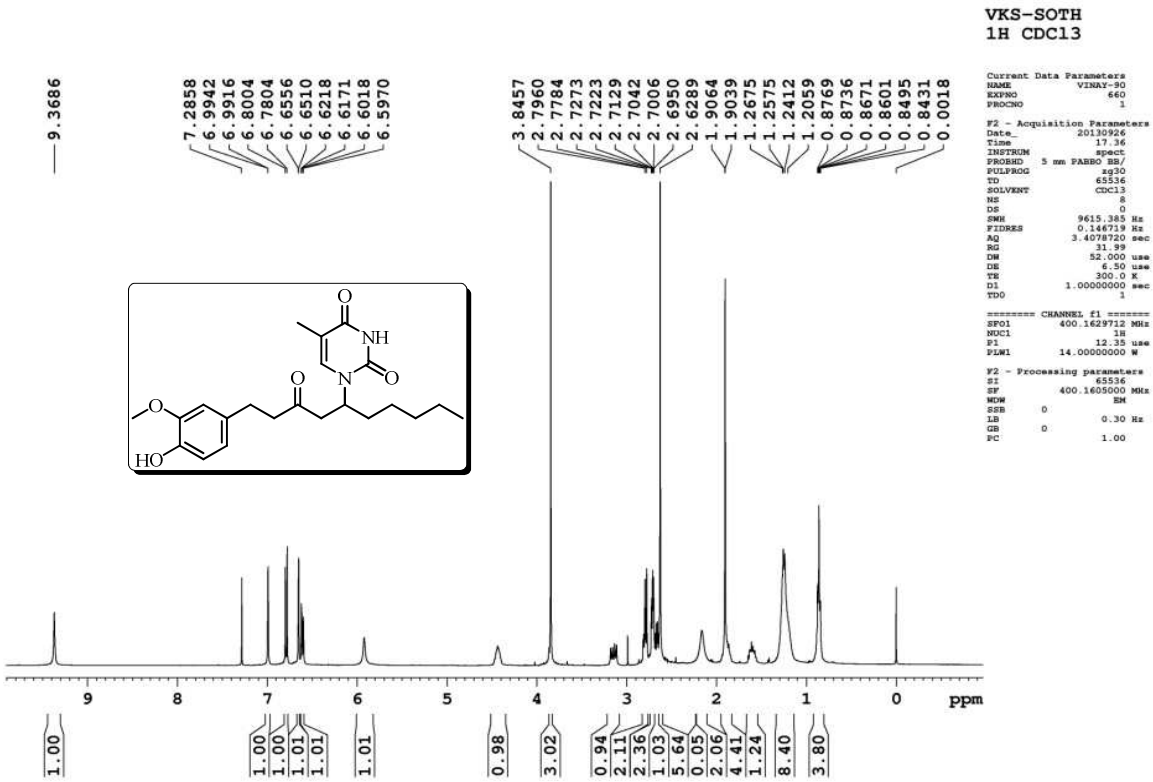

Figure 4. ^{1}H NMR spectrum of 2 (400 MHz, $CDCl_3$)

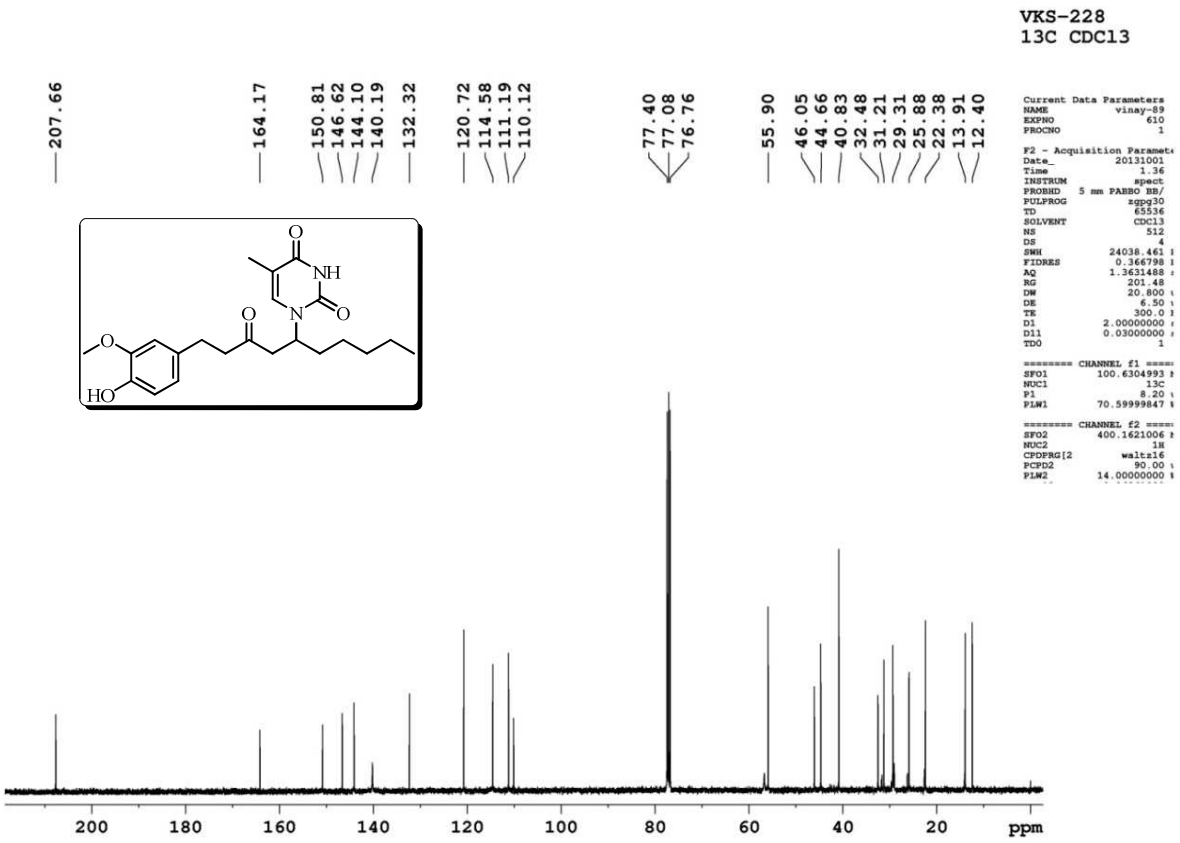

Figure 5. ^{13}**C NMR spectrum of 2 (100 MHz, $CDCl_3$)**

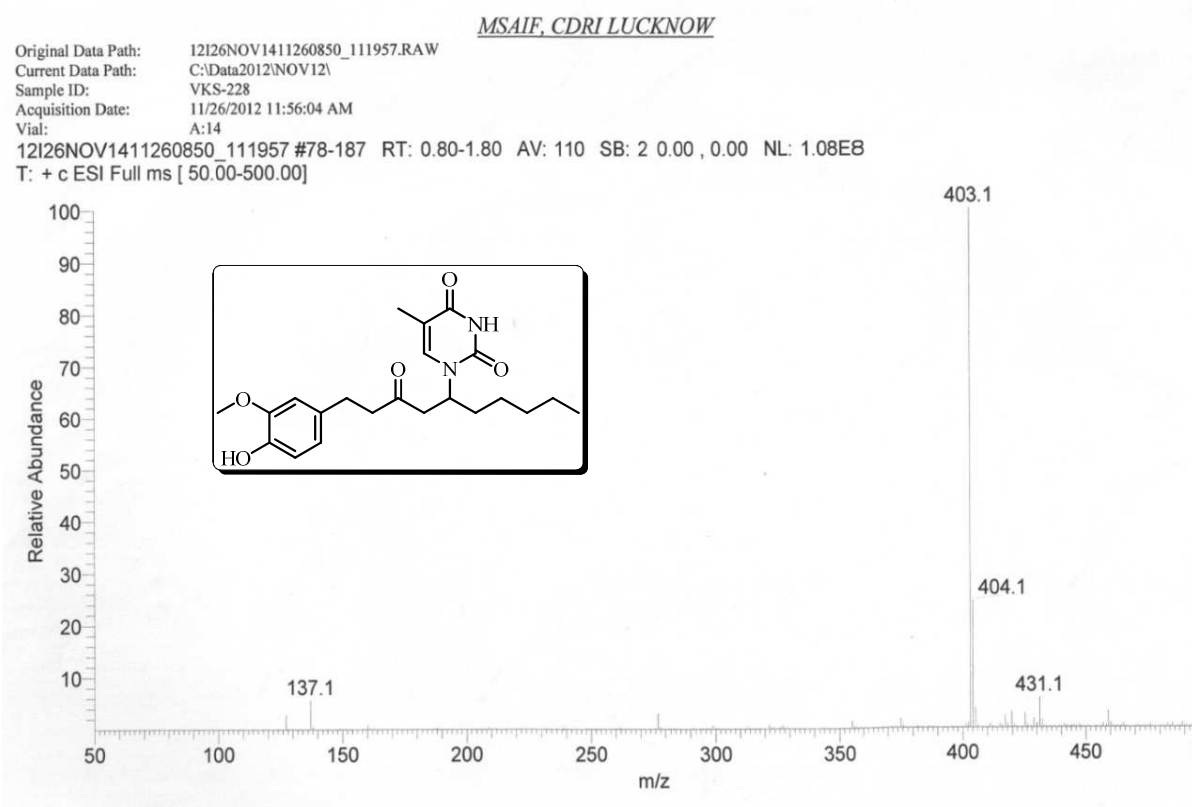

Figure 6. MS (ESI) of 2

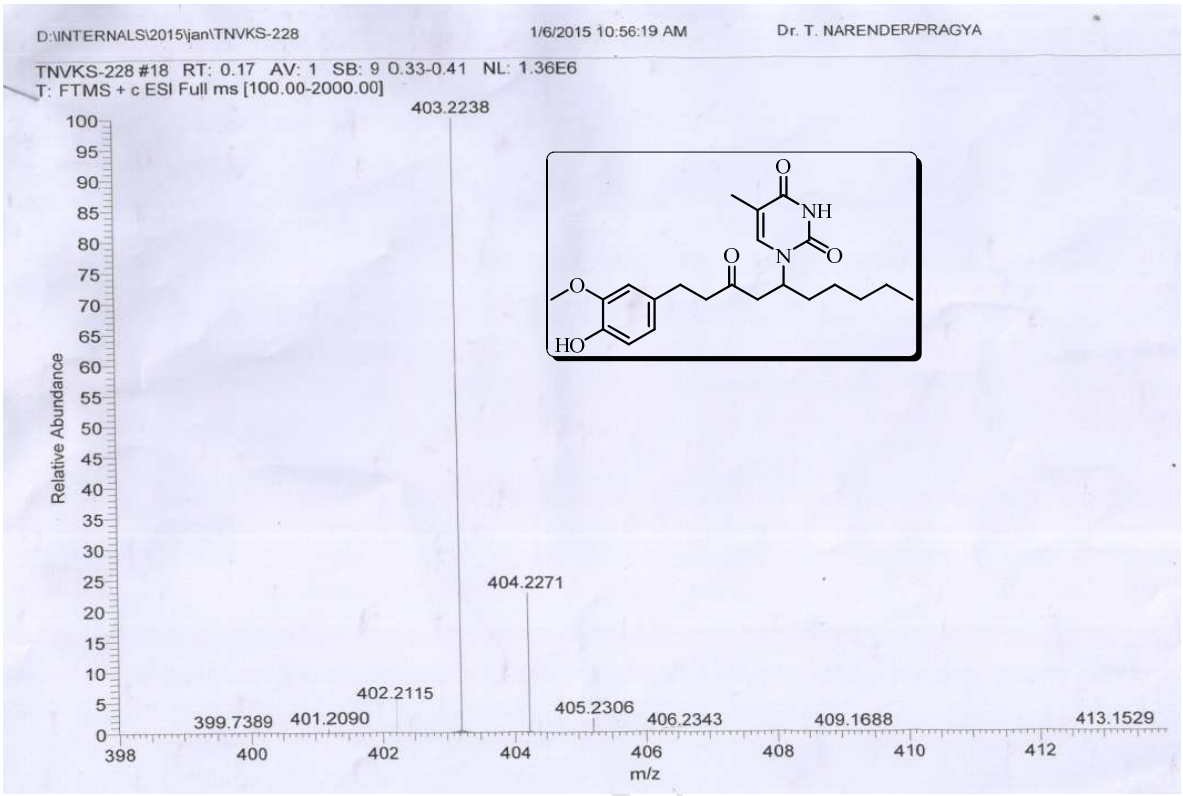

Figure 7. HRMS of 2

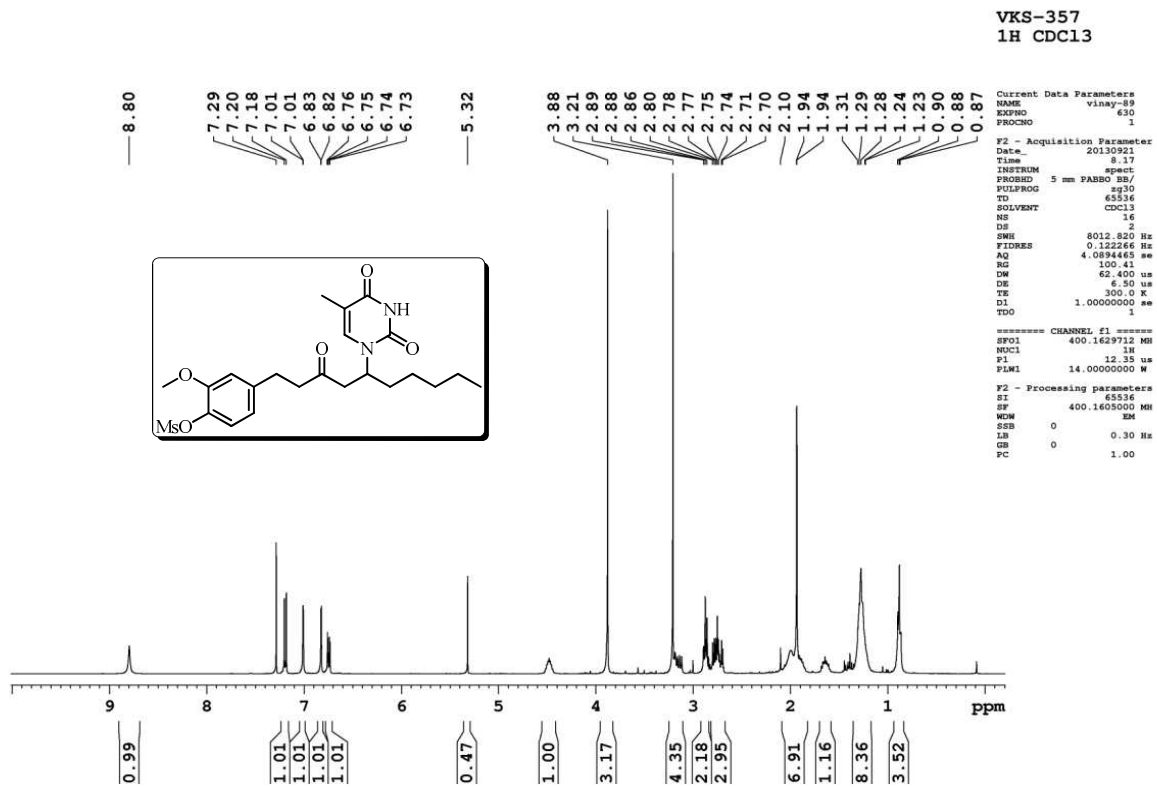

Figure 8. ^{1}H NMR spectrum of 2a (400 MHz, $CDCl_3$)

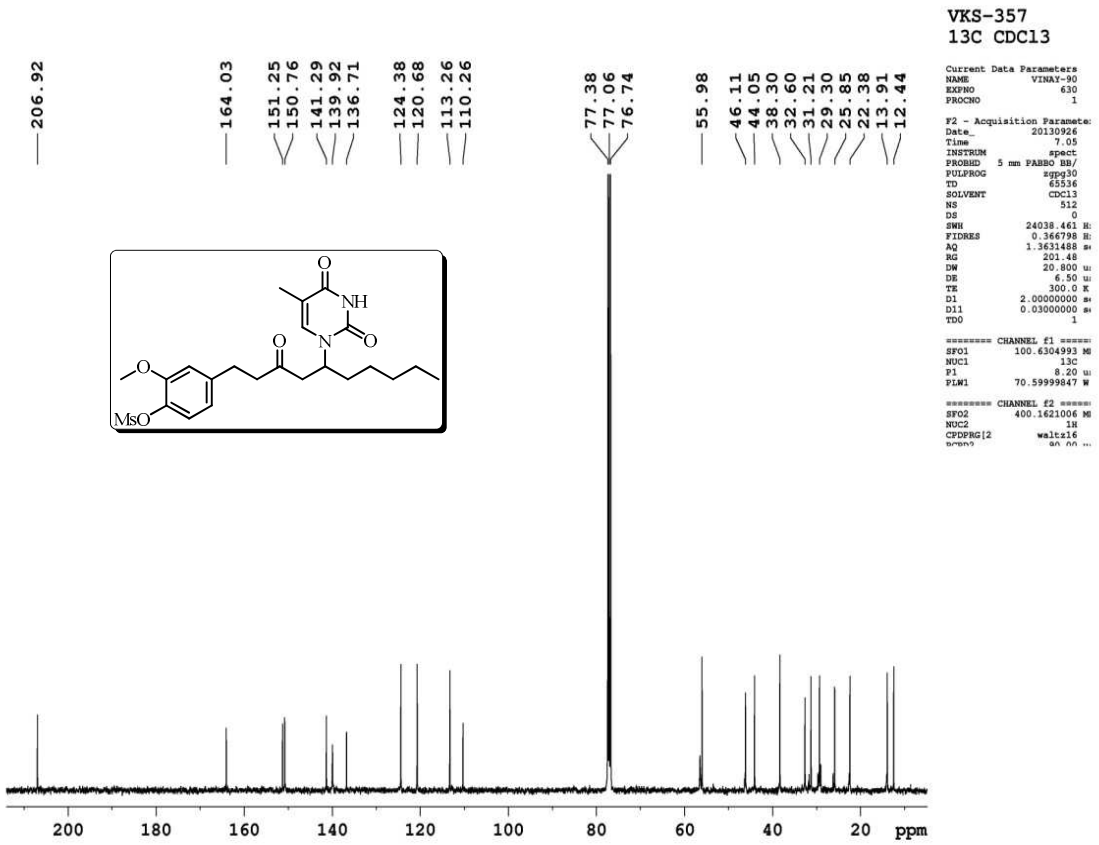

Figure 9. ^{13}C NMR spectrum of 2a (100 MHz, $CDCl_3$)

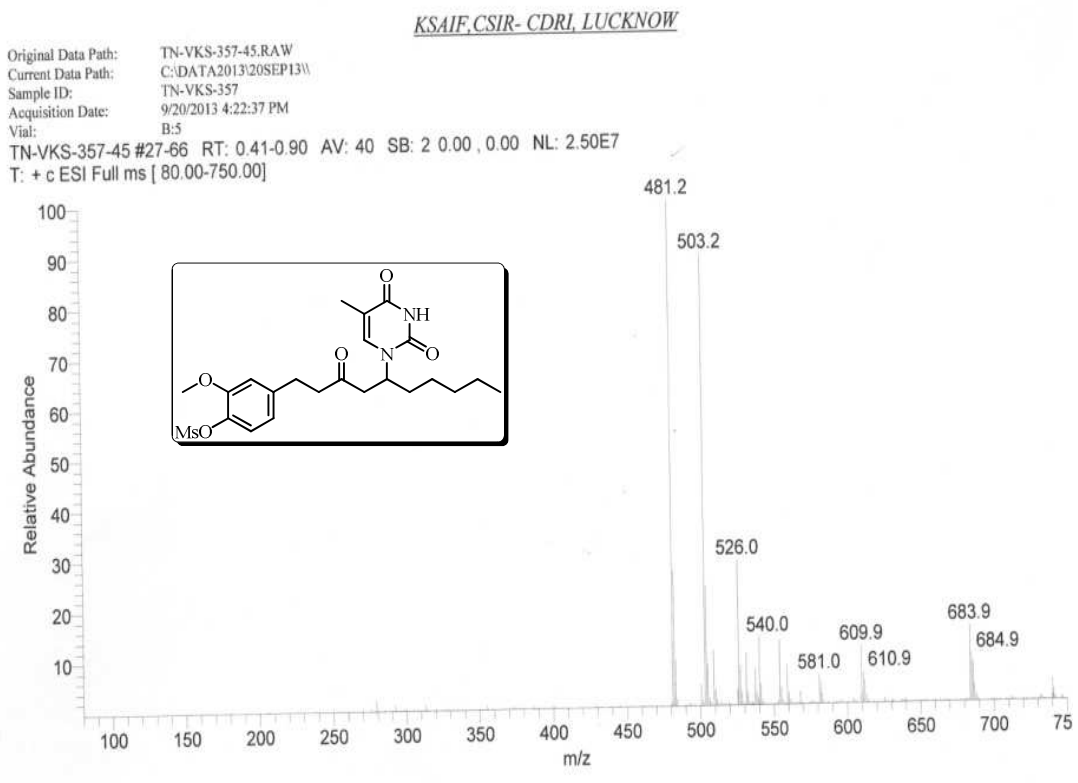

Figure 10. MS (ESI) of 2a

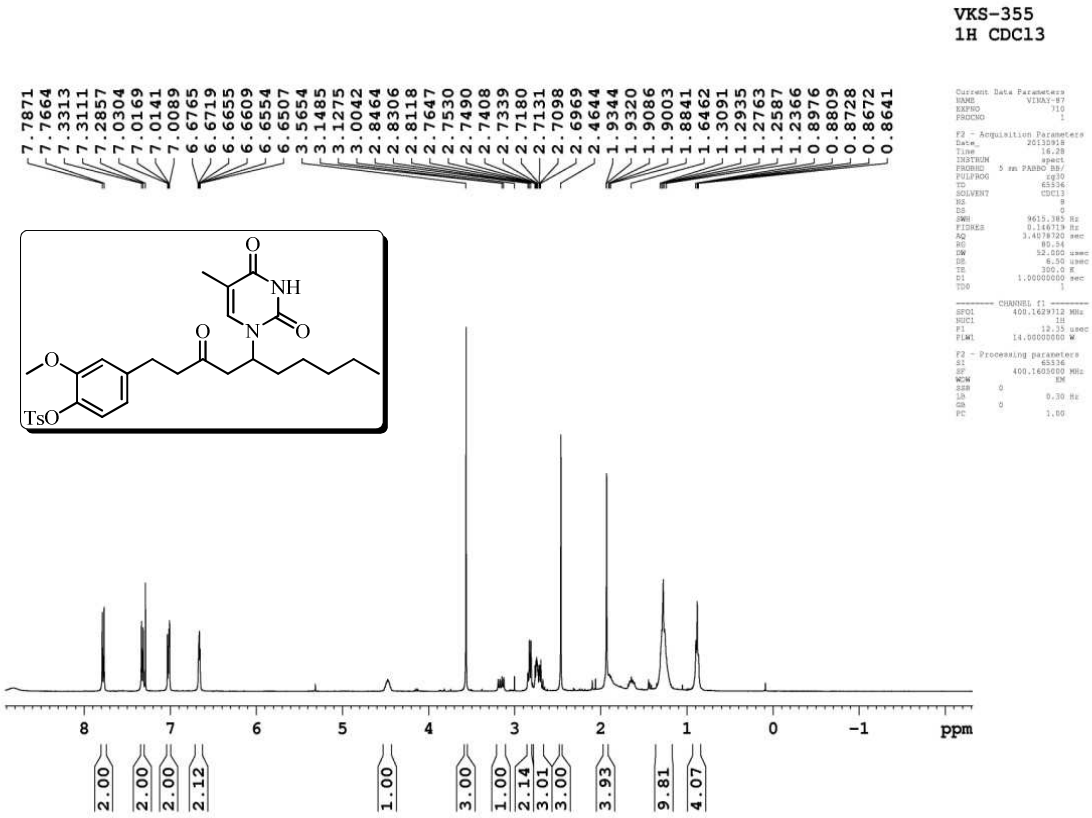

Figure 11. ^{1}H NMR spectrum of 2b (400 MHz, $CDCl_3$)

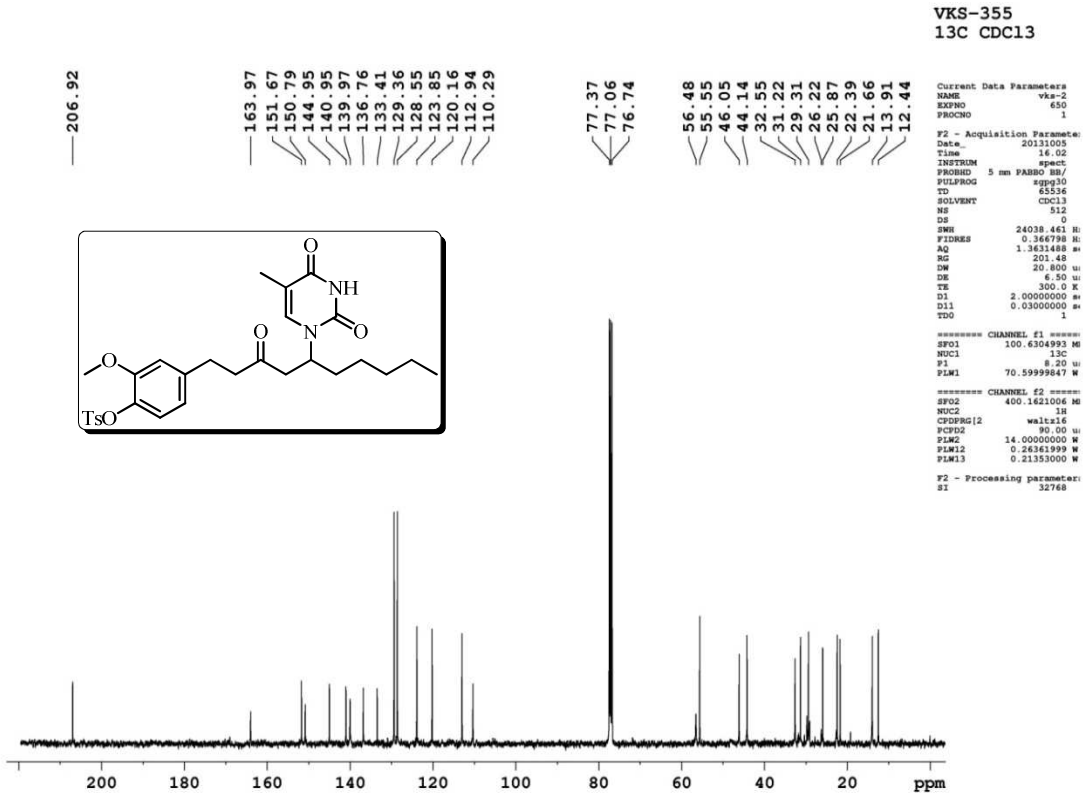

Figure 12. ^{13}C NMR spectrum of 2b (100 MHz, $CDCl_3$)

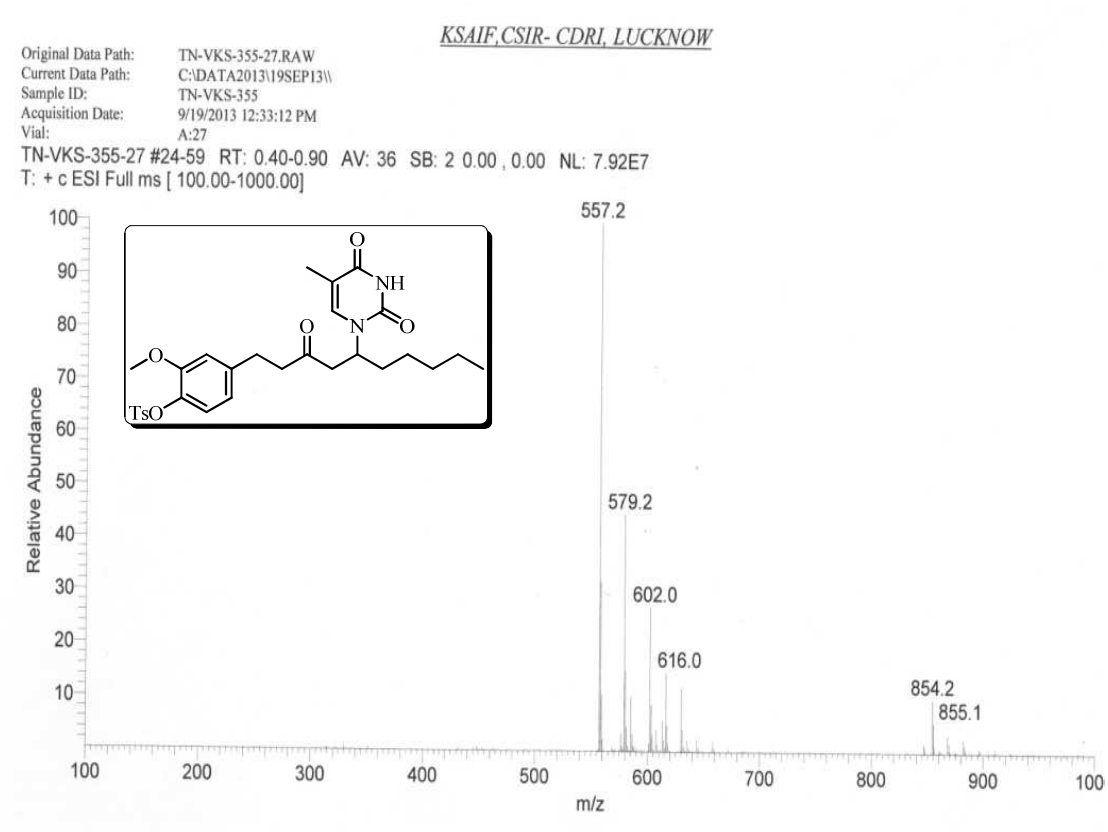

Figure 13. MS (ESI) of 2b

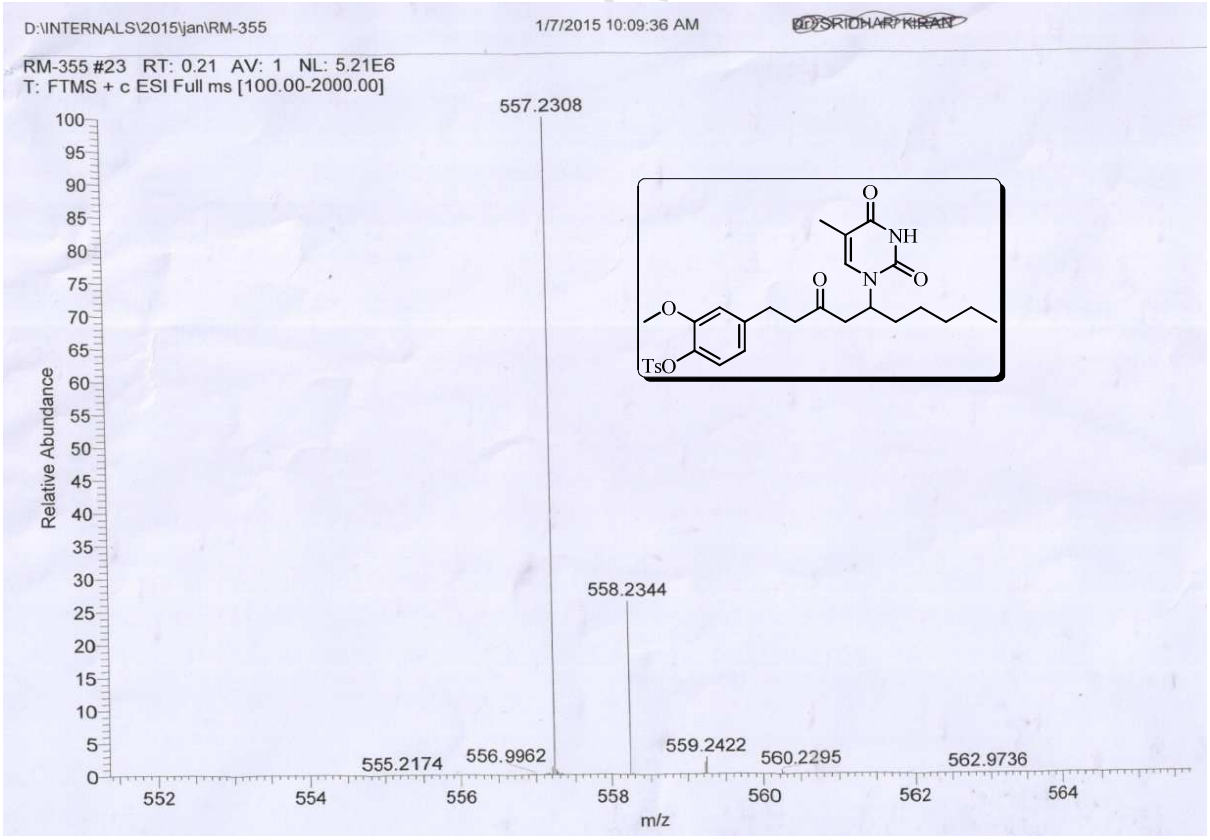

Figure 14. HRMS of 2b

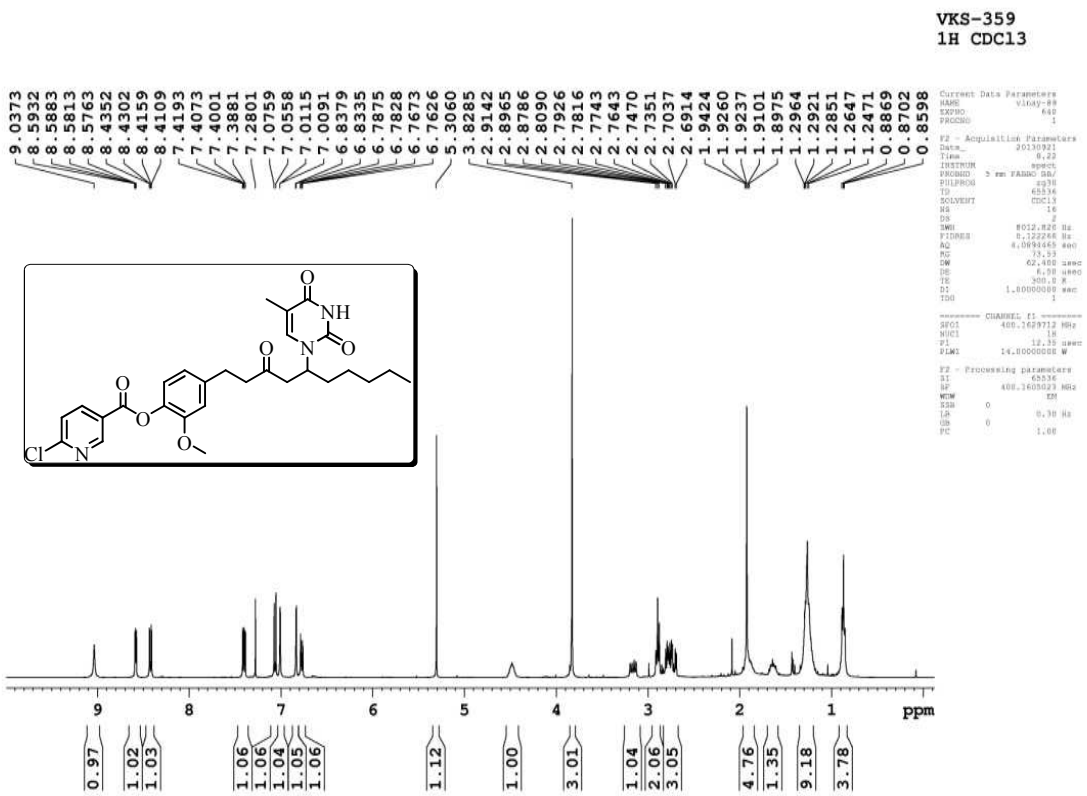

Figure 15. ^{1}H NMR spectrum of 2c (400 MHz, $CDCl_3$)

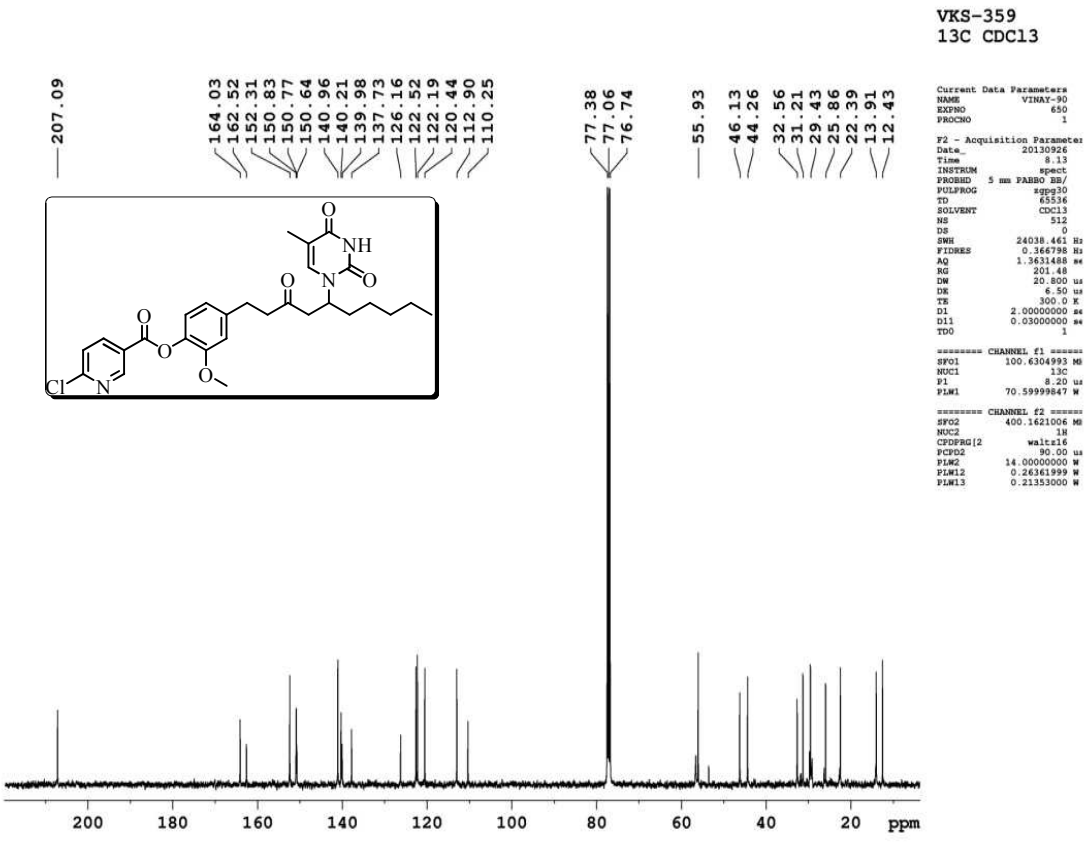

Figure 16. ^{13}C NMR spectrum of 2c (100 MHz, $CDCl_3$)

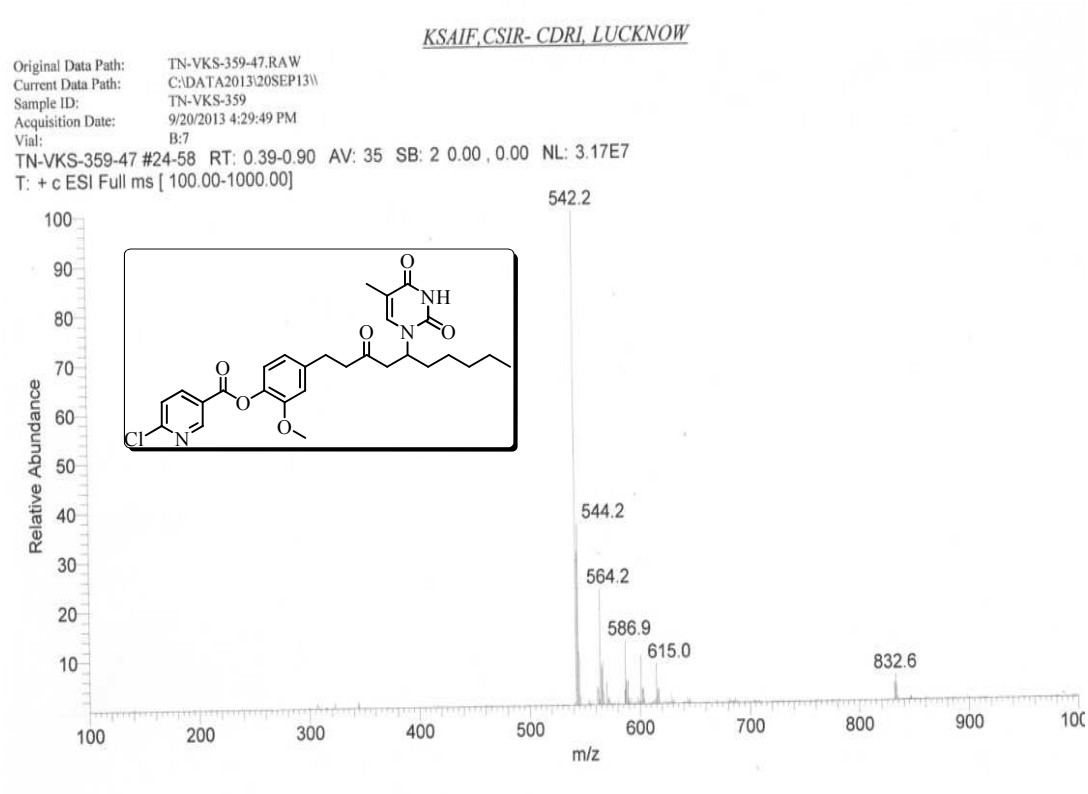

Figure 17. MS (ESI) of 2c

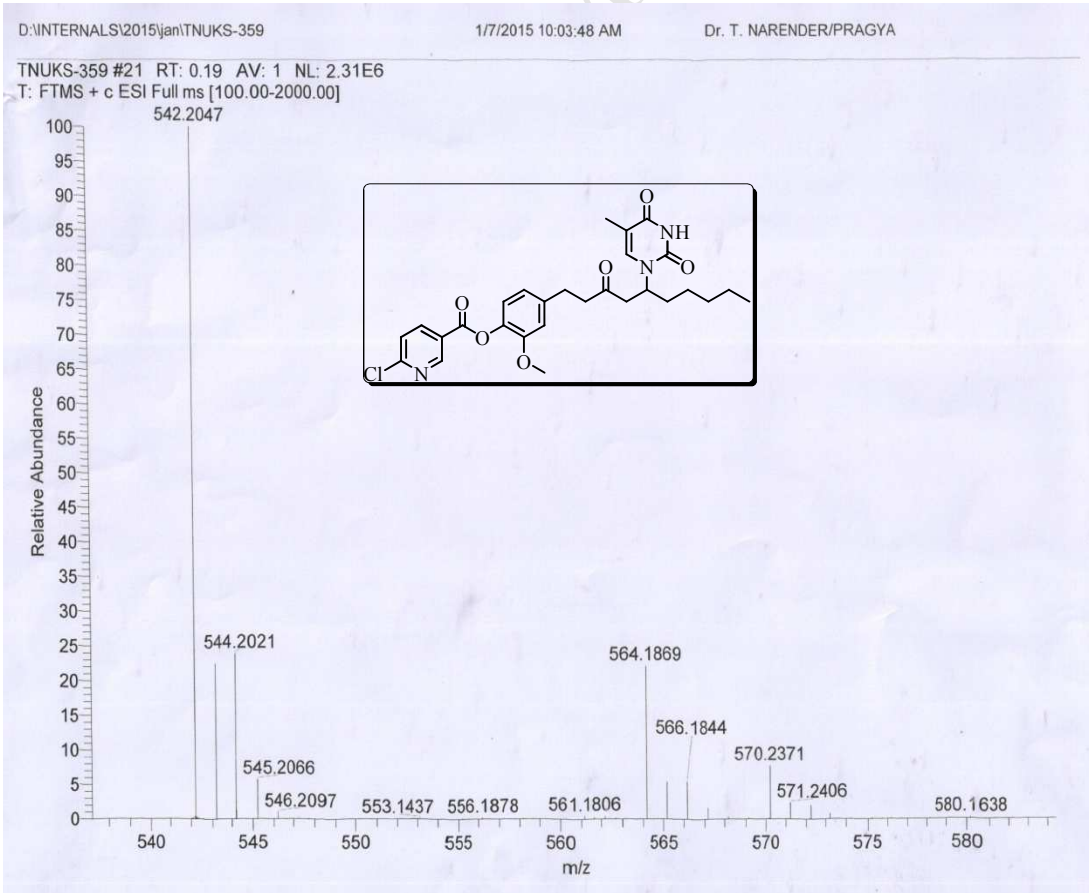

Figure 18. HRMS of 2c

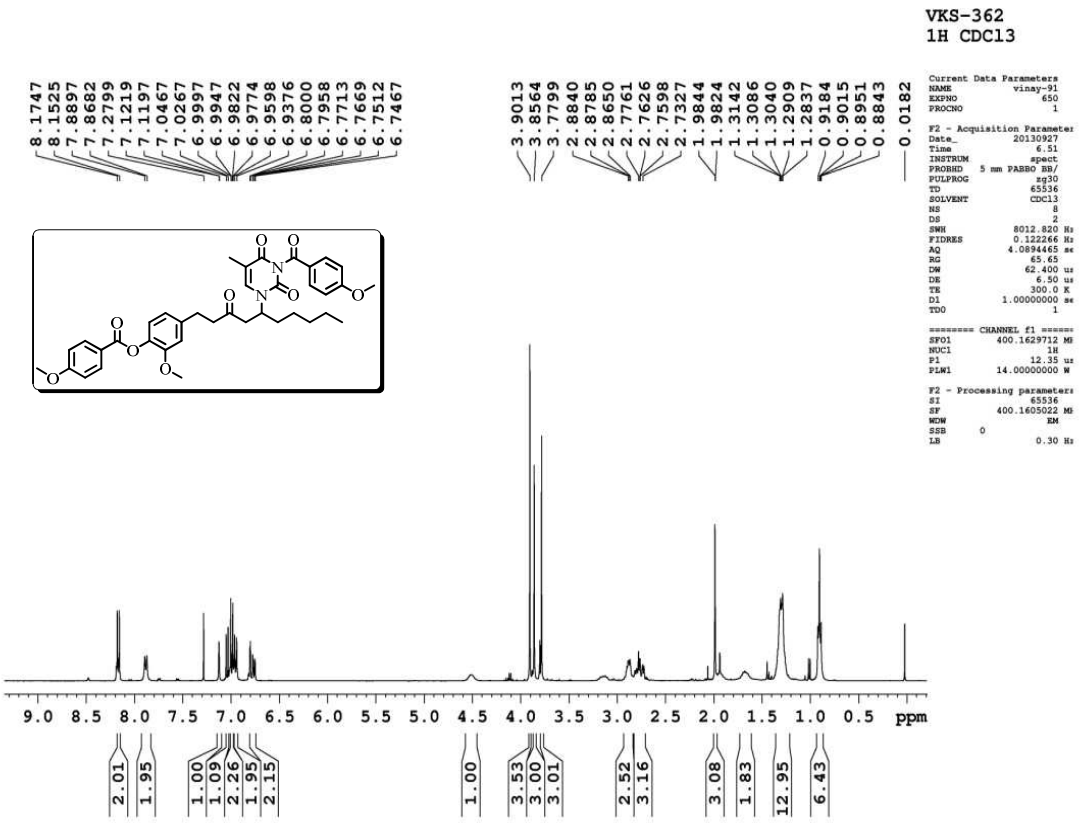

Figure 19. ^{1}H NMR spectrum of 2d (400 MHz, $CDCl_3$)

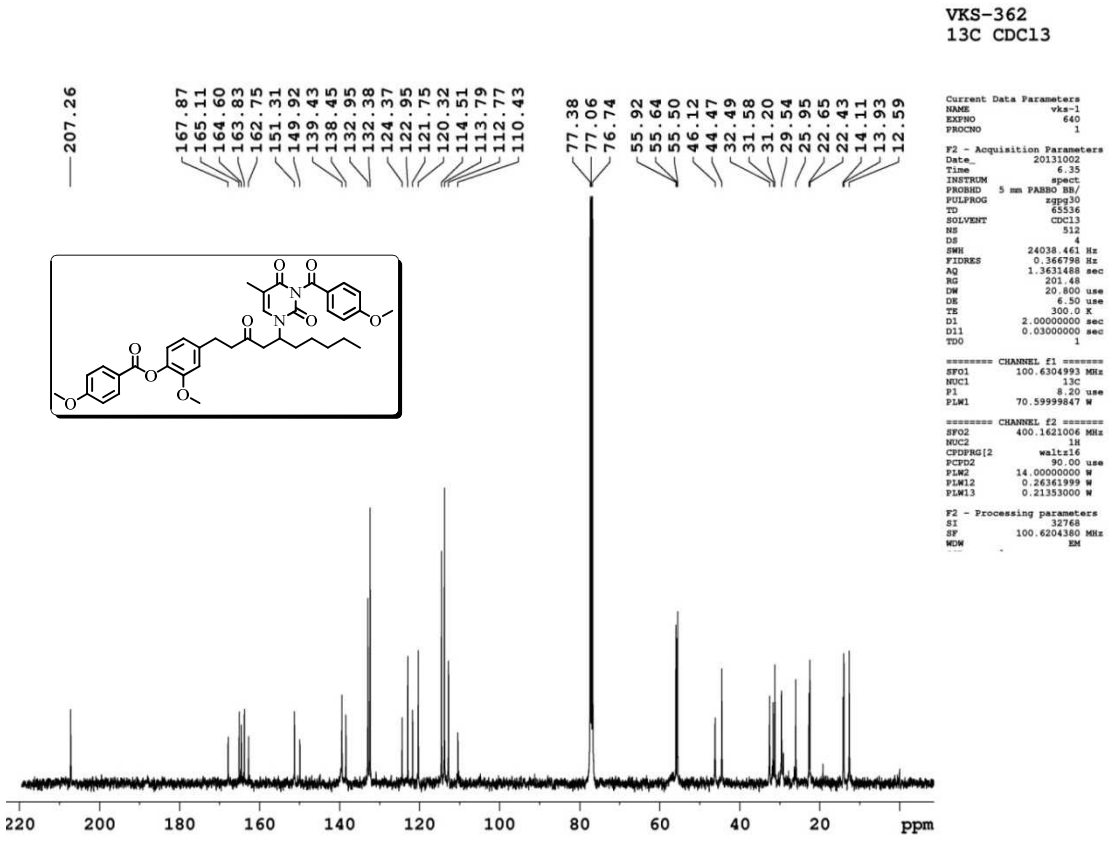

Figure 20. ^{13}C NMR spectrum of 2d (100 MHz, $CDCl_3$)

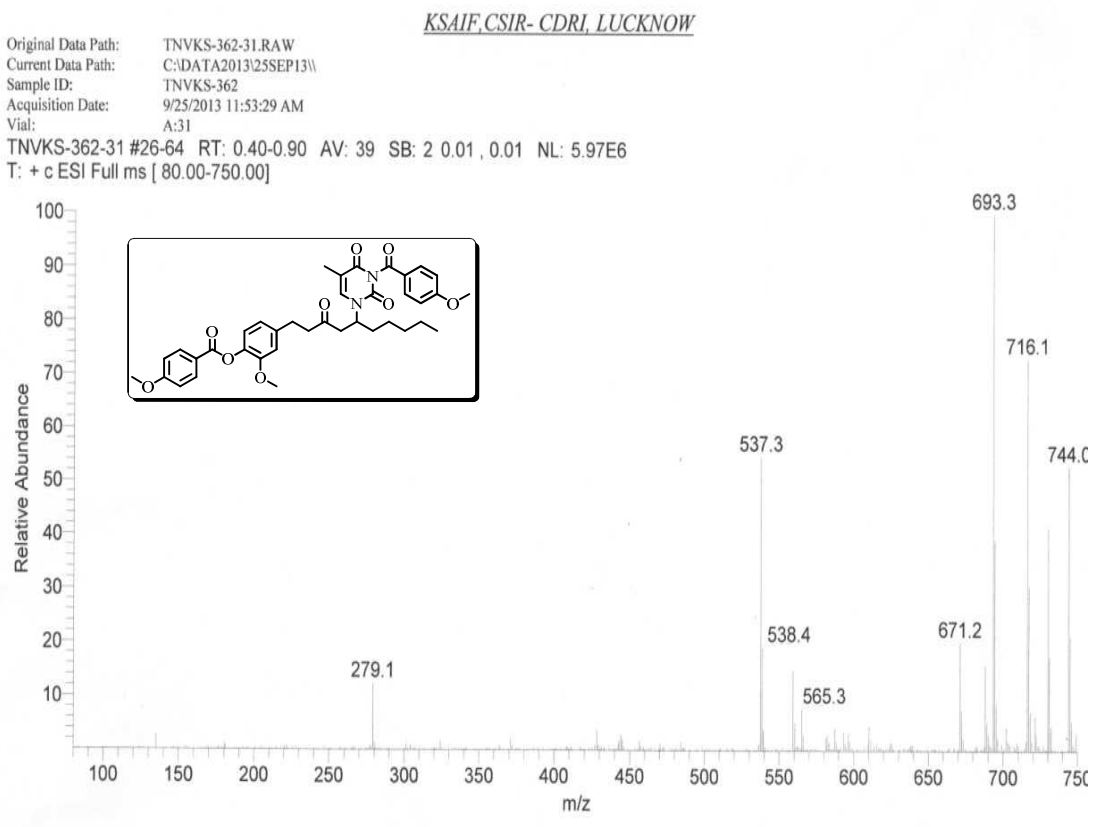

Figure 21. MS (ESI) of 2d

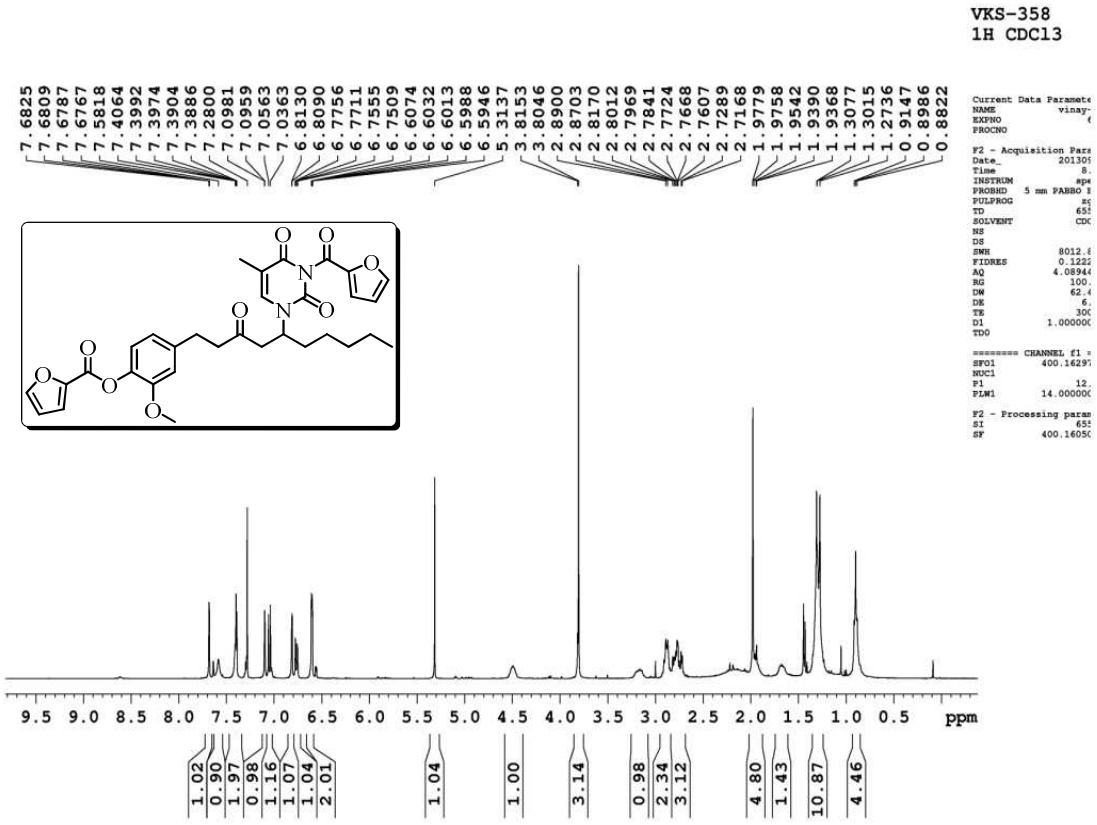

Figure 22. ^{1}H NMR spectrum of 2e (400 MHz, $CDCl_3$)

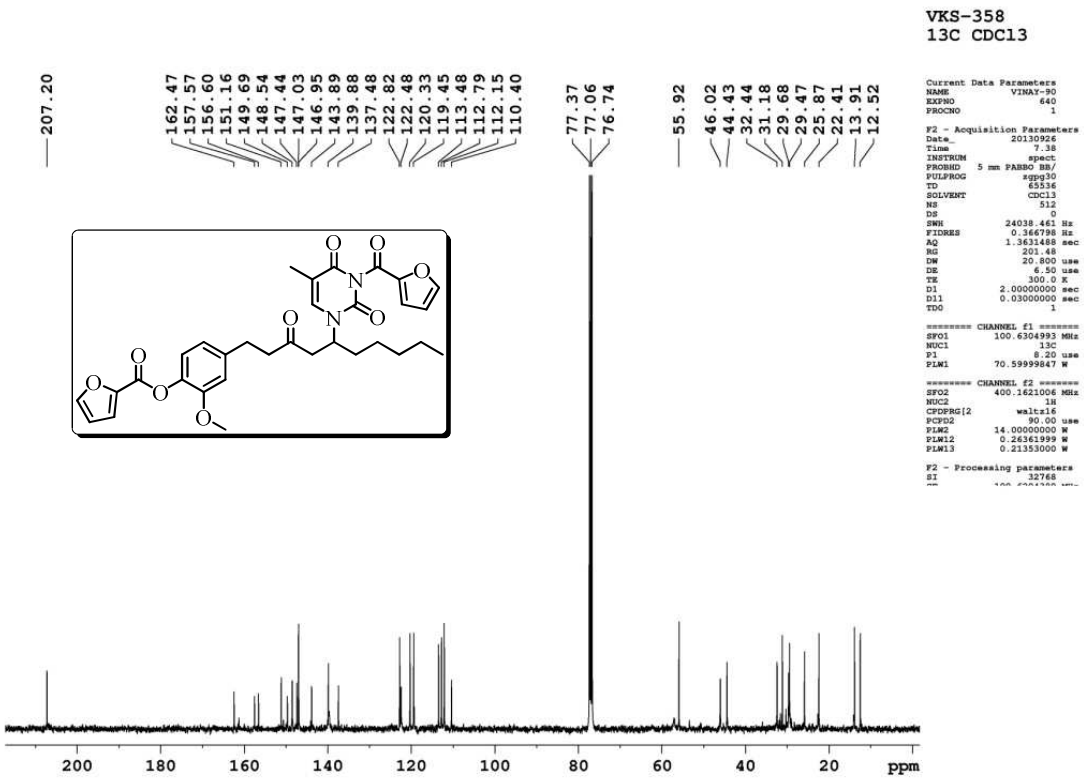

Figure 23. ^{13}C NMR spectrum of 2e (100 MHz, $CDCl_3$)

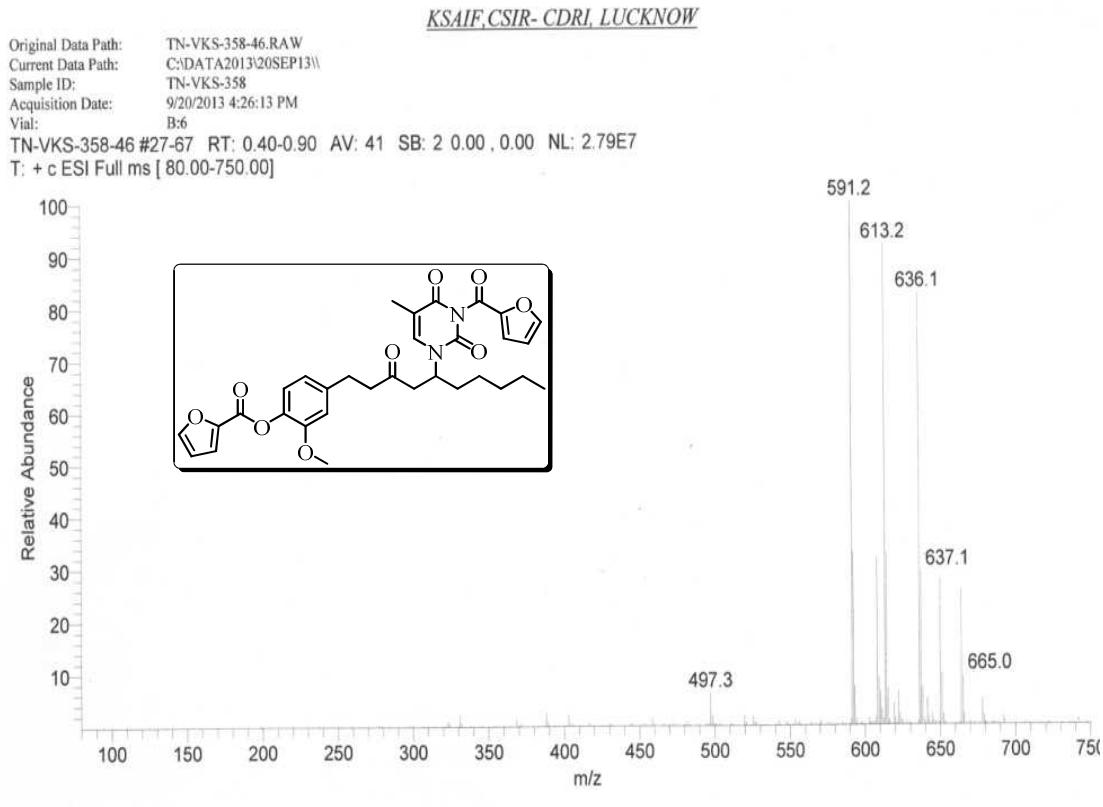

Figure 24. MS (ESI) of 2e

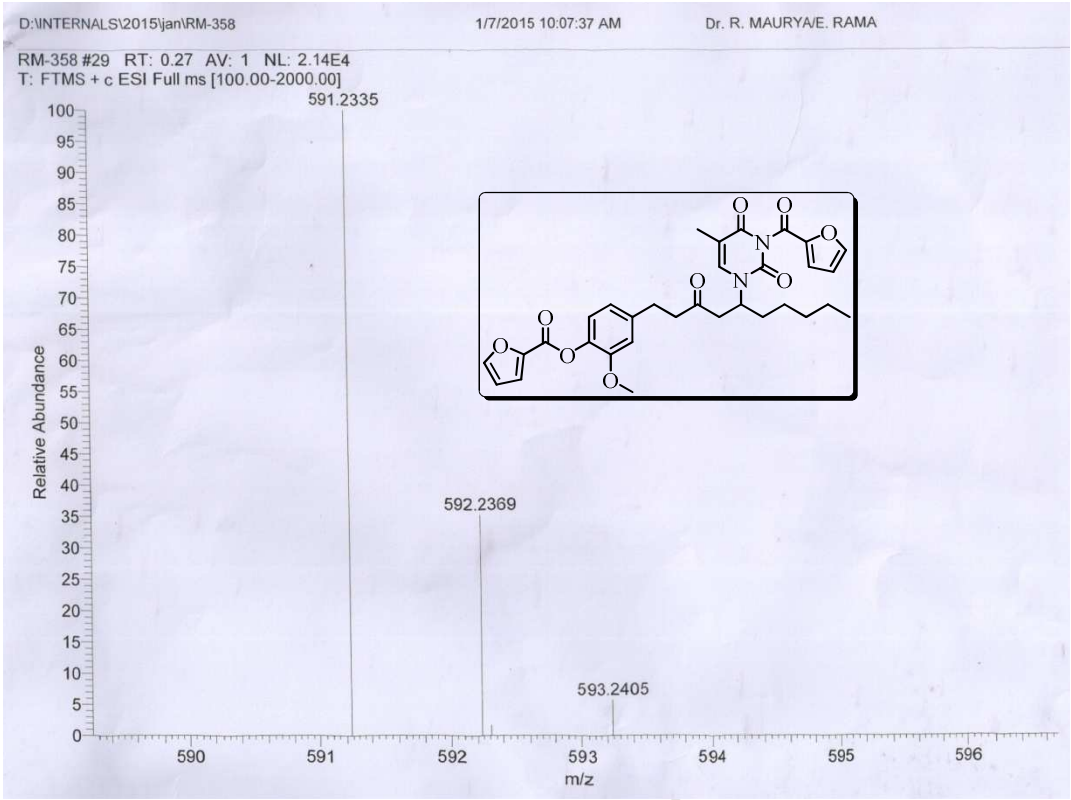

Figure 25. HRMS of 2e

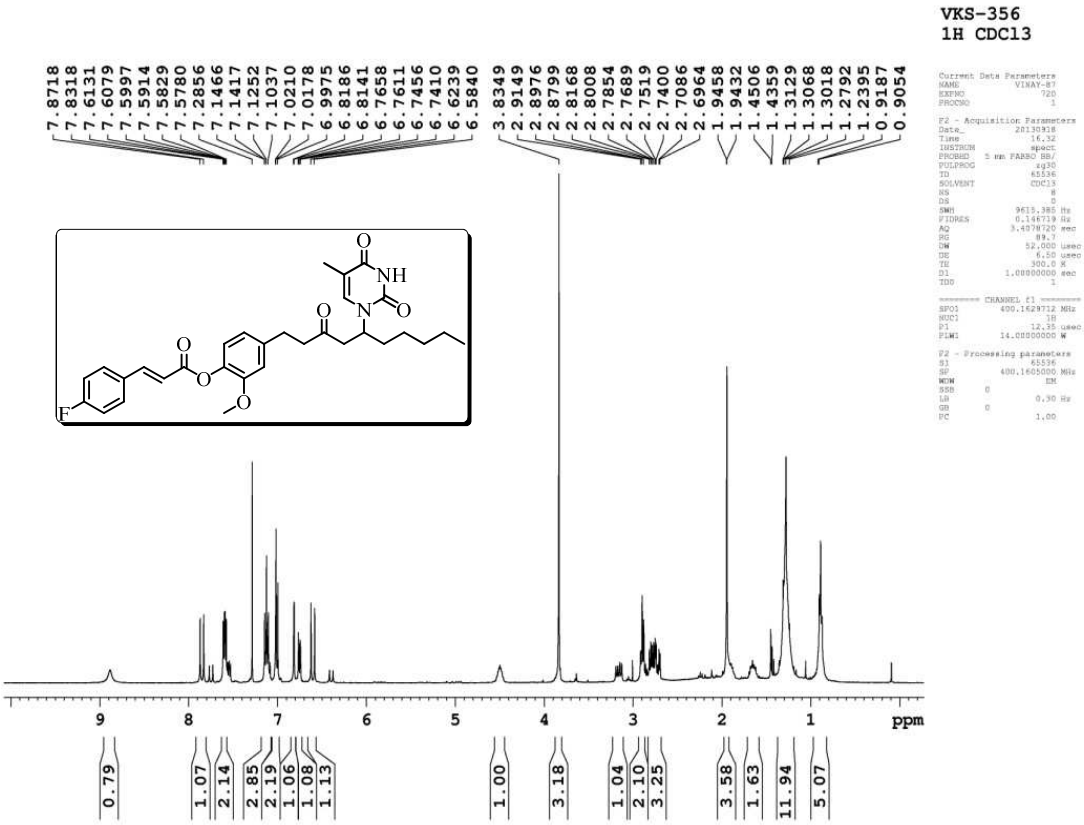

Figure 26. ^{1}H NMR spectrum of 2f (400 MHz, $CDCl_3$)

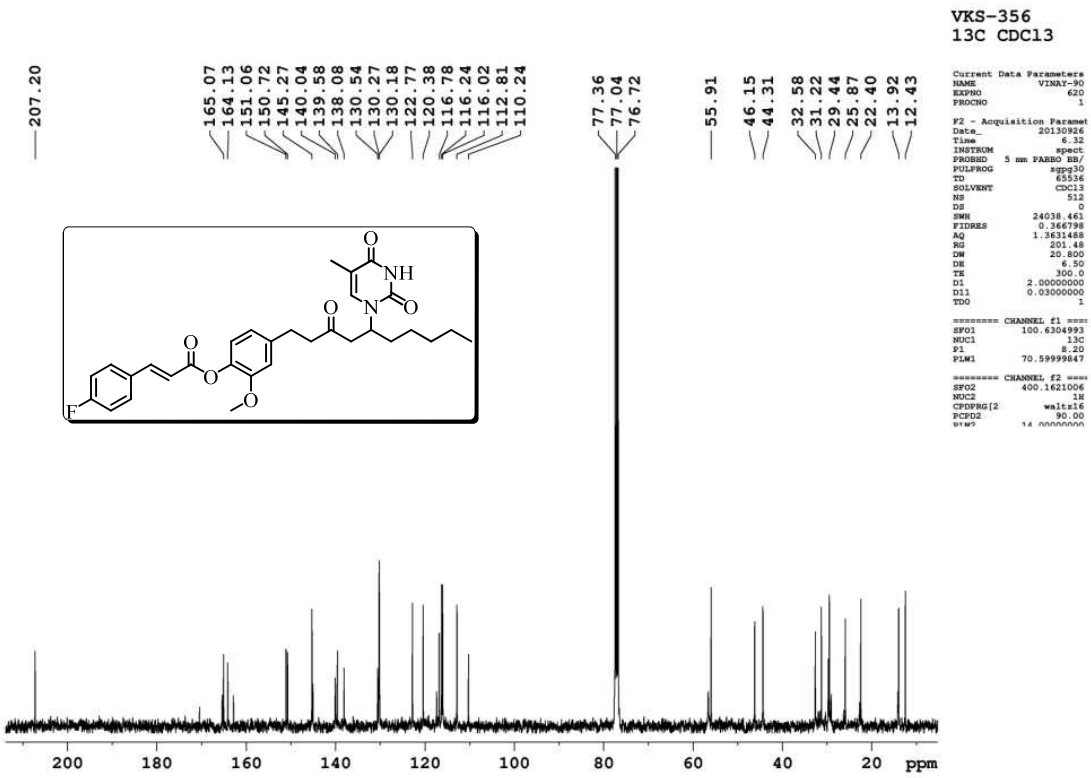

Figure 27. ^{13}C NMR spectrum of 2f (100 MHz, $CDCl_3$)

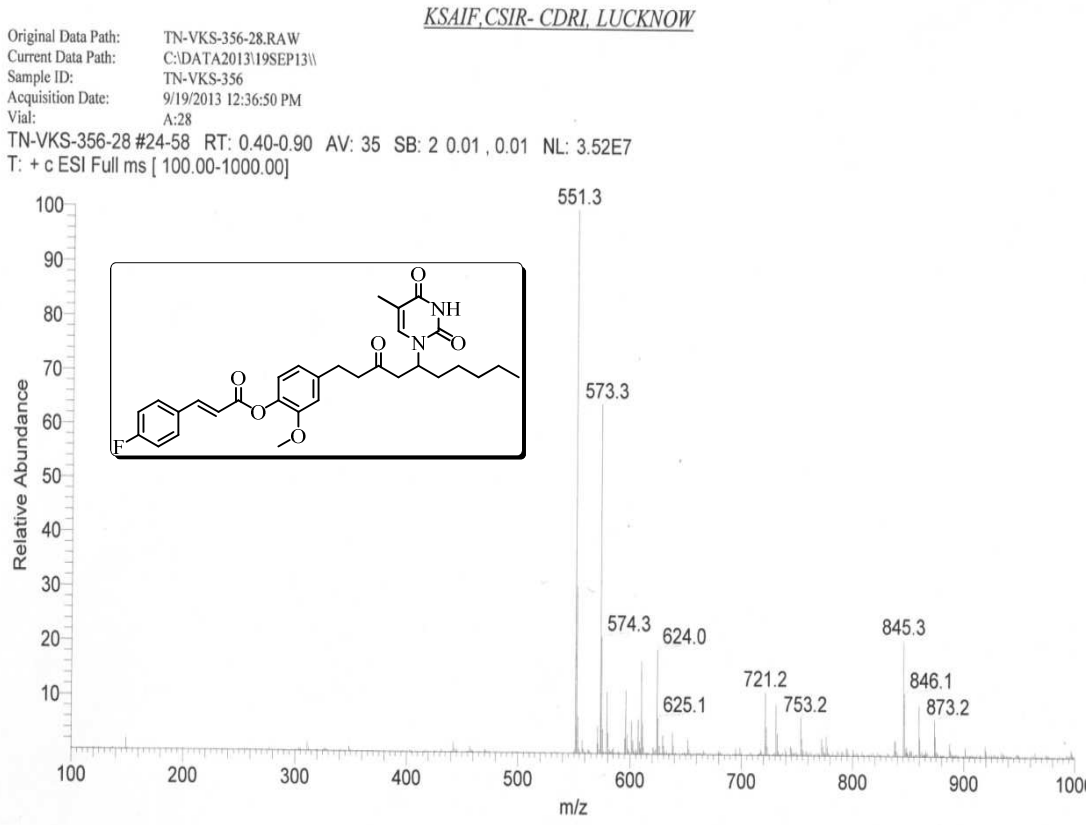

Figure 28. MS (ESI) of 2f

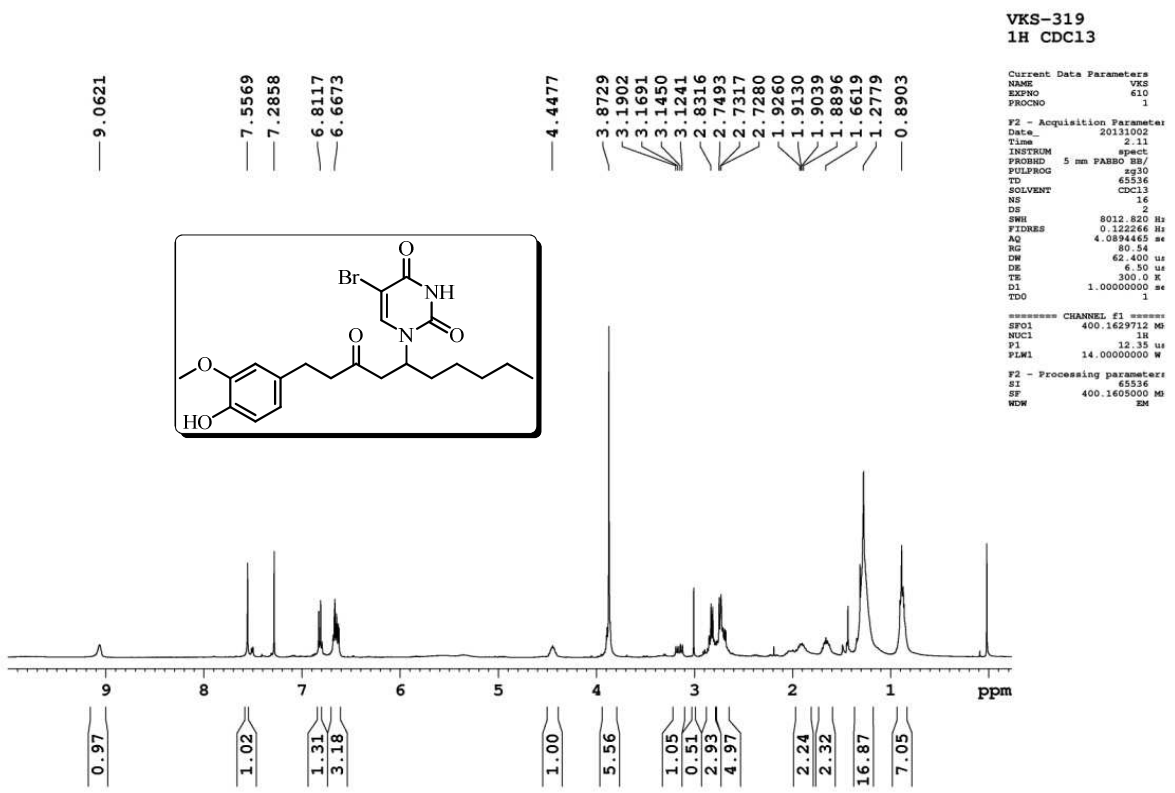

Figure 29. ^{1}H NMR spectrum of 3 (400 MHz, $CDCl_3$)

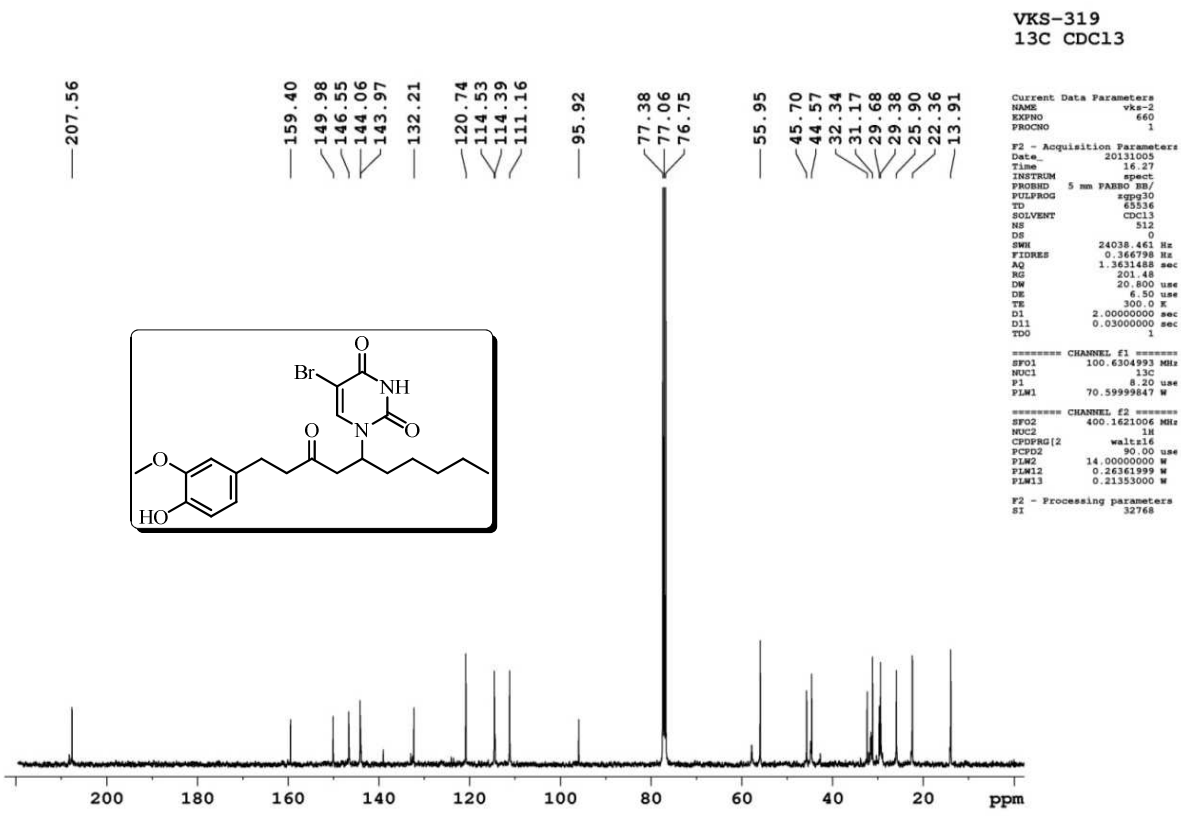

Figure 30. ^{13}C NMR spectrum of 3 (100 MHz, $CDCl_3$)

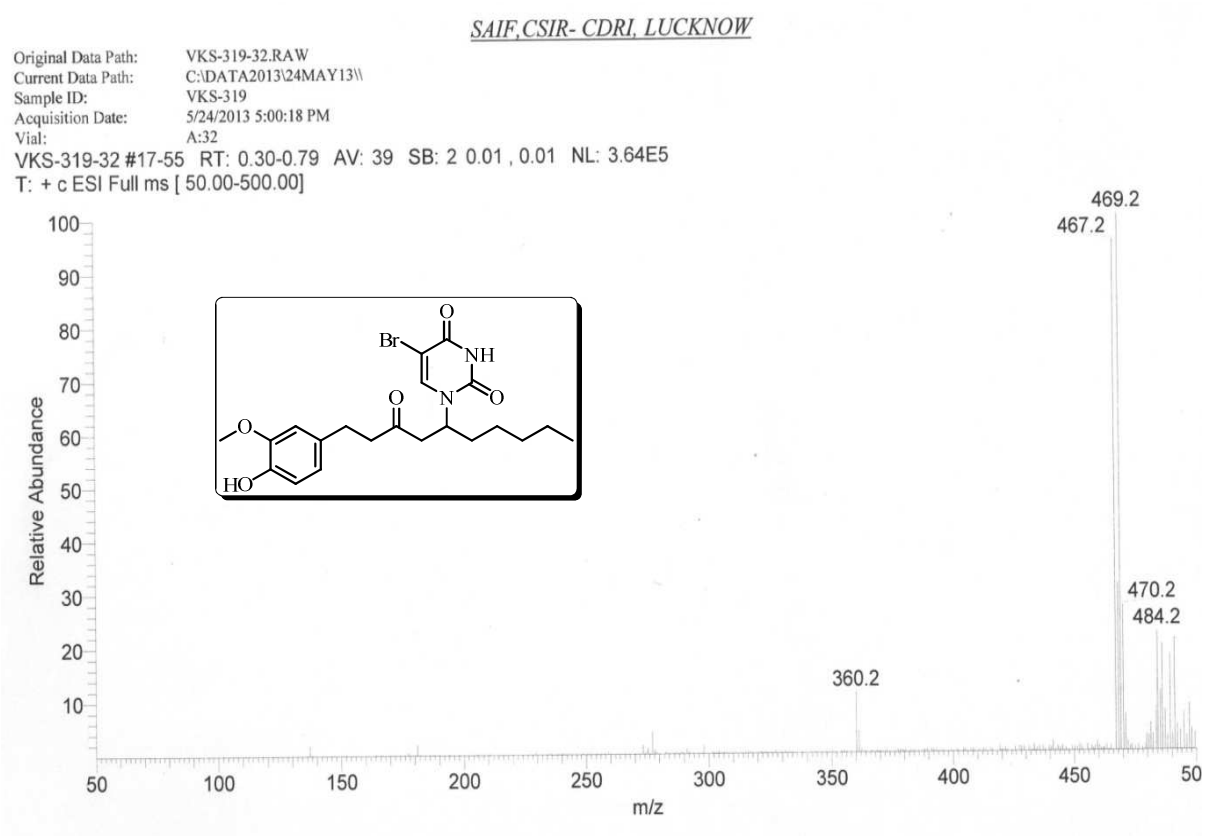

Figure 31. MS (ESI) of 3

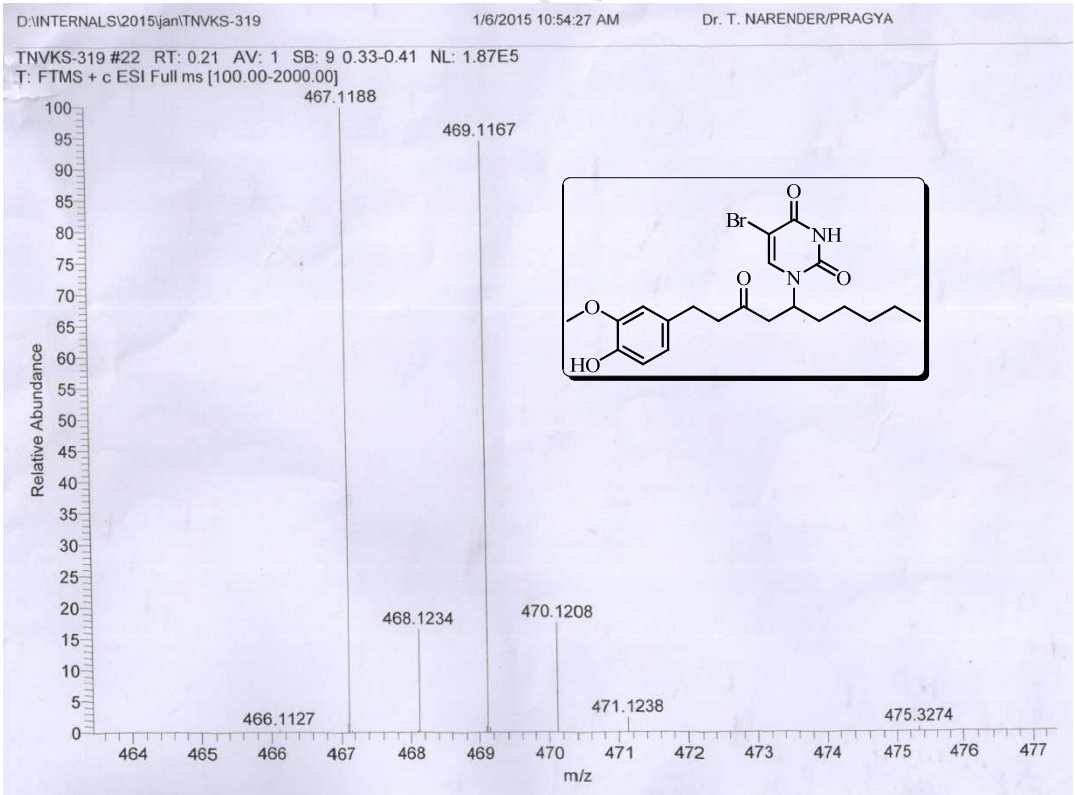

Figure 32. HRMS of 3

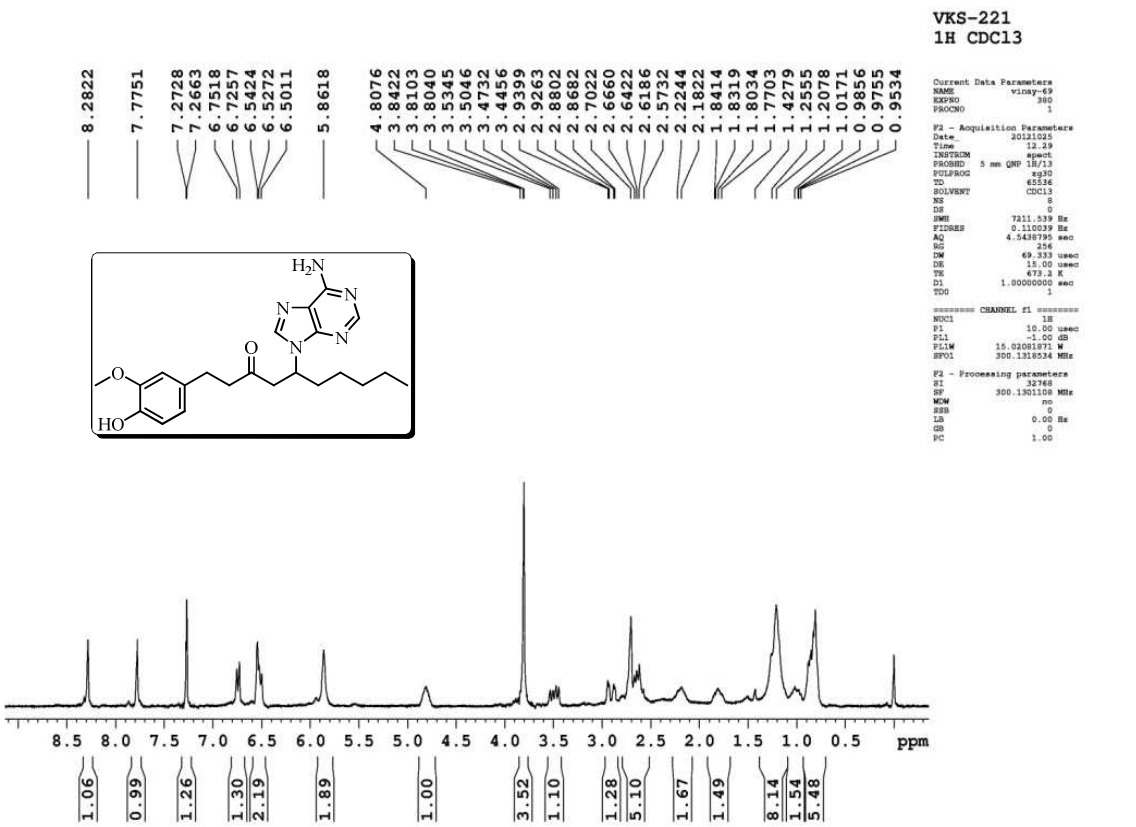

Figure 33. ^{1}H NMR spectrum of 4 (300 MHz, $CDCl_3$

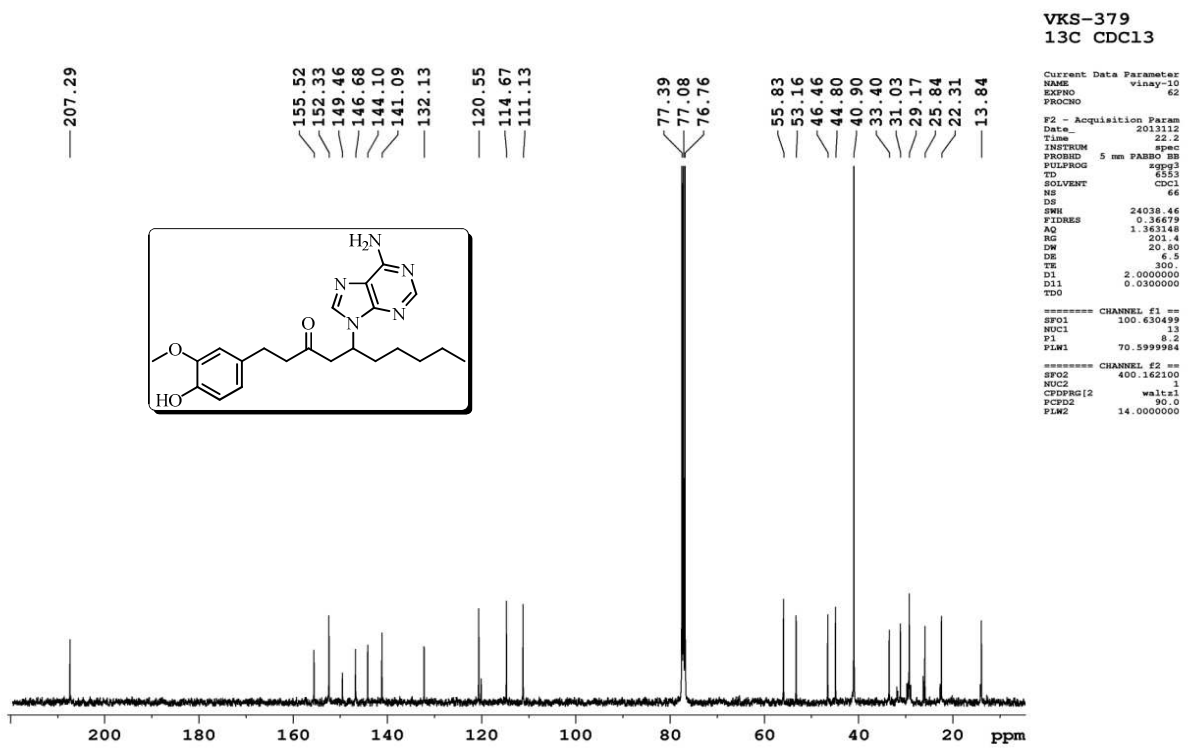

Figure 34. ^{13}C NMR spectrum of 4 (100 MHz, $CDCl_3$)

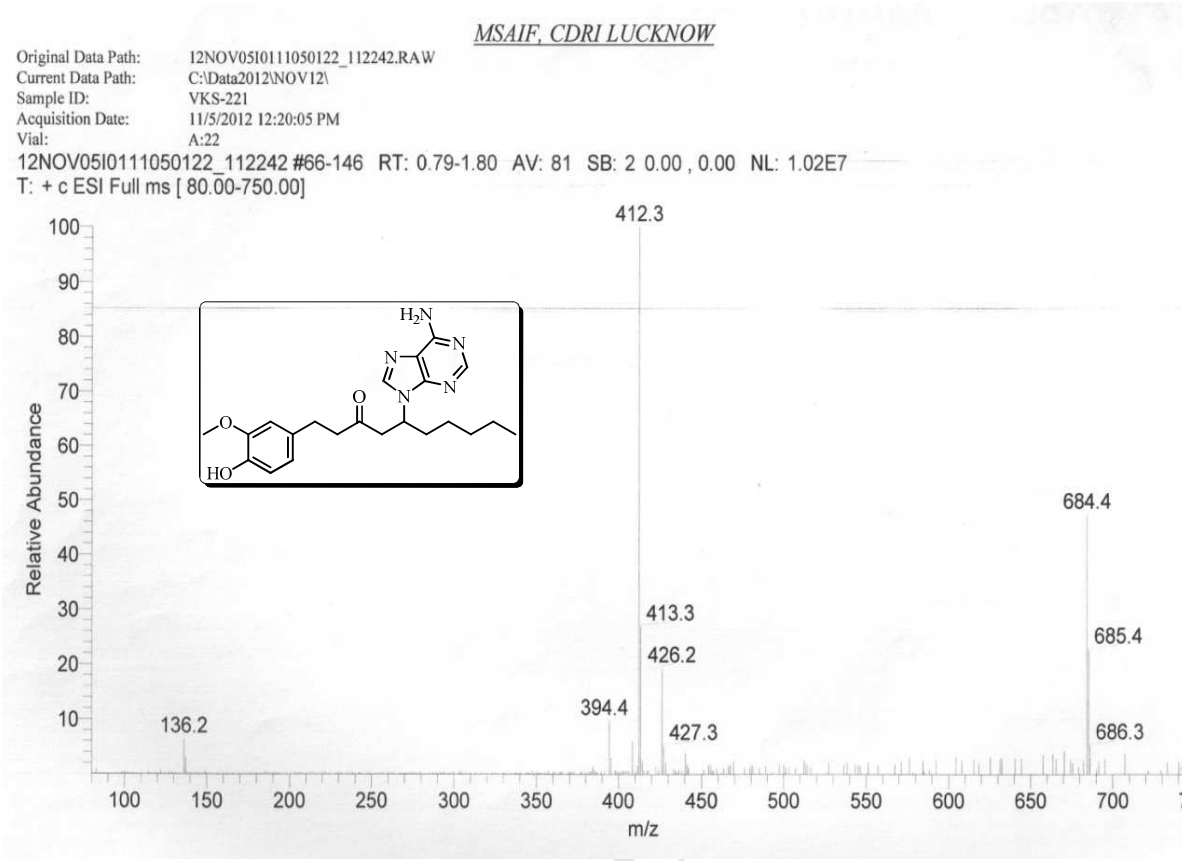

Figure 35. MS (ESI) of 4

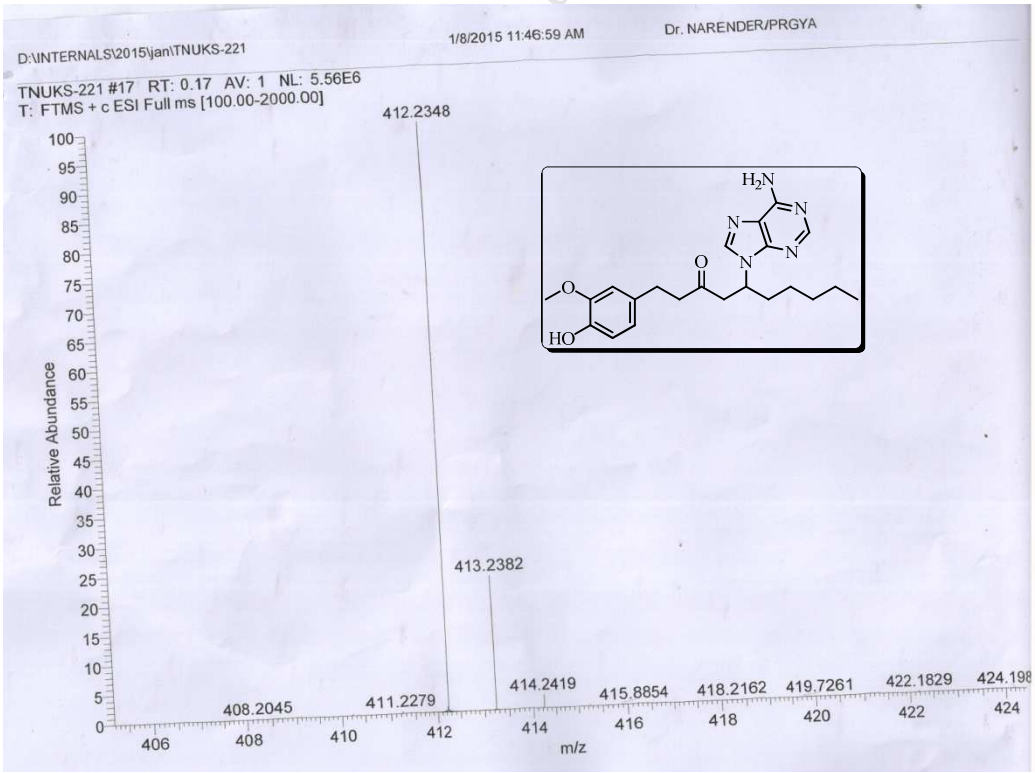

Figure 36. HRMS of 4

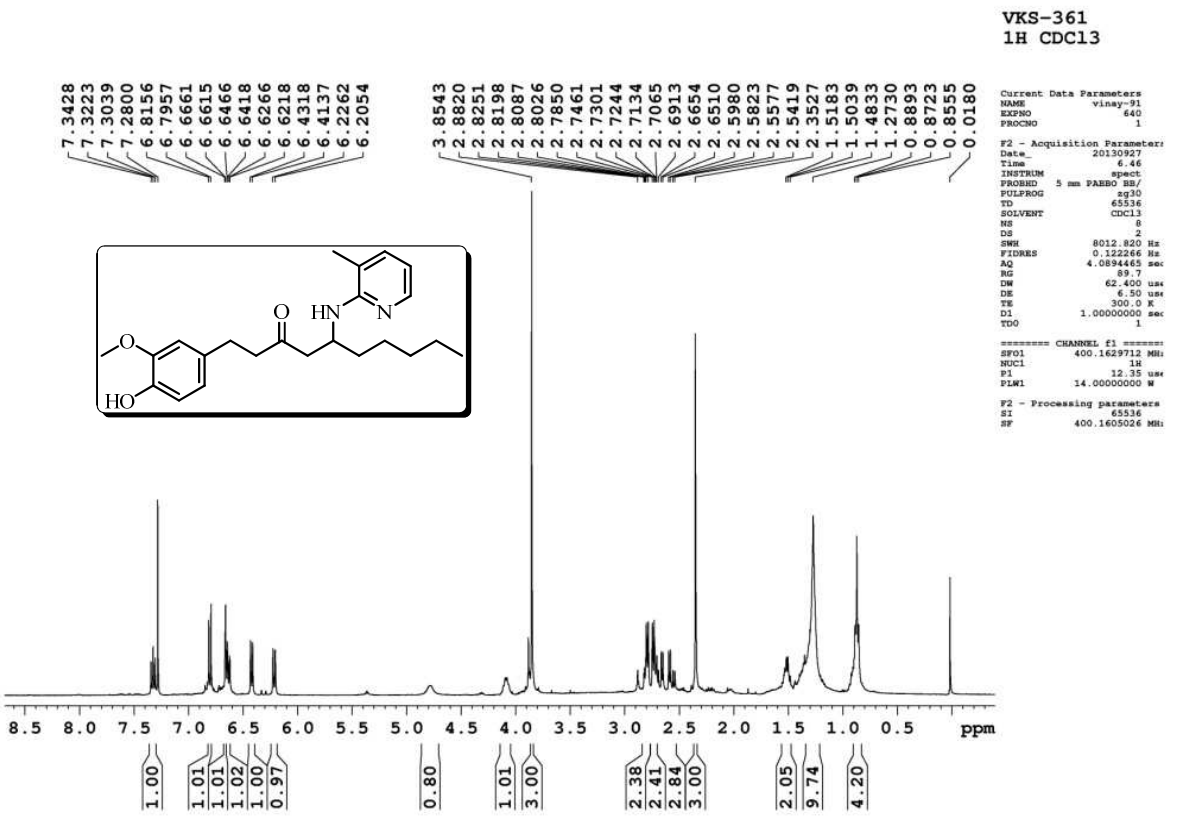

Figure 37. ^{1}H NMR spectrum of 5 (400 MHz, $CDCl_3$)

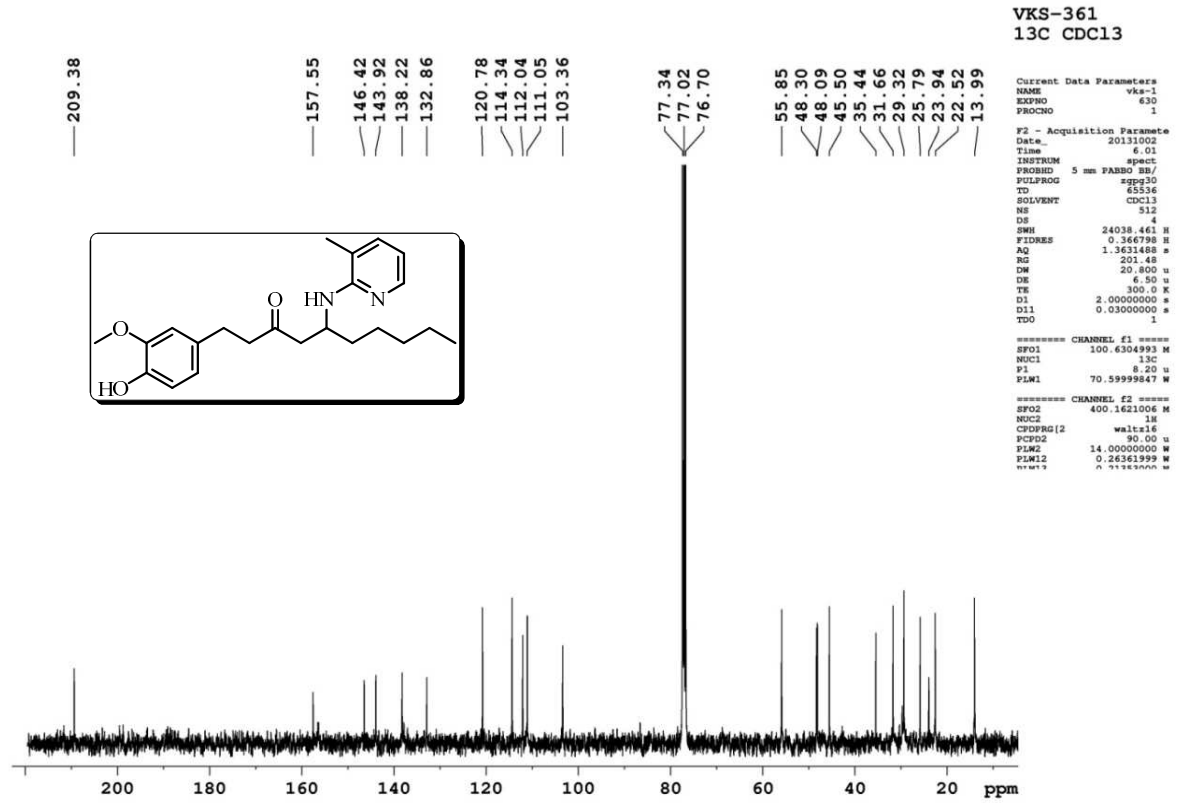

Figure 38. ^{13}C NMR spectrum of 5 (100 MHz, $CDCl_3$)

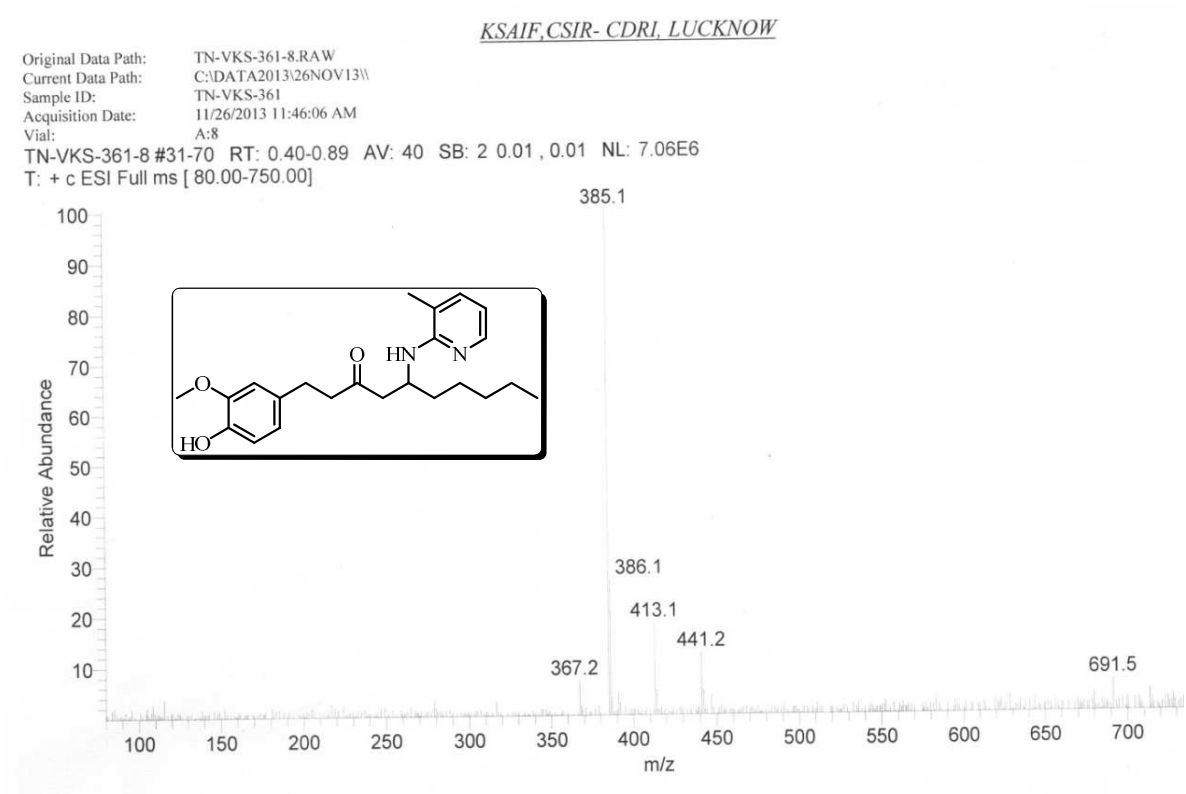

Figure 39. MS (ESI) of 5

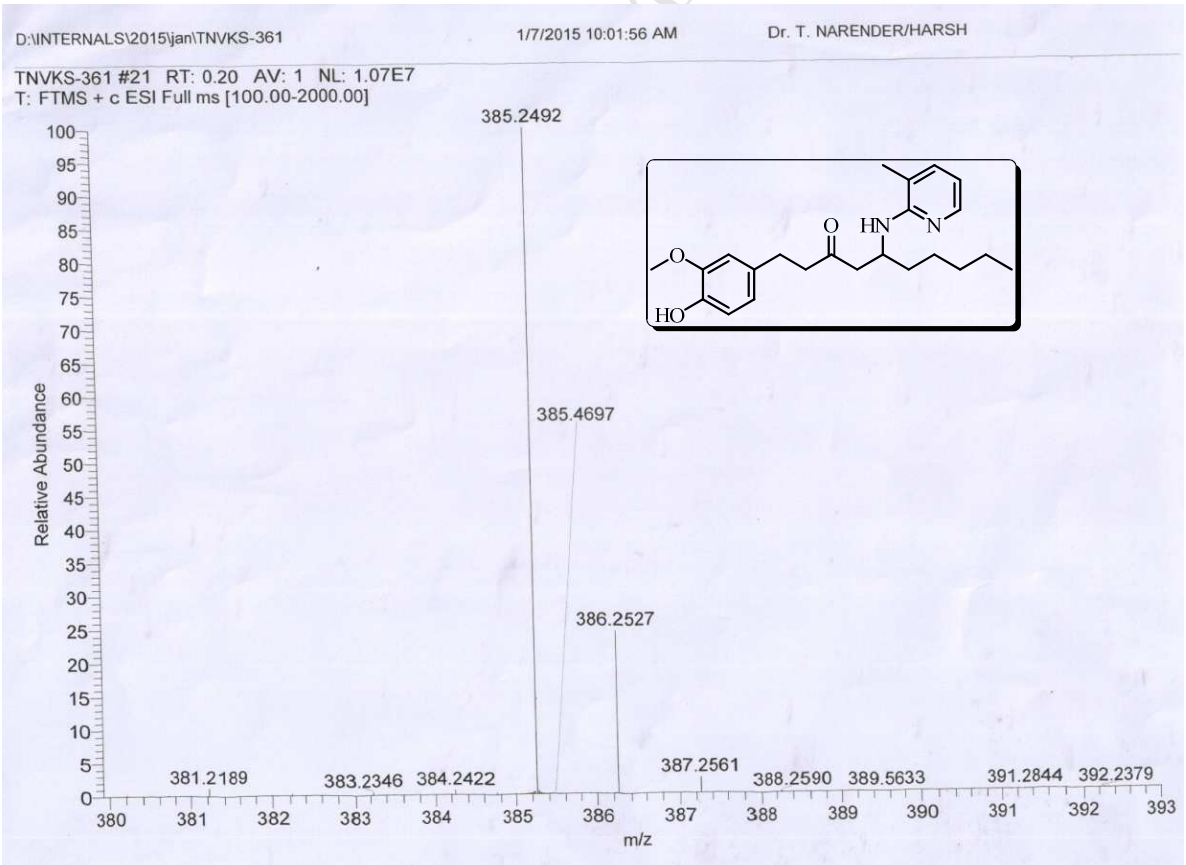

Figure 40. HRMS of 5

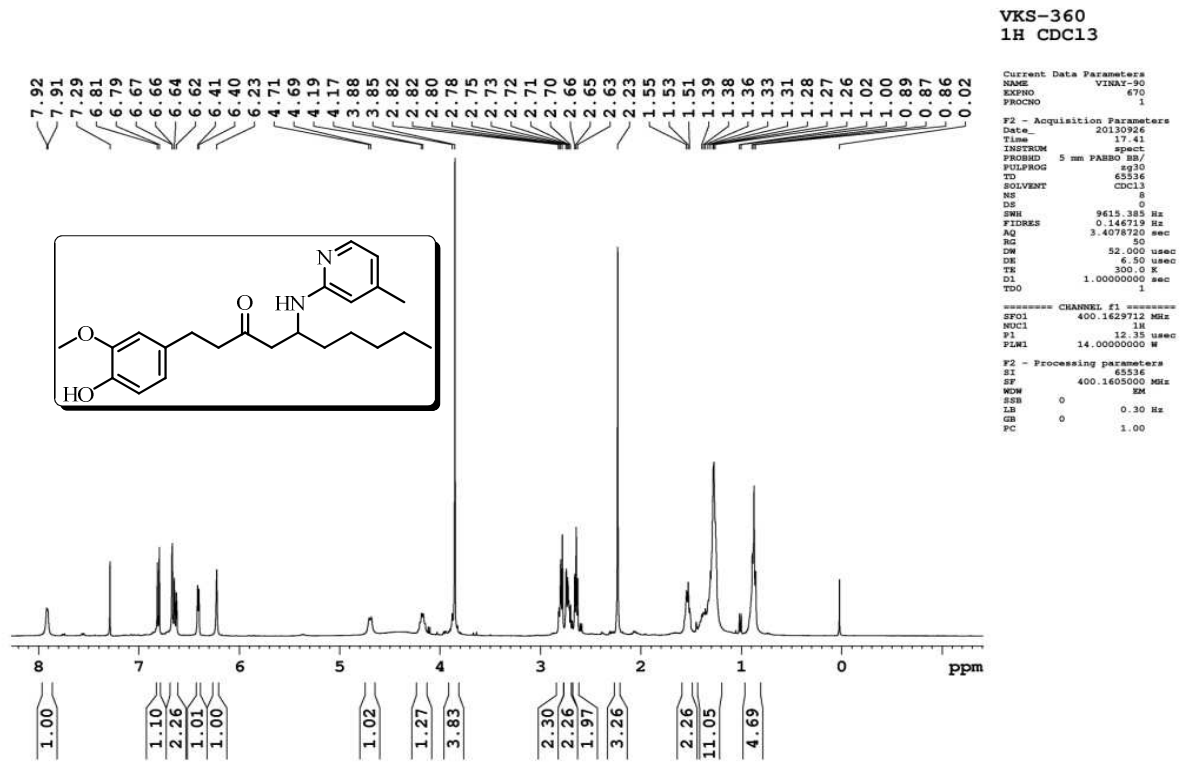

Figure 41. ^{1}H NMR spectrum of 6 (400 MHz, $CDCl_3$)

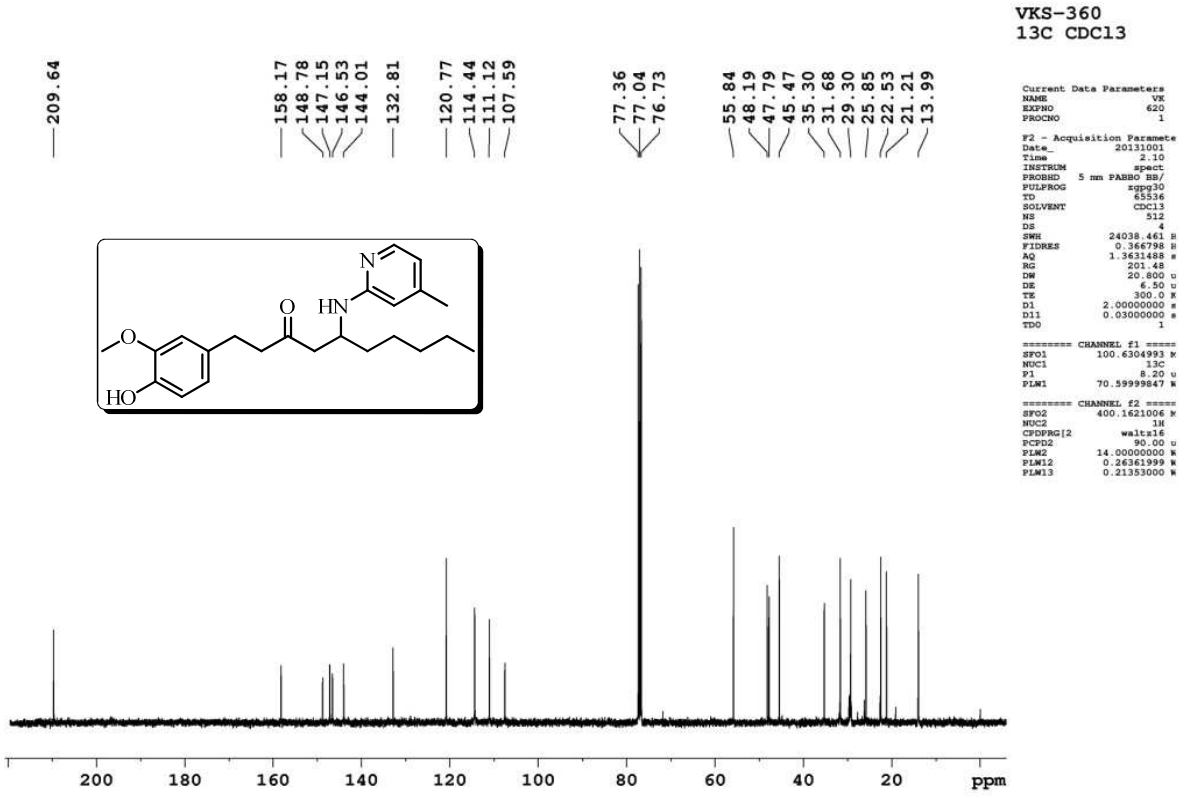

Figure 42. ^{13}C NMR spectrum of 6 (100 MHz, $CDCl_3$)

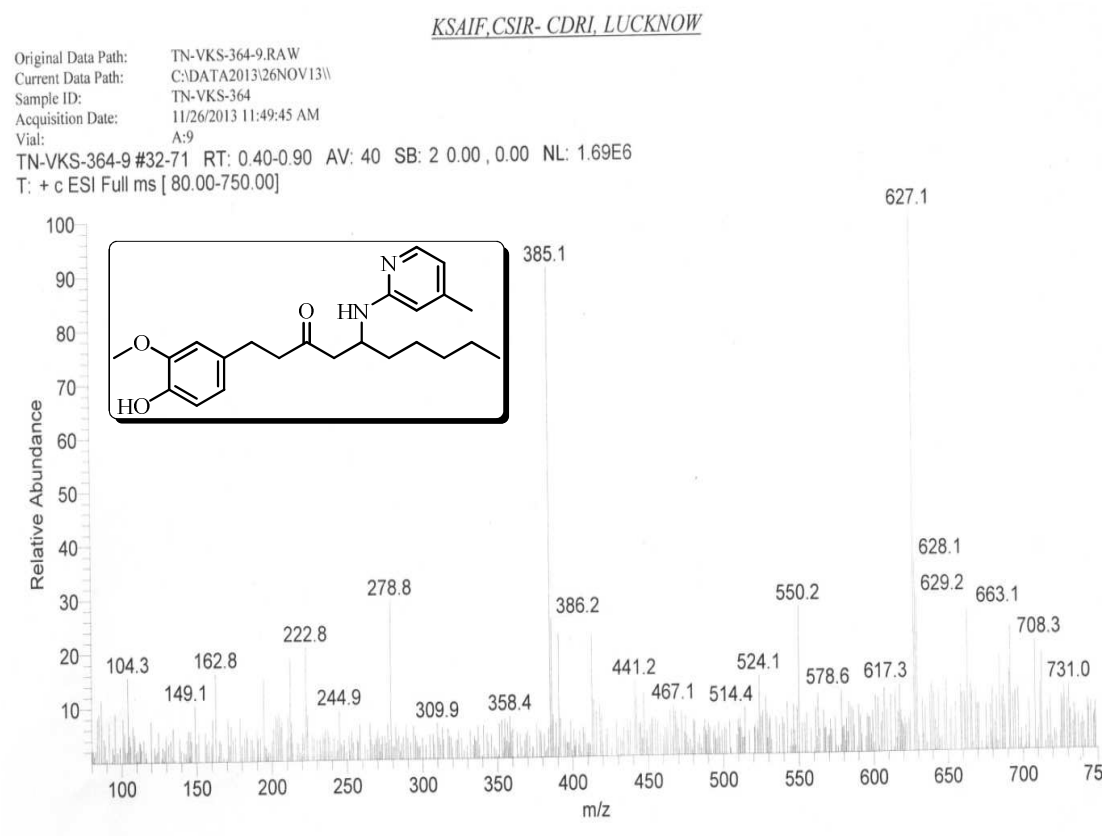

Figure 43. MS (ESI) of 6

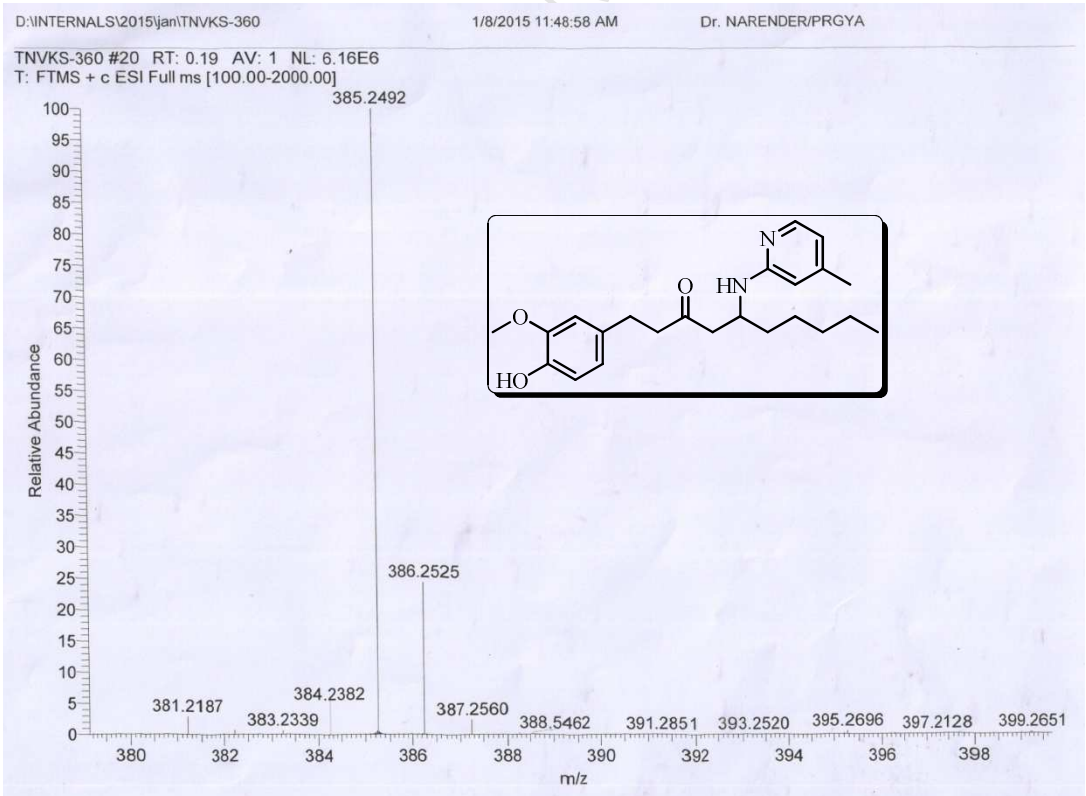

Figure 44. HRMS of 6

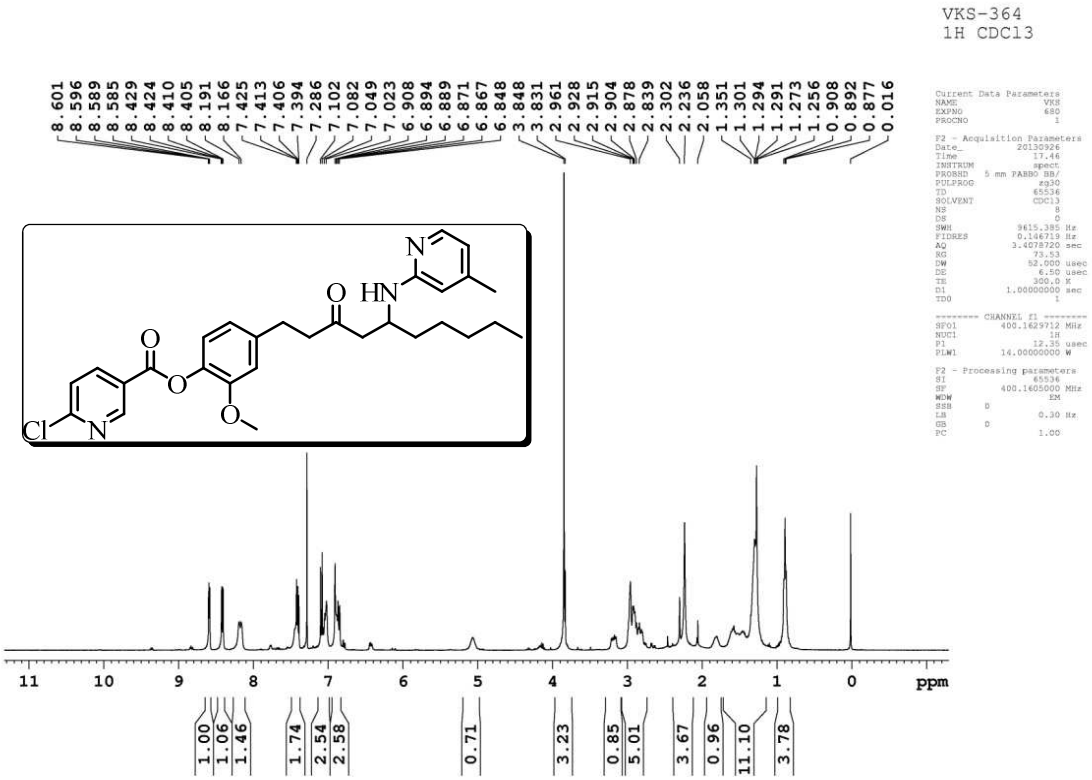

Figure 45. ^{1}H NMR spectrum of 6a (400 MHz, $CDCl_3$)

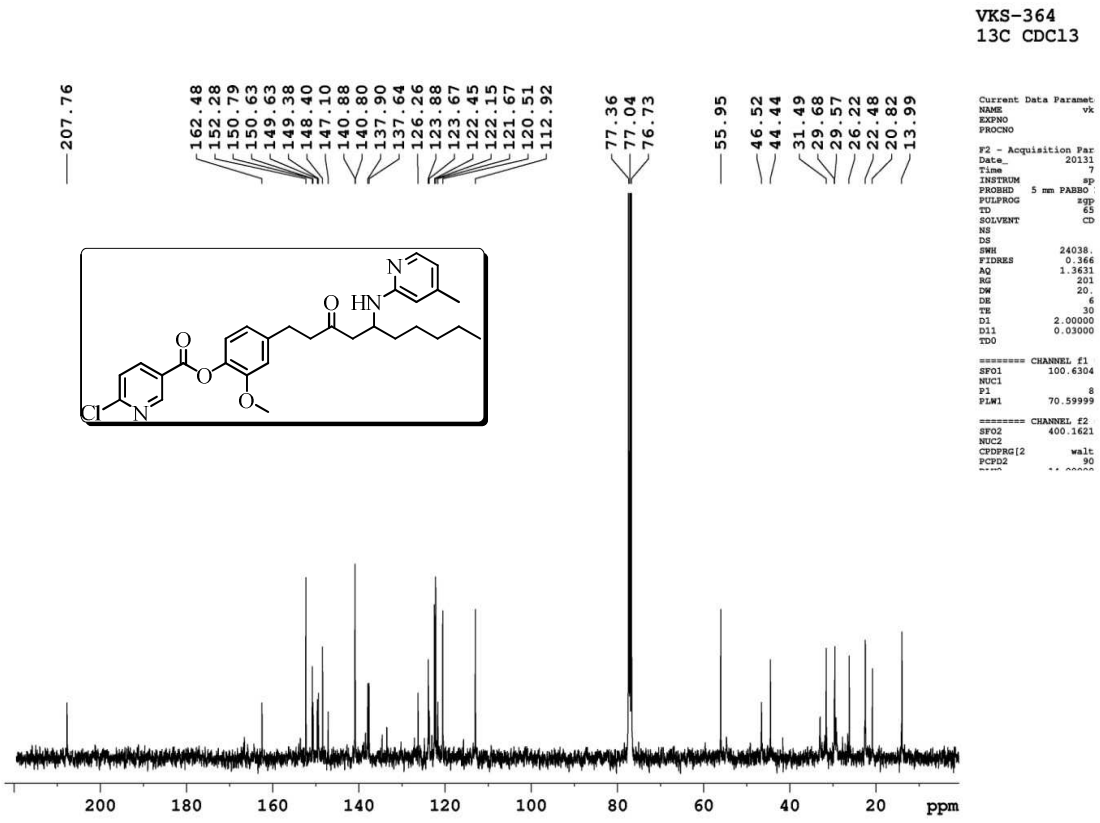

Figure 46. ^{13}C NMR spectrum of 6a (100 MHz, $CDCl_3$)

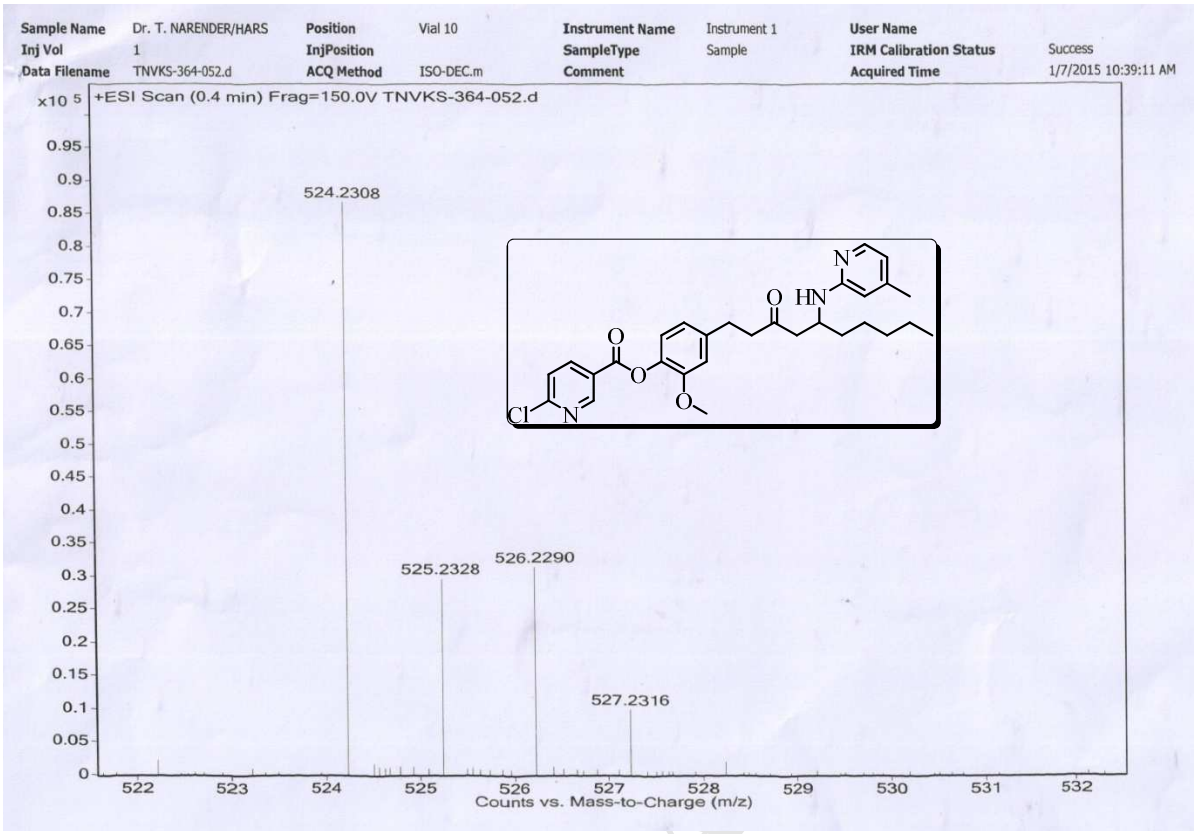

Figure 47. HRMS of 6a

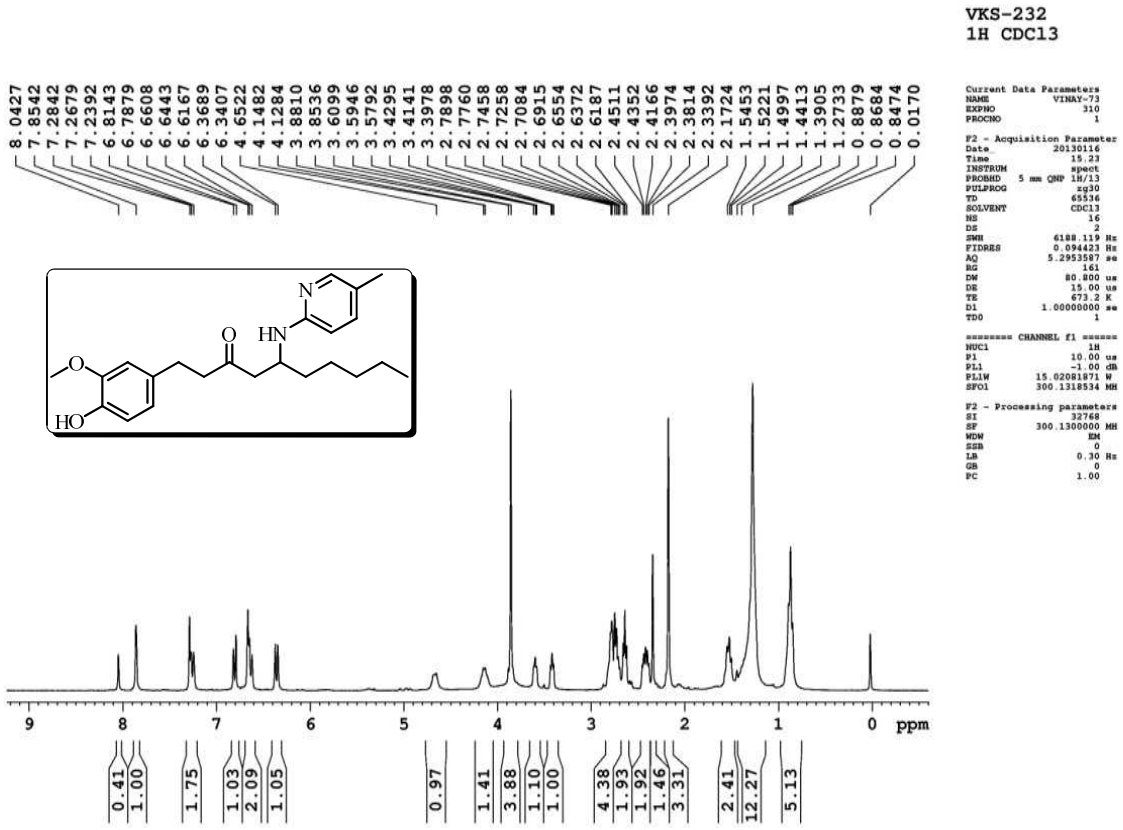

Figure 48. ^{1}H NMR spectrum of 7 (300 MHz, $CDCl_3$)

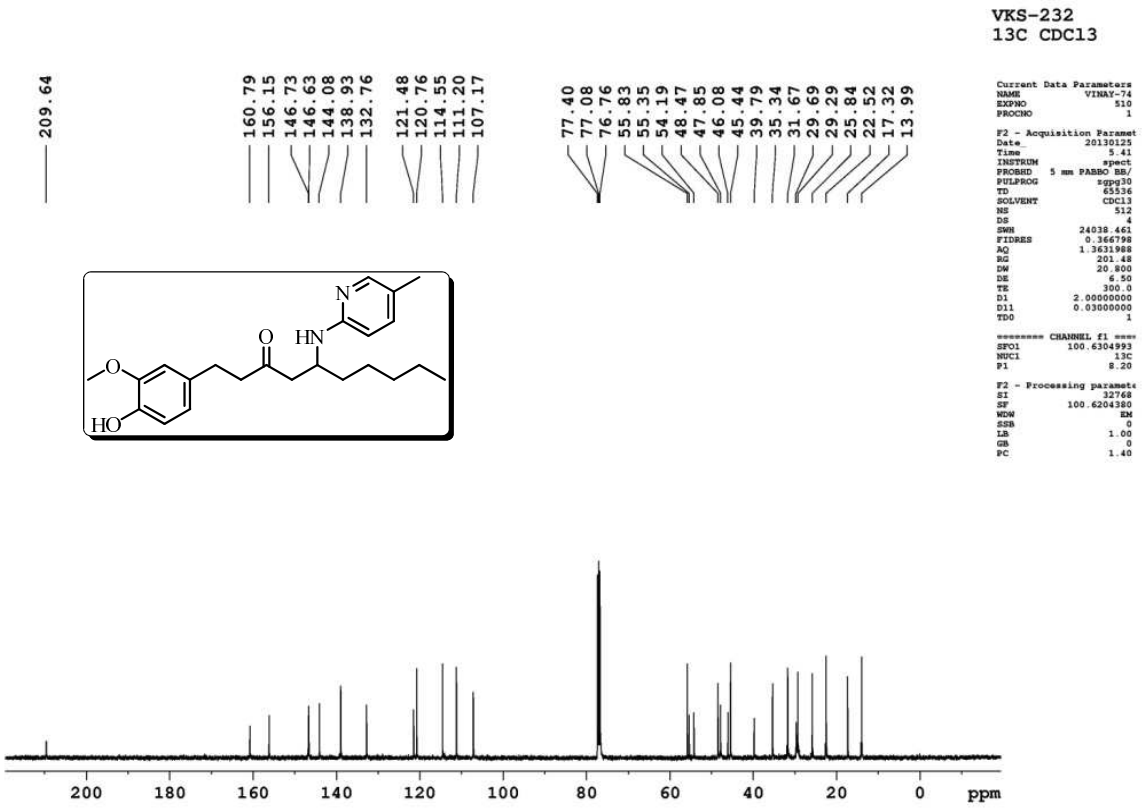

Figure 49. ^{13}C NMR spectrum of 7 (100 MHz, $CDCl_3$)

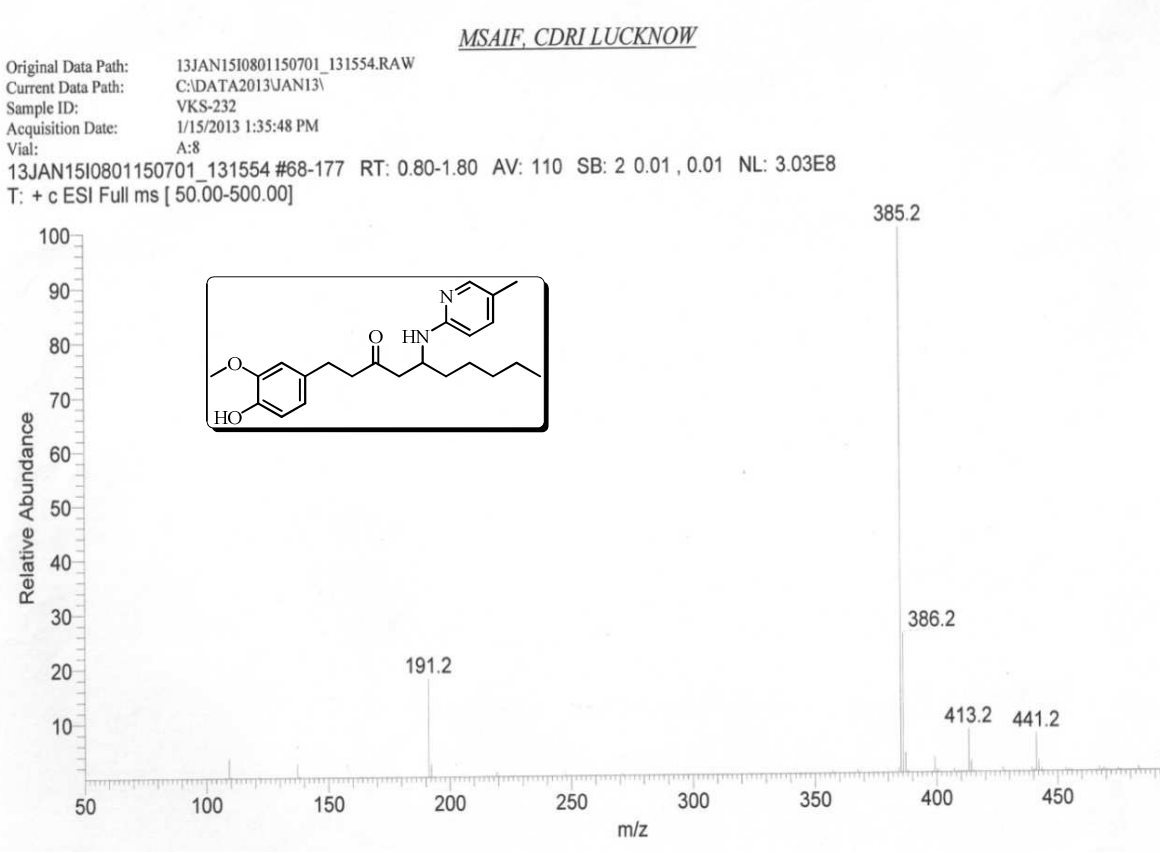

Figure 50. MS (ESI) of 7

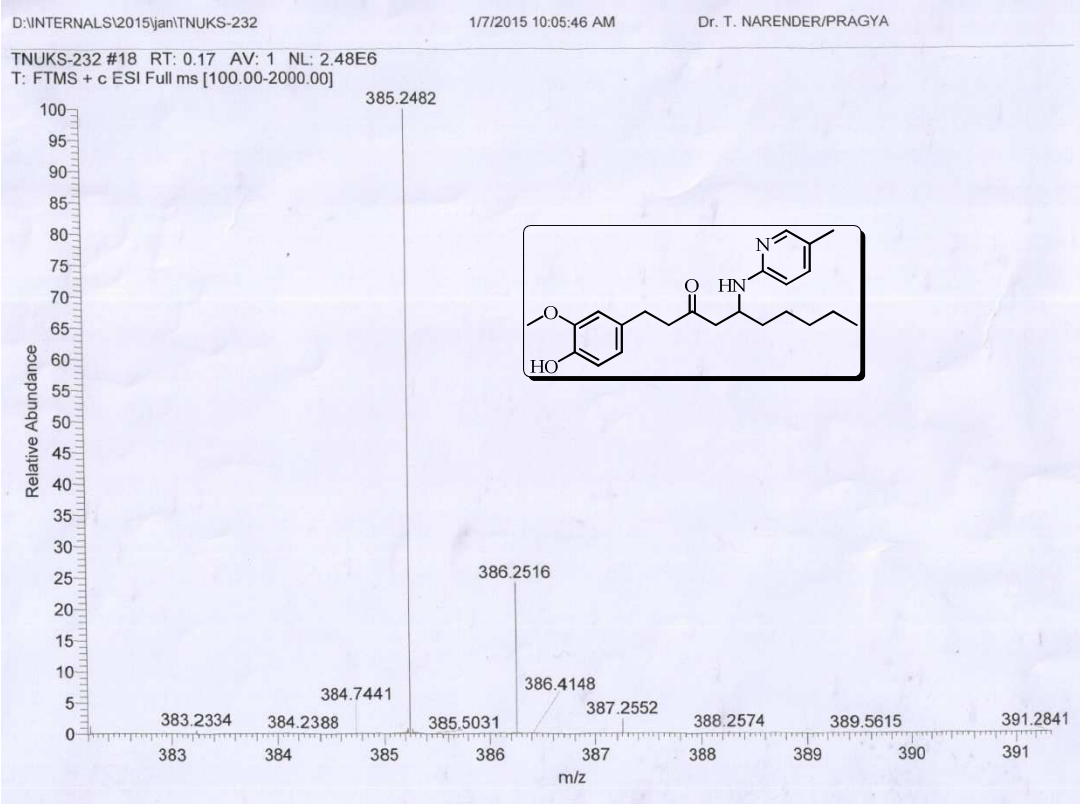

Figure 51. HRMS of 7

Figure 52: Predicted binding pose of inhibitors in TMP binding site of HsTMK

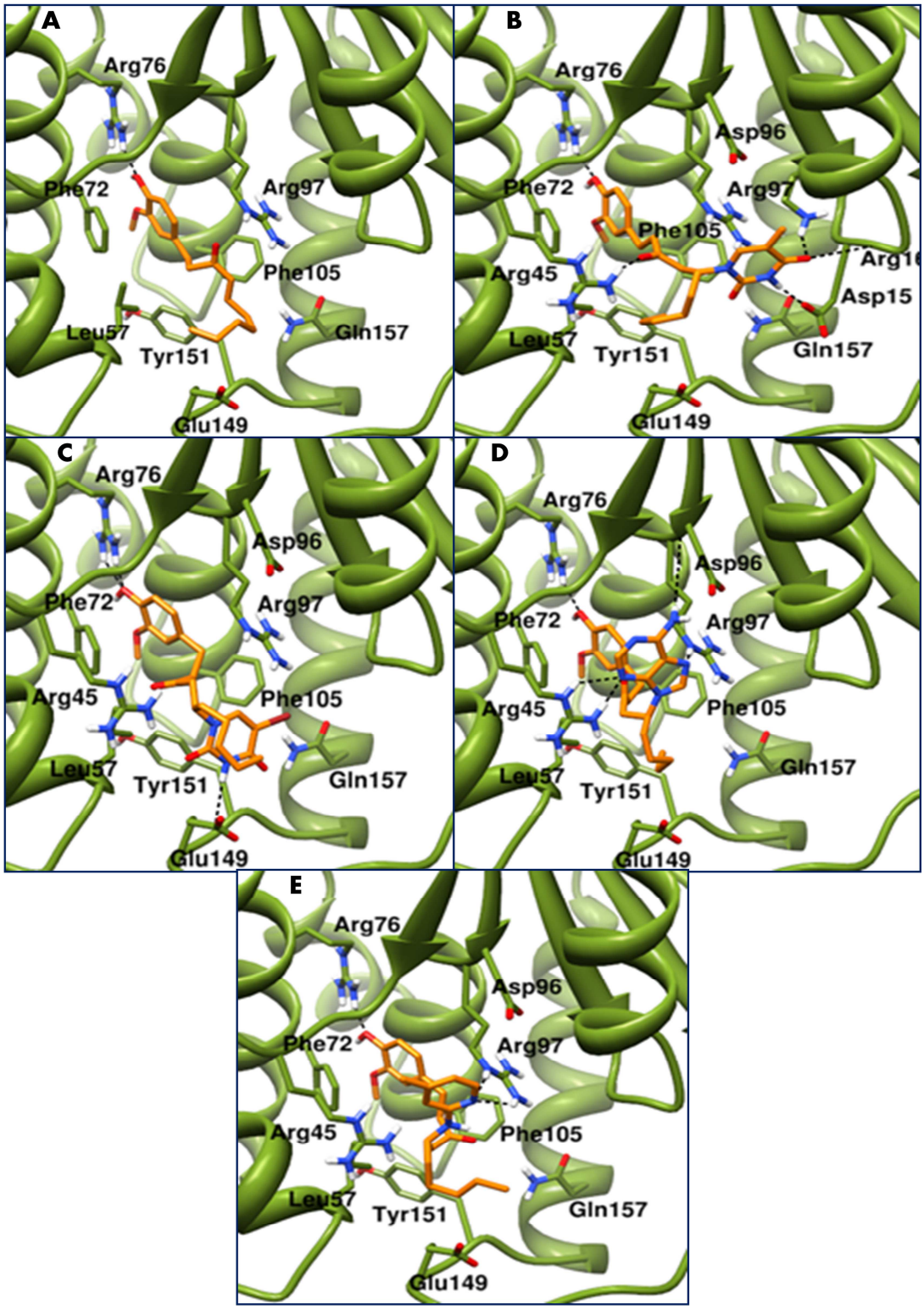

Figure 42: Predicted binding pose of [6]-shogaol **1** (A); **2** (B); **3** (C); **4** (D), and **5** (E) in TMP binding site of HsTMK. Hydrogen bonds are shown in black dotted line. Protein is shown in mixed representation (ribbon and stick). Only important residues involved in interaction are shown.